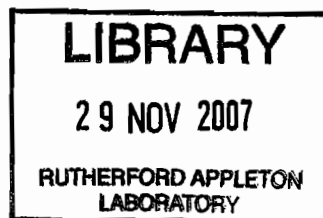




RAL-TR-2006-028
COPY 1.

Vibrational Spectroscopy at Central Facilities



**Stewart F. Parker, Gianfelice Cinque, Paul Dumas,
Peter Gardner, Anthony W. Parker, Keith Refson,
Elaine Seddon, Kevin Smith, John V. Wood**

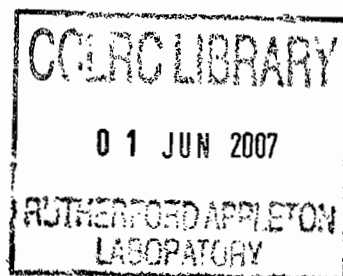
31st October 2006

Vibrational Spectroscopy at Central Facilities

On the 31st August 2006, a joint meeting of the Royal Society of Chemistry Molecular Spectroscopy Group and the Infrared and Raman Discussion Group (IRDG) was held at the Rutherford Appleton Laboratory with the theme 'Vibrational Spectroscopy at Central Facilities'. The meeting attracted around 35 people from a diverse range of backgrounds, both academic and industrial. The event provided a snapshot of the many activities in vibrational spectroscopy that are carried out at central facilities, particularly those of CCLRC. In addition, the meeting provided a forward look at the next generation infrared beamline at Diamond and an update on the progress and possibilities of 4GLS, a free-electron laser facility that will span the infrared to the X-ray regions.

This report contains the presentations of all the speakers and provides an overview of a field that is undoubtedly one of CCLRC's strengths and emphasises the world-leading capabilities in both experimental and computational science.

Stewart F. Parker



Vibrational Spectroscopy at Central Facilities:
*A joint meeting of the Royal Society of Chemistry
Molecular Spectroscopy Group and the Infrared and
Raman Discussion Group*

Thursday 31st August 2006

Venue: Conference Rooms 12 & 13, Rutherford Appleton Laboratory

- 10:00 Coffee and Registration
- 10:30 Introduction to CCLRC
Professor John Wood, CEO CCLRC
- 10:45 High-Resolution Infrared Studies at the RAL Molecular Spectroscopy Facility.
Dr Kevin Smith, Atmospheric Science, CCLRC
- 11:20 Time Resolved Vibrational Spectroscopy of DNA.
Professor Tony Parker, Central Laser Facility, CCLRC
- 11:55 DFT Analysis of Vibrational Spectra
Dr Keith Refson, Computational Materials Science Group, CCLRC
- 12:25 Vibrational Spectroscopy with Neutrons: Catalysts, Hydrides and Polyethylene
Dr Stewart Parker, ISIS Facility, CCLRC
- 13:00 Lunch and photograph
- 14:00 Synchrotron Infrared Microspectroscopy
Dr Paul Dumas, Soleil Synchrotron, Paris
- 14:50 Synchrotron Reflection Absorption Infrared Spectroscopy
Dr Peter Gardner, School of Chemical Engineering and Analytical Science, The University of Manchester
- 15:25 The Infrared Beamline at the New Diamond Facility.
Dr Gianfelice Cinque, Diamond Light Source
- 15:35 Update on 4GLS
Dr Elaine Seddon, Synchrotron Radiation Source, CCLRC
- 16:00 Closing Remarks
Tours of facilities (ISIS, CLF, MSF) available by prior appointment
-



Why do we need a research strategy, and how do we develop it?

Professor John Wood

Professor John Wood

CCLRC

August 2006



Why do we need a strategy?



- Enabling research
- Building partnerships
- Getting it right for science
- Engaging with society
- Exploiting own potential
- Developing strategy

... ..



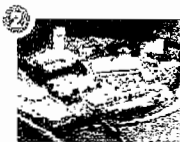
- One of eight UK research councils
- Formed by Royal Charter on 1 April 1995
- Funded by Department of Trade and Industry (Office of Science and Technology)
- 7,000 users annually
- Operating turnover £240m (2004-5)

... ..

Three world class research laboratories...



CCLRC Rutherford
Appleton Laboratory
Oxfordshire



CCLRC Daresbury
Laboratory
Cheshire



CCLRC Chilbolton
Observatory
Hampshire





www.ukri.ac.uk



Wholly owned facilities:

- **Laser – Vulcan, Astra**
- **Neutron - ISIS**
- **Synchrotron - SRS**
- **Computing – HPCx**

Shareholder in:

- **Diamond (majority shareholder on behalf of the UK government)**
- **ILL/ESRF**



www.ukri.ac.uk



- Particle Physics
- Space Science and Technology
- Instrumentation and sensors
- E-science and grid technology
- Micro and nano-fabrication
- Energy
- Radio Communications
- Engineering design
- Knowledge transfer

Increased Capacity

Increased capacity

Increased capability

New opportunities for

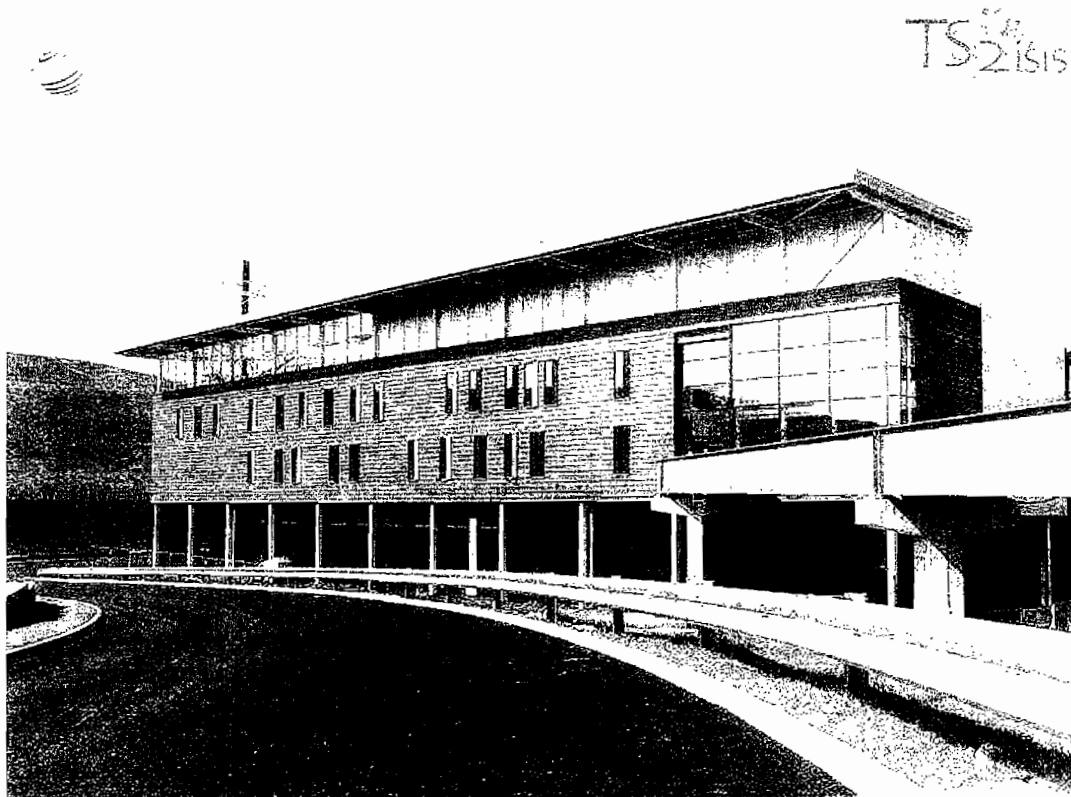
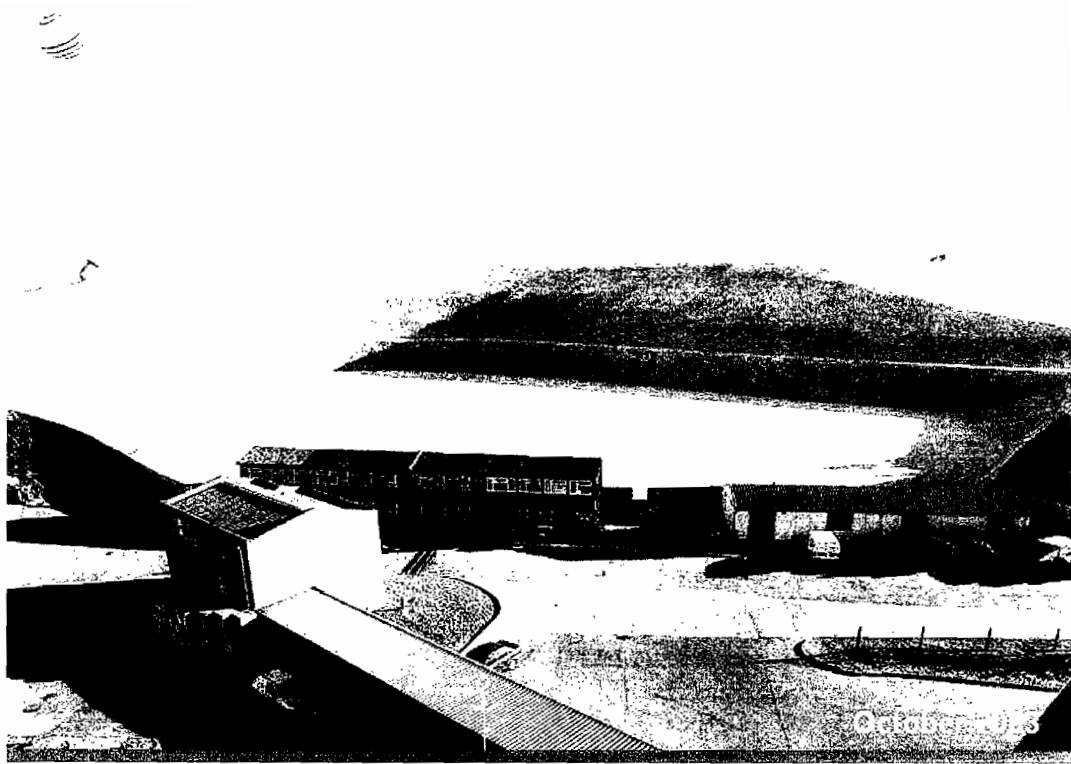
- Soft Matter
- Advanced Materials
- Biomolecular Systems

Nanoscience

ISIS TS2



May 2003

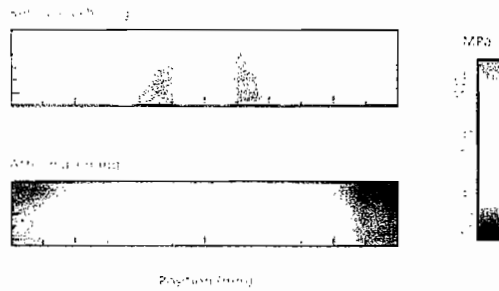


TS-21515

Neutron Strain Measurements

EMOX-X

- Neutron Strain Measurements

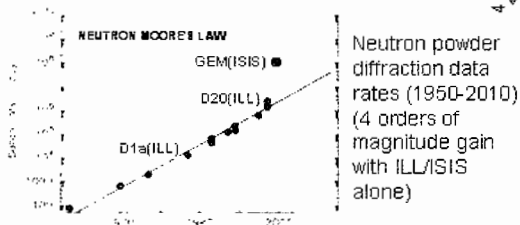


A380 wing section

Data curation

Data curation

- Volume of data increasing dramatically
- Issues of filtering, mining, storage and management



- Conserving experimental data for future research
- the next big challenge



Sources of X-rays



10/16

Sources of mixed mode, high intensity X-rays and synchrotron light

- SRS
- ESRF
- Diamond
- 4GLS



4



Lasers for Science



High power, state-of-the-art laser facilities

Vulcan

- the world's highest intensity focused laser
- Recreating conditions on the sun in the lab

Astra

- high power, ultra short pulse titanium-sapphire laser
- Following chemical and biological reactions

Lasers for Science

- optical tweezers

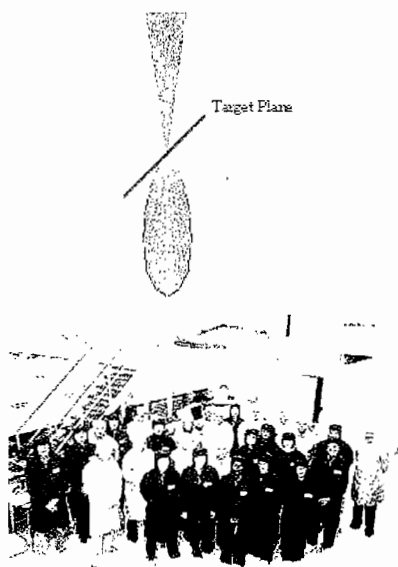


Electron Acceleration in Laser-Produced Plasmas

- Electron acceleration studies in gas jets
- EMP (electromagnetic pulse measurements) + buried layer heating studies
- Solid target interaction studies
- Studies of advanced fast ignitor concept for ICF (Inertial Confinement Fusion)
- Electron transport measurements in solids
- Ultra high density plasma investigations



Electron Acceleration in Laser-Produced Plasmas



- Highest energy accelerating field in plasma
- Brightest Gamma ray beam ever produced
- Largest laser induced nuclear conversion
- Highest flux ever delivered from a laser plasma interaction
- Capable of producing a beam with an intensity of 10^{21} w/cm².

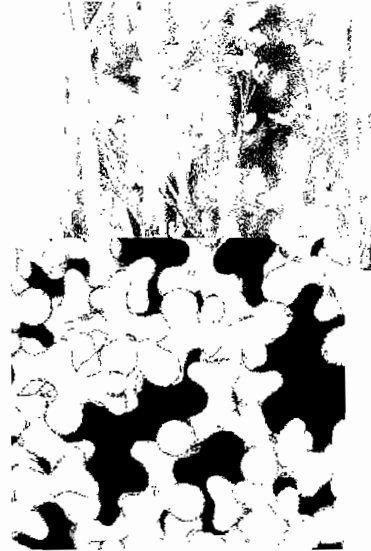




High Performance Computing

HPCx

- Europe's most powerful academic computer
- Quantum mechanics of proteins – calculations of unprecedented scale
- Electronic structure of Crambin (extracted from Abyssinian Cabbage)
- Calculation was 10 times more challenging than any published before
- Similar techniques will be used to study proteins of greater scientific value e.g. the redox potentials of Rusticyanin, a blue copper protein involved in electron transport in plants and bacteria

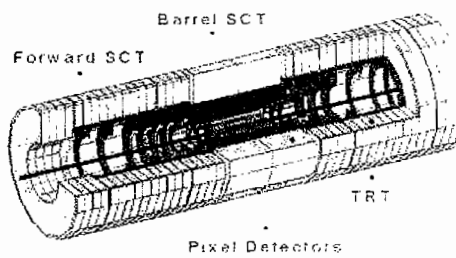


High Energy Physics

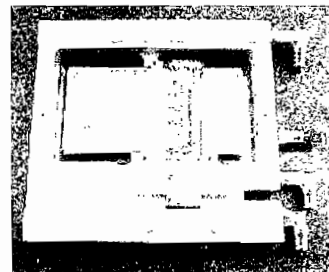
Experiments at

- CERN:** ATLAS, CMS, LHCb
- DESY:** H1, ZEUS
- FNAL:** MINOS
- SLAC:** BaBar
- ILL:** Neutron edm
- Boulby:** Dark matter
- R&D:** Linear Collider, Neutrino Factory

ATLAS Semiconductor Tracker



ATLAS Tracker Modules

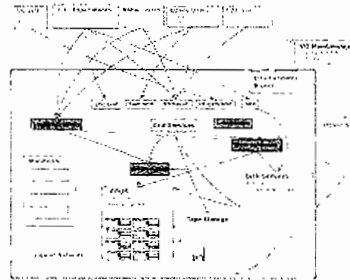




Grid enabling CCLRC facilities

Grid enabling CCLRC facilities

- Portals
- Data storage architecture
- Computing resources
- Visualisation



Europe's largest space science and technology department



Europe's largest space science and technology department

167 instruments in space

Collaborations with:

- NASA
- ESA
- PPARC, NERC

Quality assured:

- ISO 9001
- TickIT

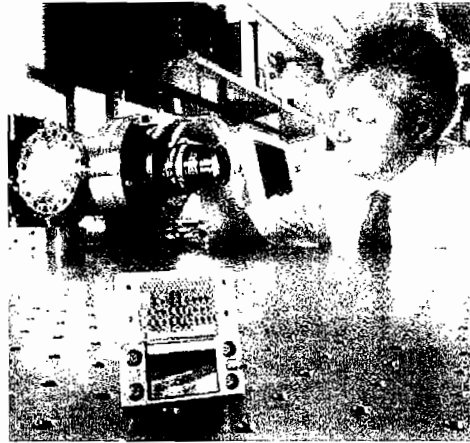




Space Technology



- CCDs and cameras
- Space Coolers
- Optical/Electronics design
- Thermal structural design
- Sensors and Detectors
- Millimetre wave components
- Orbit dynamics/mission analysis
- Smart technology
- Payload operations systems



Space Technology

SMART-1 - Europe's first mission to the Moon

- testing innovative technologies for future deep space missions (low mass, low volume, low power)
- D-CIXS - Demonstration Compact Imaging X-ray Spectrometer, designed and built at RAL
- Producing the first X-ray map of the Moon

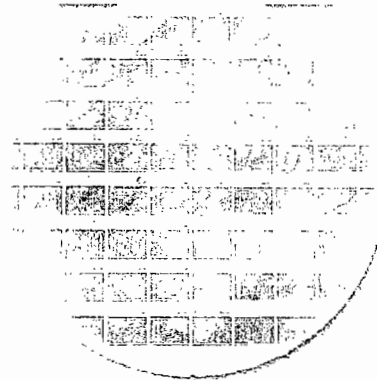


www.ral.ac.uk

Underpinning CCLRC science

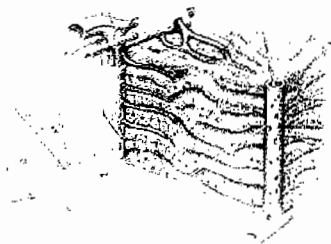


- **Microelectronics design**
- **Detector design**
- **Data acquisition electronics**
- **Control systems design**



Nature's design

Nature's design



Powder blasted tissue scaffold to form sinusoid

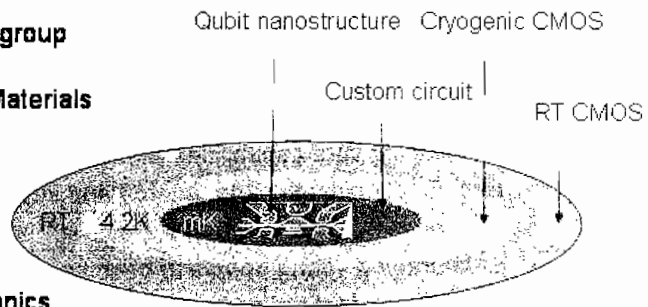
- **Project aims to simulate complex tubes which carry blood around the liver**
- **Constructing nanometre scaffolding in which to grow liver cells**
- **Artificial liver will be used for testing drugs in the laboratory**

School of Pharmaceutical Sciences, University of Nottingham
Central Microstructure Facility, CCLRC & Mechanical Engineering, University of Leeds



Spin-out companies from CCLRC

- **CCLRC Microelectronics group**
- **Oxford – Department of Materials**
- **Hitachi Cambridge**
- **Oxford instruments**
- **Cambridge – Microelectronics Research Centre, Cavendish Lab**



CLIC Ltd will manage and develop the intellectual property rights in the microelectronics technology developed by the CCLRC Microelectronics group.



Spin-out companies from CLIC Ltd

CLIC Ltd

- formed in March 2002
- to stimulate and nurture start up and licensing opportunities for CCLRC
- Rainbow Seed Corn Fund

4 spin-out companies formed in the last 12 months:

- L3T – near patient cholesterol testing
- Microvisk – diagnostics for blood viscosity and clotting measurements
- Oxsensis – sensors for hellish environments such as jet engines
- Thruvision – terahertz imaging for security screening



- **Promoting the added value of bringing together core teams to deliver world class science and to exploit innovations for the UK**
 - **Developing core capabilities with national and international partners (e.g. focal points in nano, energy and space)**
 - **Encouraging young people to become actively involved in vibrant science and technology**
-

High-Resolution X-Ray Spectroscopy

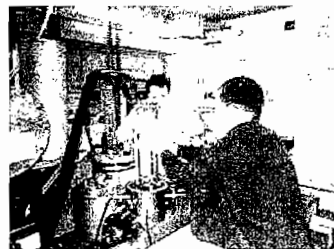
Dr. Kevin Smith - Principal Investigator

Office of the Director, National Science Foundation
Washington, D.C. 20540

1

Summary

The proposed research project is a continuation of the work done in the past few years on the development of a high-resolution X-ray spectrometer. The spectrometer is designed to measure the energy of X-rays with a resolution of 1 eV. This is a significant improvement over the current state-of-the-art spectrometers which have a resolution of 10 eV. The spectrometer is based on a novel design that uses a series of curved mirrors to focus the X-rays onto a detector. This design allows for a much larger acceptance angle than traditional spectrometers, which is essential for measuring the energy of X-rays from a wide range of sources. The spectrometer is currently under development and is expected to be completed in the next few years.



The spectrometer is currently under development and is expected to be completed in the next few years. The project is supported by the National Science Foundation and is part of a larger program on X-ray spectroscopy. The spectrometer is designed to measure the energy of X-rays with a resolution of 1 eV. This is a significant improvement over the current state-of-the-art spectrometers which have a resolution of 10 eV. The spectrometer is based on a novel design that uses a series of curved mirrors to focus the X-rays onto a detector. This design allows for a much larger acceptance angle than traditional spectrometers, which is essential for measuring the energy of X-rays from a wide range of sources.

2

Figure 2.10.1.8

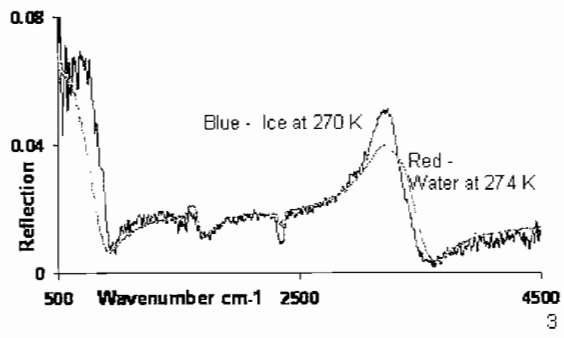
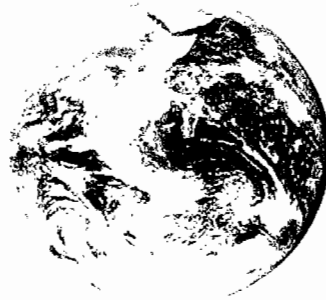
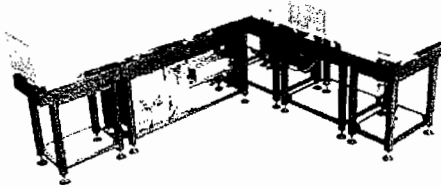
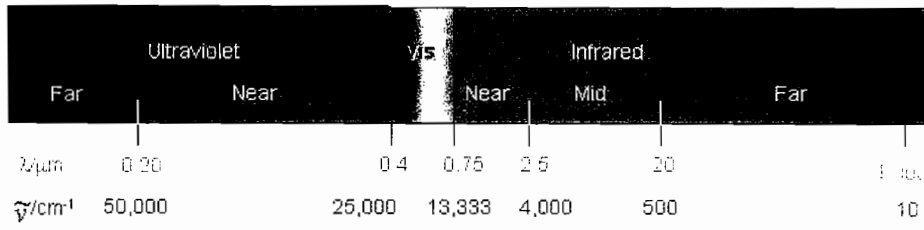


Figure 2.10.1.9



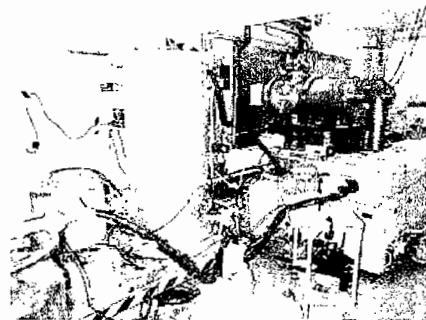
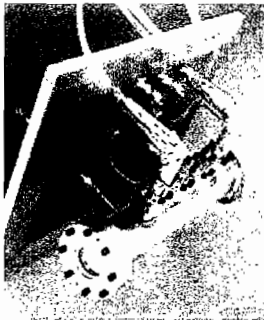
4

Spectrometers



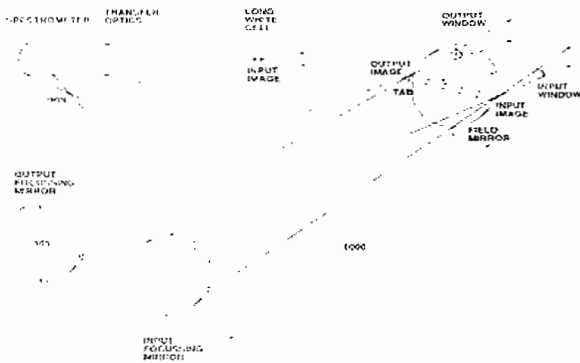
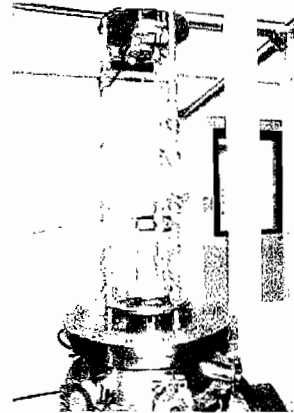
5

Gas cells



6

039 101 5



039 101 5

039 101 5 Water vapour (University of Reading)

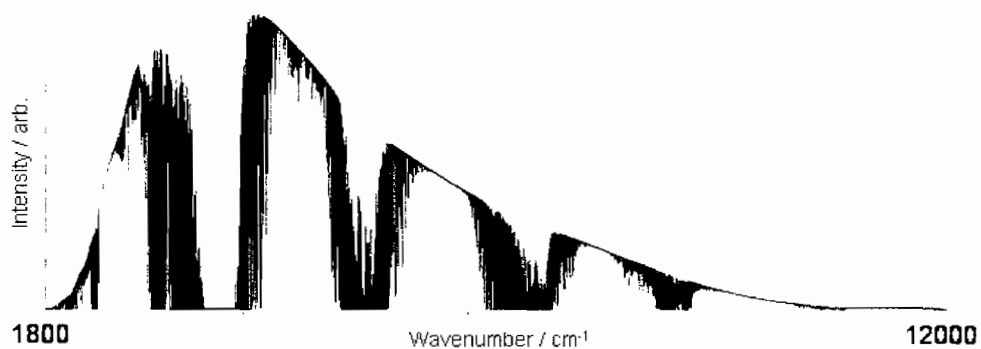
039 101 5 Methane (University of Oxford)

039 101 5 PSCs, mineral dust (University of Oxford, The Open University)

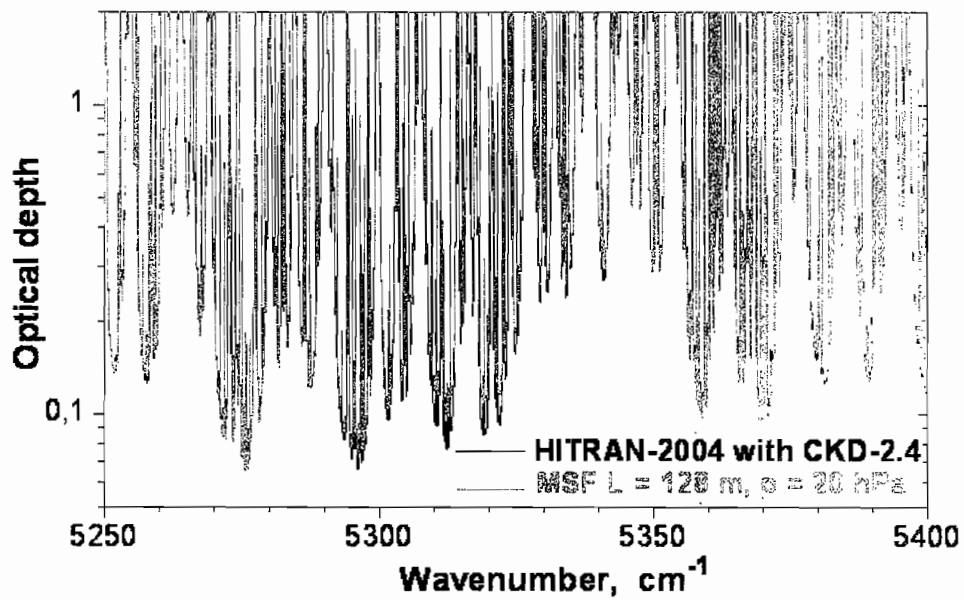
039 101 5 PAN (University of Leicester)



Optical depth vs. Wavenumber

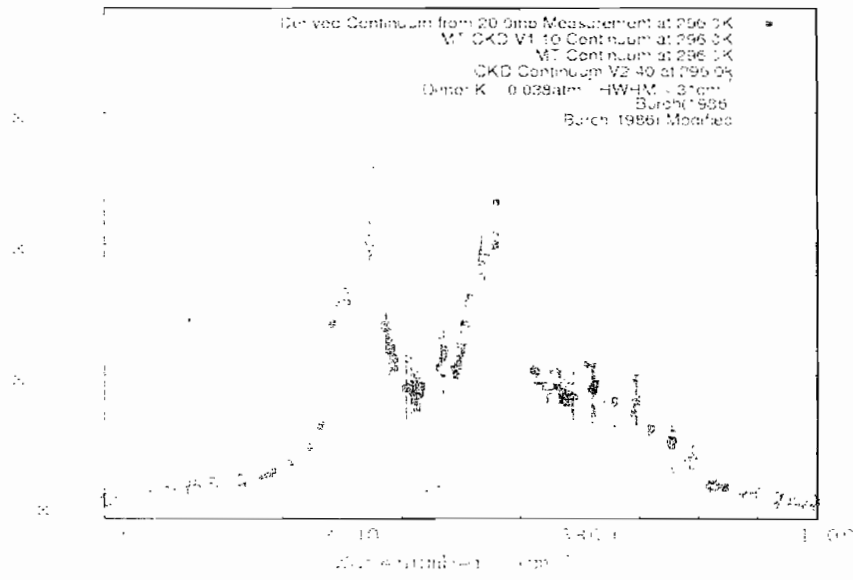


Optical depth vs. Wavenumber (5250-5400 cm⁻¹)



10

2.13.0. 5000 cm⁻¹ to 1000 cm⁻¹



11

2.13.0. 5000 cm⁻¹ to 1000 cm⁻¹

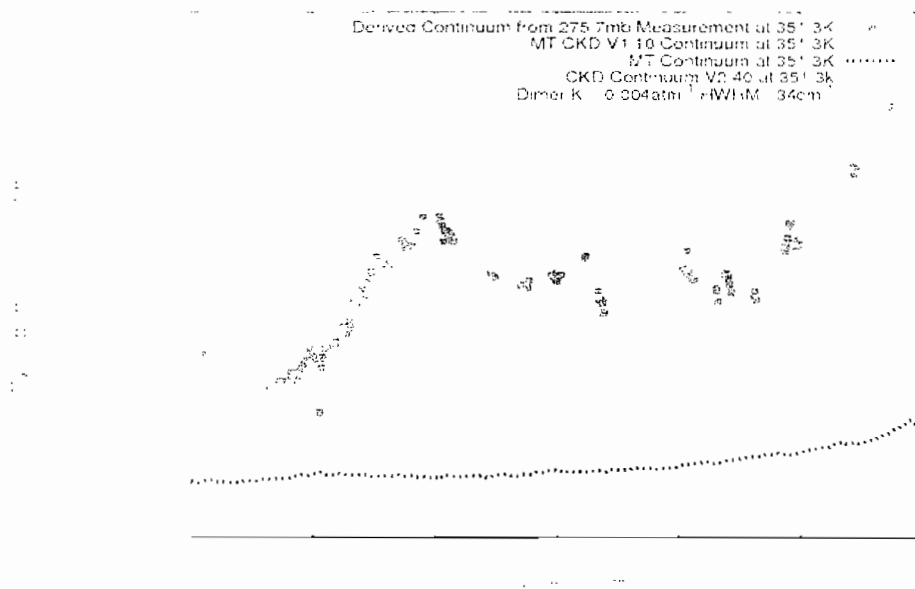
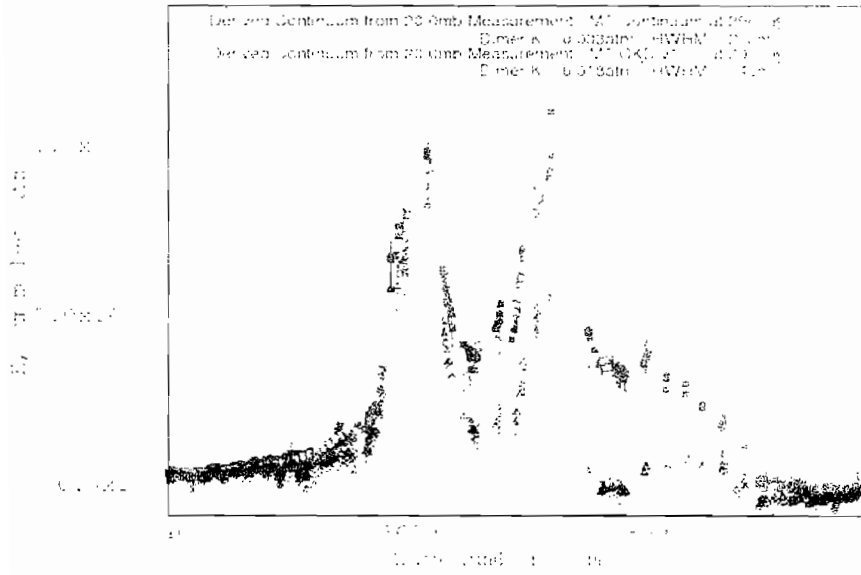
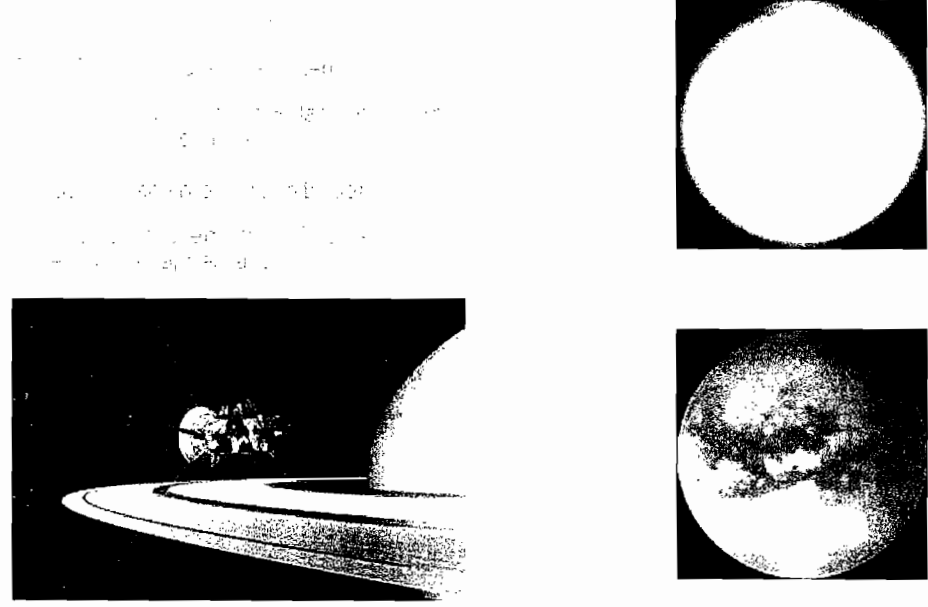


Figure 13.10: W_{eff} vs λ



13

Figure 13.11: W_{eff} vs λ

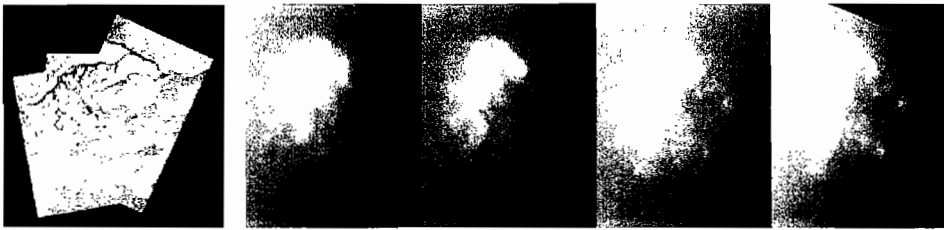


14

Figure 46. IR spectra of methane

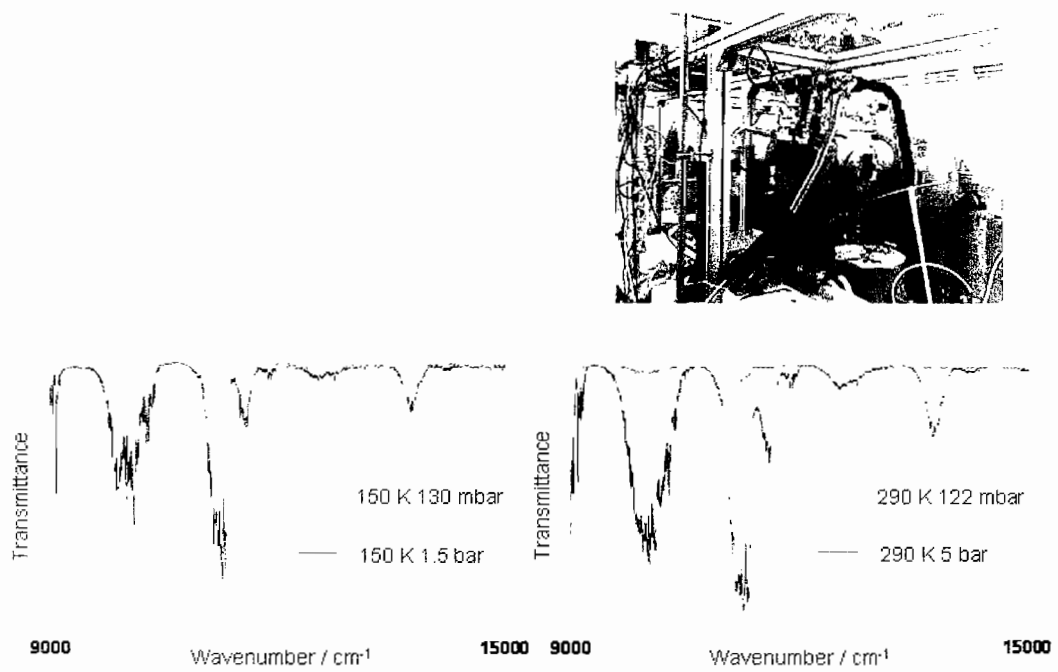


Figure 47. Laser spectroscopic data on methane below 1.1 μm (above 900 cm^{-1})



15

Figure 48. IR spectra of methane



24

Aerosols

• Particles of solid or liquid matter suspended in a gas

• Can be natural or man-made



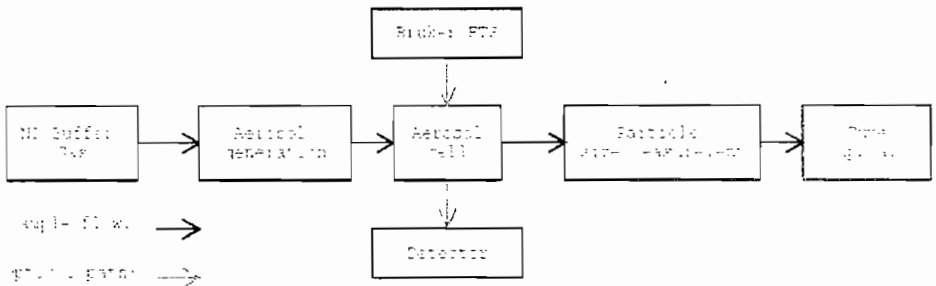
Volcanic ash and smoke, Organic aerosols (from forest), Smoke from forest, Volcanic eruption

17

Aerosols

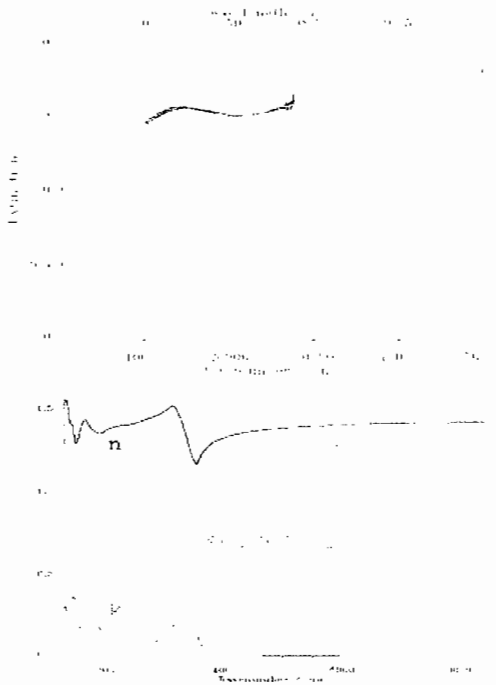
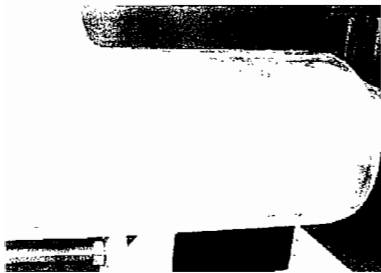


• Can be natural or man-made



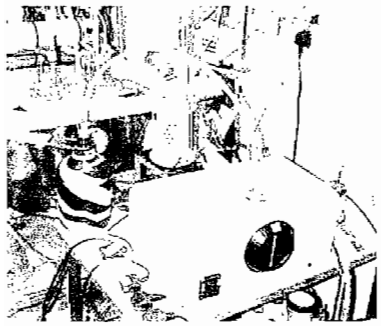
18

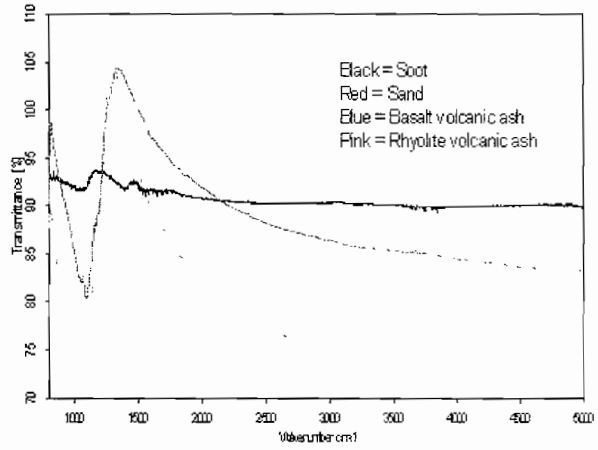
WIND TUNNEL TEST RESULTS



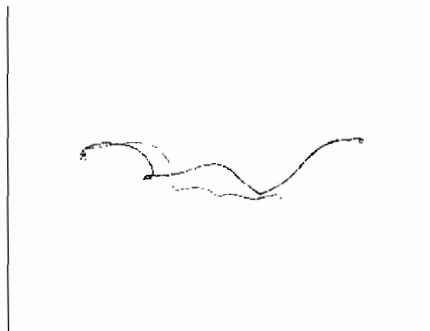
19

WIND TUNNEL TEST RESULTS

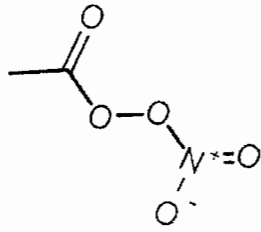




Analysis



Chemische Strukturformel eines Salzes



23

23

Chemische Strukturformel eines Salzes



24

Diagram of PAB on a SA's orbit

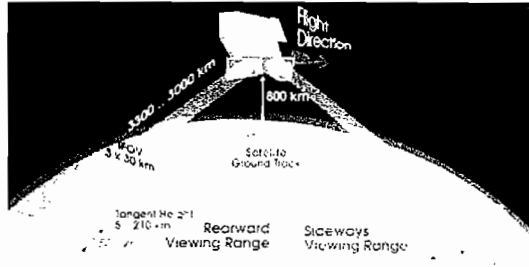
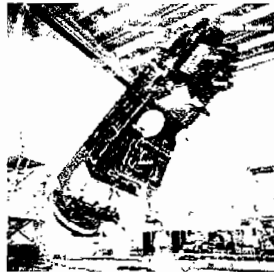


Diagram of view from a SA's orbit

Diagram illustrating the view from a satellite's orbit, showing the ground track and the viewing range.

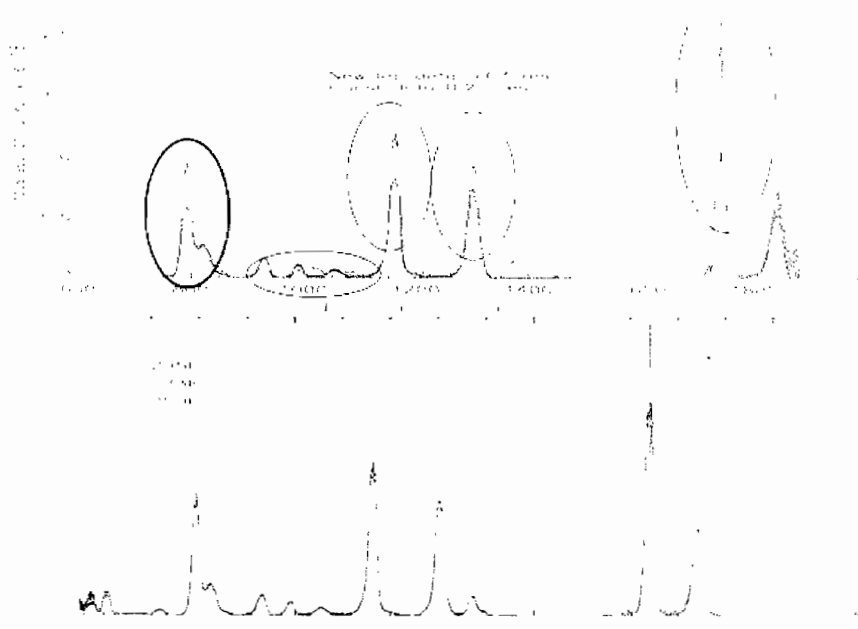


Figure 10: MIPAS atmospheric radiance spectra

Figure 10 shows the MIPAS atmospheric radiance spectra for the 1000-1100 cm⁻¹ region. The plot displays the radiance spectra (black line) and the corresponding cross sections (red line) for the 1000-1100 cm⁻¹ region. The x-axis represents the wavenumber in cm⁻¹, ranging from 1000 to 1100. The y-axis represents the radiance in K, ranging from 0 to 10. The red line represents the cross sections, and the black line represents the MIPAS atmospheric radiance spectra. The plot shows a complex structure with many absorption lines, particularly in the 1000-1100 cm⁻¹ region.

RED = fit based on MIPAS cross sections

BLACK = MIPAS atmospheric radiance spectra

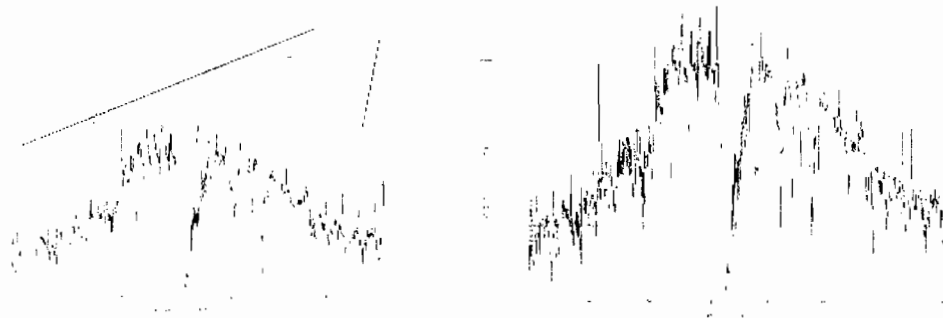
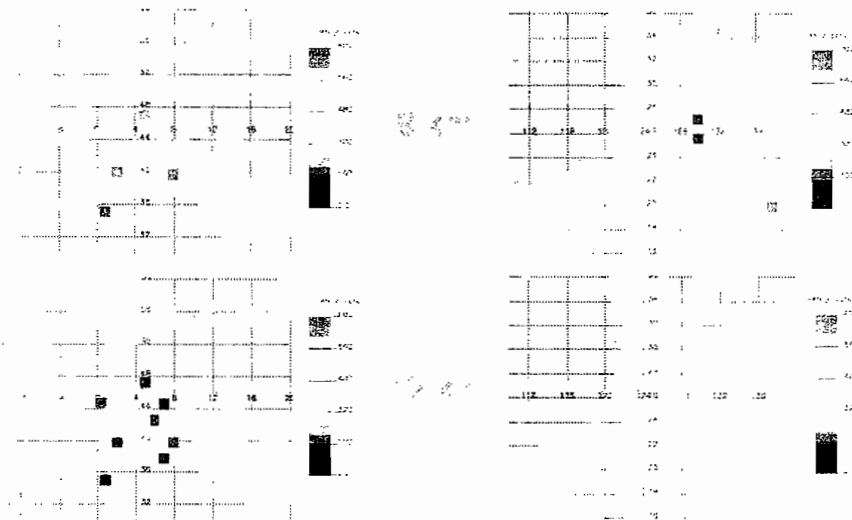


Figure 11: MIPAS atmospheric radiance spectra



10-00000000

17

67 NATIONAL
68 ENVIRONMENT
69 AND ENERGY

10-00000000

10-00000000

Time Resolved Vibrational Spectroscopy of DNA

Anthony W. Parker (a.w.parker@rl.ac.uk)

❖ PURATE

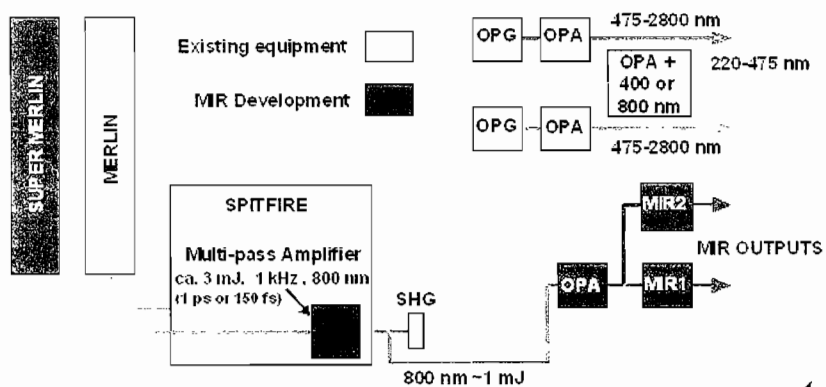
❖ Molecular Structure of Transient Intermediates

Nucleic Acid Bases

UV Excitation

Photoionisation

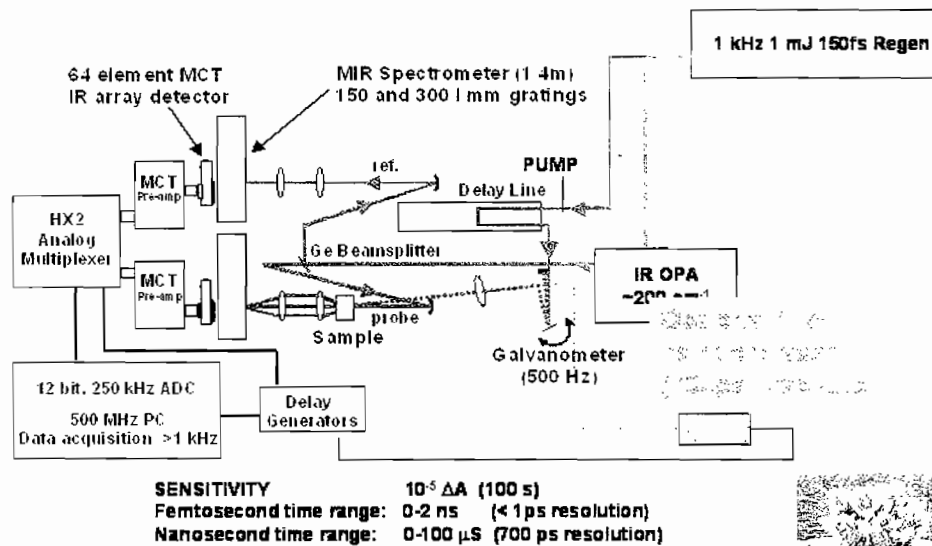
Schematic layout of the laser system and OPAs



Picosecond Infra Red Absorption Transient Excitation



The Broadband Pump-Probe TRIR Spectrometer



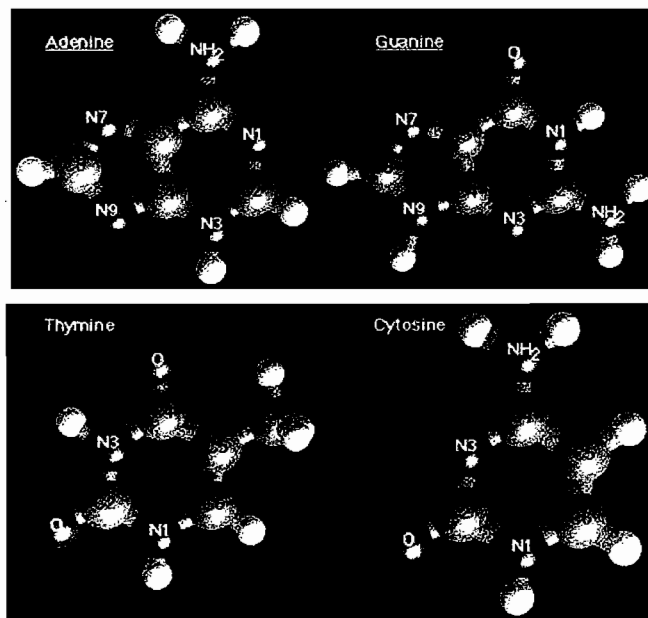
A High-Sensitivity Femtosecond to Microsecond Time-Resolved Infrared Vibrational Spectrometer
 M. Towne,* A. Gabrielsson, P. Matousek, A. W. Parker, A. M. Blanco Rodriguez, and A. Vliček, JR.

Levels of "potential" DNA Damage & measurement†

- **Solar Radiation - Sunny Day**
 ~ 200 W/m² gives potentially 8×10^{18} potentially harmful events per cell/day.
- **Background Radiation -**
 ~ 100 mrem/year inflicting c. 2 harmful events per cell/day
- **Physical carcinogens (chemical pollution)**
 say 1 ppm, air exchanged between average lung per day ~ 7000 l, equivalent to 0.01g toxin per day, assuming 0.1% activity, studies show pollutants generate 10^{18} radicals per gram. With finite probability of these generating deleterious effects estimated c. 3×10^4 potentially harmful effects per cell/day
- **Detectivity - DNA damage detection using immuno assay (apurine /apyrimidine) utilising anti-AP and fluorescence 100 units per DNA**

Effects of electronic excitation on DNA bases, polynucleotides and DNA

Nucleic Acid Bases & DNA



http://www.bic.arizona.edu/Molecular_Graphics/DNA_Structure/DNA_Tutorial.HTML#helixaxis

UV Excitation of DNA & Components

- **UV radiation gives**

singlet	triplets
<i>lifetimes</i> < 1ps	$\Phi_T \leq 0.01$
$\Phi_I \leq 10^{-4}$	$E_T \sim 300 \text{ kJ mol}^{-1}$

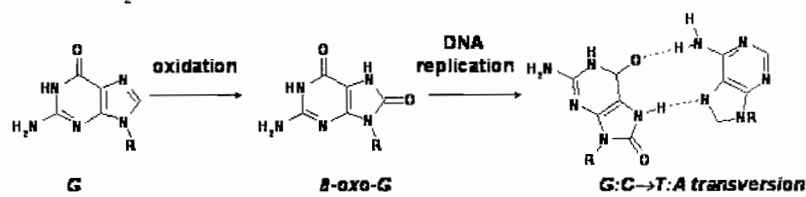
- **Chemical reactions**
cyclobutane pyrimidine dimers

- **Photoionisation**

Base + $h\nu \rightarrow \text{Base}^{**} + \text{electron}$

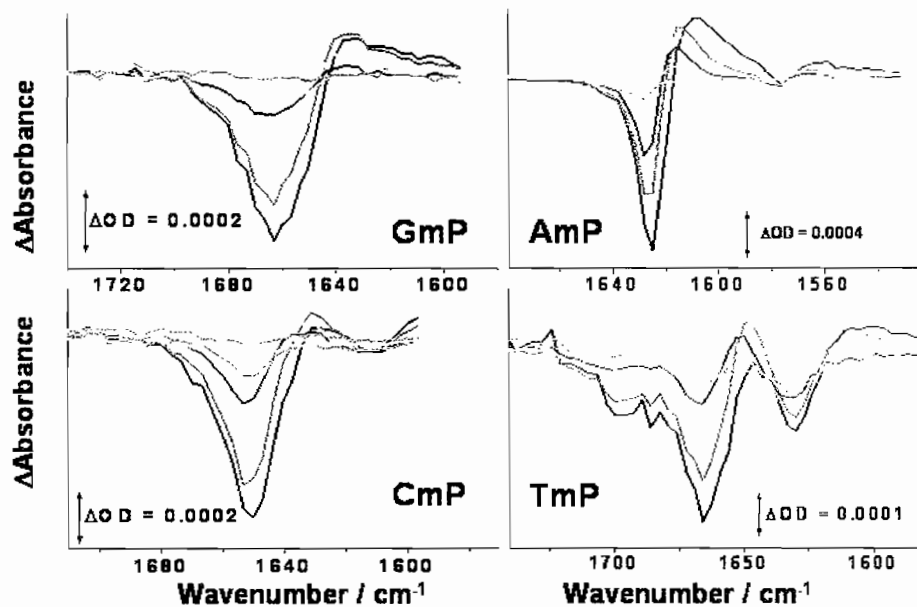
Base^{**} + H₂O → 8-oxo-G

GG/C-C can give AA/C-C on replication

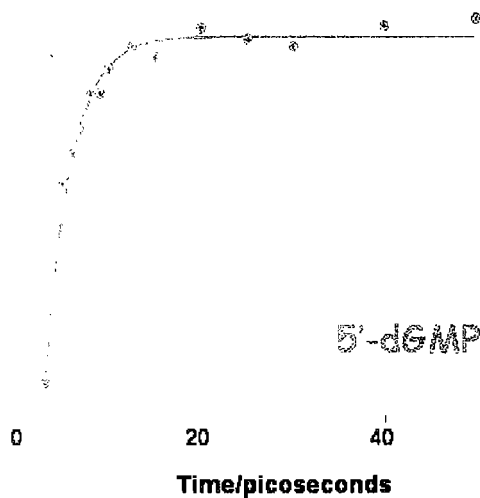


Orlov et al. - Tetra Lett 1976, vol 48, p4377; Fernando (LeBreton) PNAS 1998 vol 95 p5550; IP in solution - 4.47/4.9 eV to 5.57/5.5 eV

267 nm pump IR probe (1-50 ps)



267 nm excitation: Kinetics

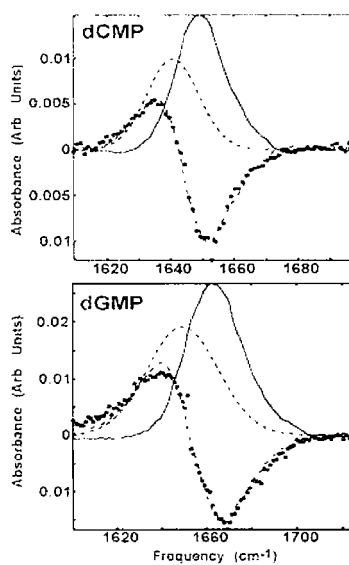


Base	lifetime
5'-dGMP	2.9 (± 0.2) ps
5'-dCMP	4.7 (± 0.3) ps
5'-dAMP	4.3 (± 0.2) ps
5'-TMP	2.2 (± 0.1) ps

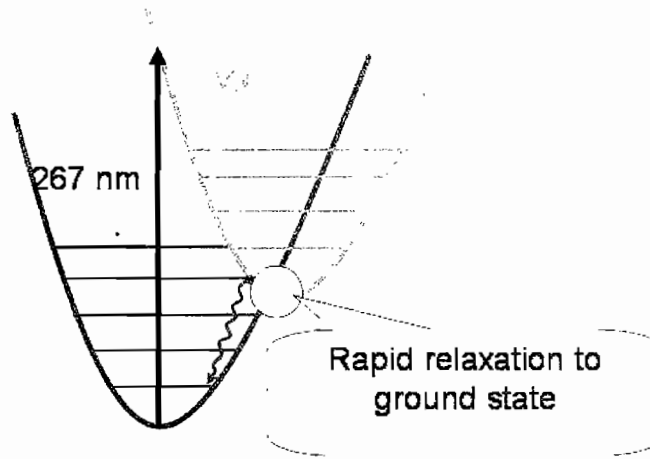
16 cm⁻¹ mode ($\tau = 400$ fs) of $\nu = 1 \rightarrow 2$ character

A. T. Krummel, P. Mukherjee and M. Zanni, *J. Phys. Chem. B.*, 2003, 107, 9165.

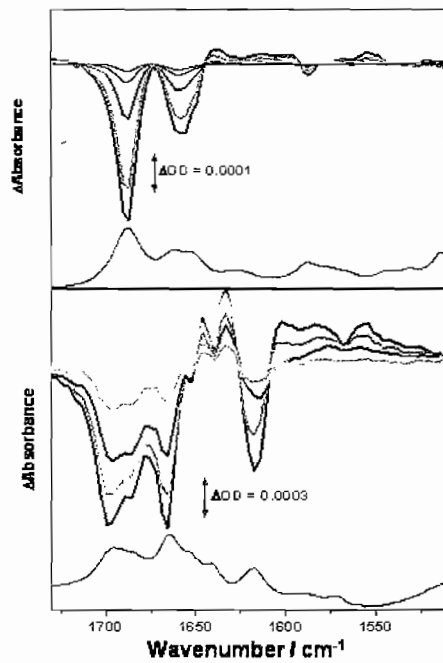
16 cm⁻¹ shift is identical to the 267 nm ps-TRIR study of β and α CMP



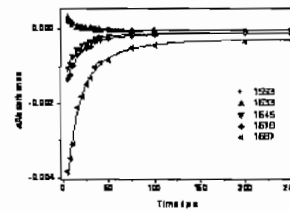
267 nm excitation: Mechanism



UV pump IR probe of poly-strands (1-1000 ps)



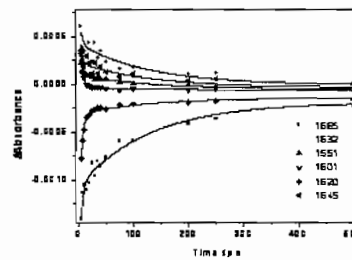
polydG-dC = polydG-dC



biexponential

$\tau = 12 \text{ \& } 50 \text{ ps}$

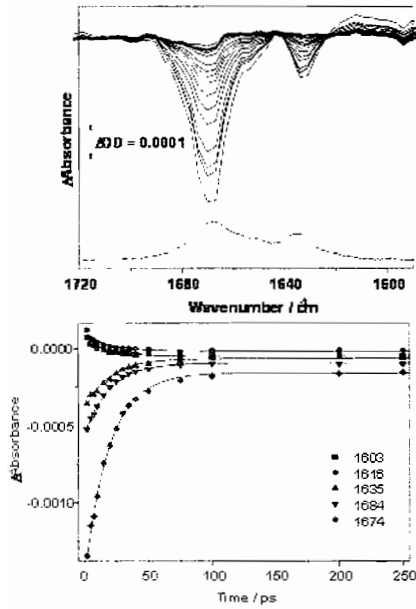
polydA-dT = polydA-dT



$\tau = 4 \text{ \& } 140 \text{ ps}$

UV pump IR probe of poly-strands (1-1000 ps)

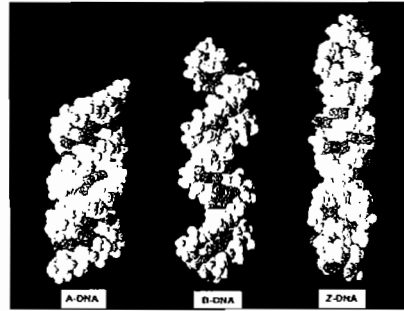
Z- polydG-dC • polydG-dC



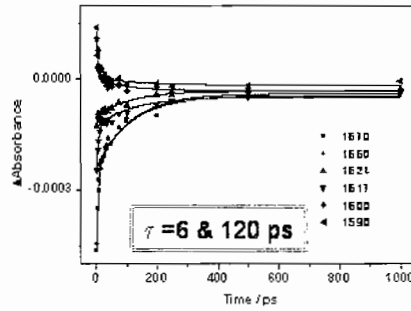
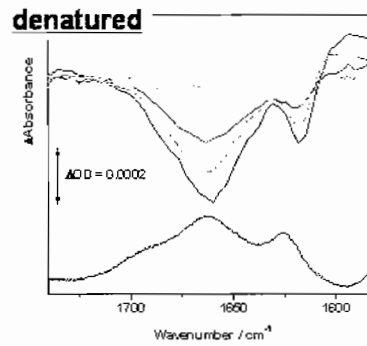
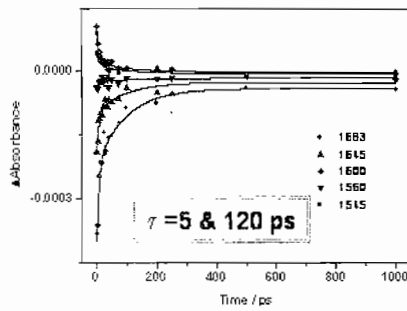
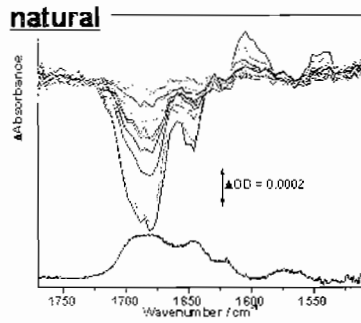
monoexponential

$$\tau = 19 \pm 3 \text{ ps}$$

- Solvation ?
- H-bonding?



UV pump IR probe CT DNA



267 nm excitation of DNA - Conclusions

- Electronic excitation leads to rapid S_1 to S_0
(in agreement with others)
- ps-TRIR used to directly observe vibrationally hot (S_0 , $\nu \geq 1$) ground state nucleobases following electronic excited state relaxation.
- Polynucleotide strands give complex spectra with longer-lived transients. Assignment is less clear

*M. K. Kuimova, J. Dyer, M. W. George, D. C. Grills, J. M. Kelly, P. Matousek, A. W. Parker, X. Z. Sun, M. Towrie and A. M. Whelan
Chem. Commun., 2005, (9), 1182 - 1184*

**Direct photoionisation of
DNA bases as a step
towards DNA
photodamage**

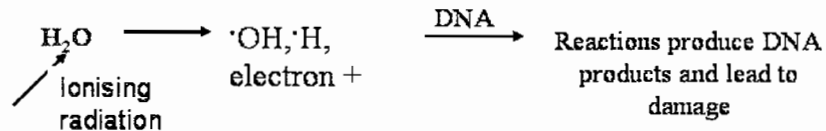
DNA Damage Through Radical Ion Formation

➤ Study the study the primary chemical processes leading to mutations (cancer) of DNA caused by strand breakages.

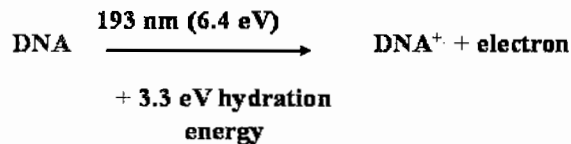
Key question does DNA act as a molecular wire?

➤ 2 processes of inflicting DNA damage

1. Ionising radiation creates radicals indiscriminate



2. Laser damage using 193 nm laser more precise - directly photoionize DNA



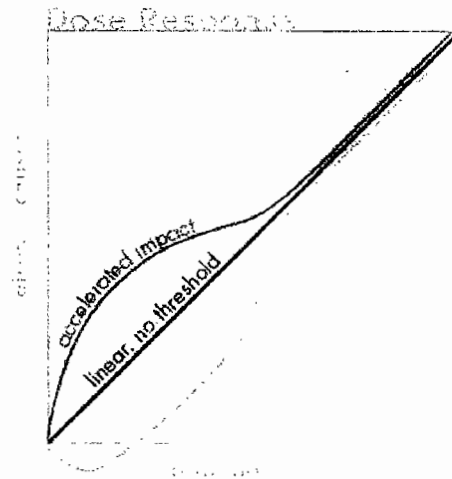
Consequence of Free Radical Damage

S. S. Wallace Free Rad Biol & Med (2002)

Lesion	Block to DNA polymerases	Lethal	Base inserted opposite in vitro	Mutagenic
Dihydrothymine	No	No		No
5-Formyluracil	No	No	A > G > C	T → C T → A
5-hydroxycytosine	No	No	G > A	C → T C → G
5-hydroxyuracil	No	No	A	C → T
8-Oxoguanine	No	No	C > A	G → T
Fapy-G	Yes	Yes	n.d.	No
8-oxoadenine	No	No	T >> G	Poor
α-Adenine	Yes	Yes	deletion	-1 deletion

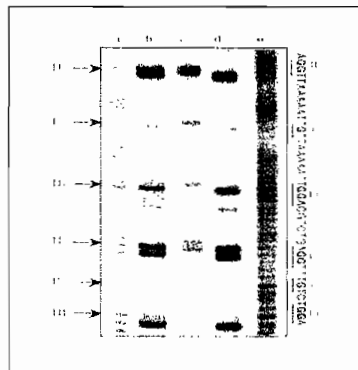
Linear no-threshold model

- The linear no-threshold model, LNT model, or LNTM is a model of the damage caused by ionizing radiation, and particularly the increased risk of cancer. It assumes that the response is linear and that this linear relationship continues to very small doses



<http://whyfiles.org/020radiation/index.php?g=4.txt>

DNA Damage - Base specific Sequence



Base sequence specificity of frank ssb (lane c, energy 5 mJ), Fpg excised damage (lane d, energy 2.5 mJ) and hot piperidine labile sites (lane b, 2.5 mJ) of the DNA 154 bp fragment ($A_5T_2GT_2A_5$) irradiated under aerobic conditions with 193nm light. Lanes a and e show Maxam-Gilbert G+C sequence markers and hydroxyl radical cleavage sites respectively.

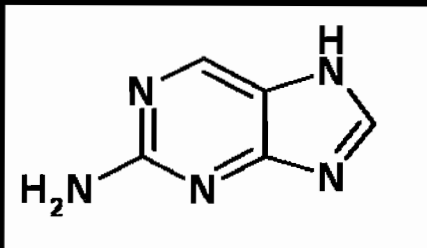
T. Melvin, S. Cunniffe, P.O'Neill, A. W. Parker & T. Roldan-Arjona
Nuc. Acids Res (1998) **21** 4935

- Study fundamental chemical events leading to DNA modification.
- 193 nm induces direct damage by monophotonic photionisation of bases.
- Strategic base sequence characterises where DNA breaks occur.
- Damage is enhanced at G sites indicating hole migration occurs (ease of oxidation $G > A > C > T$)
- Work shows that photoionisation results in a sequence dependent intra- *not* inter-strand charge migration of the radical cation of the nucleobases to G located with a few base pairs of the initial site of ionisation.

Direct DNA / bases ionisation



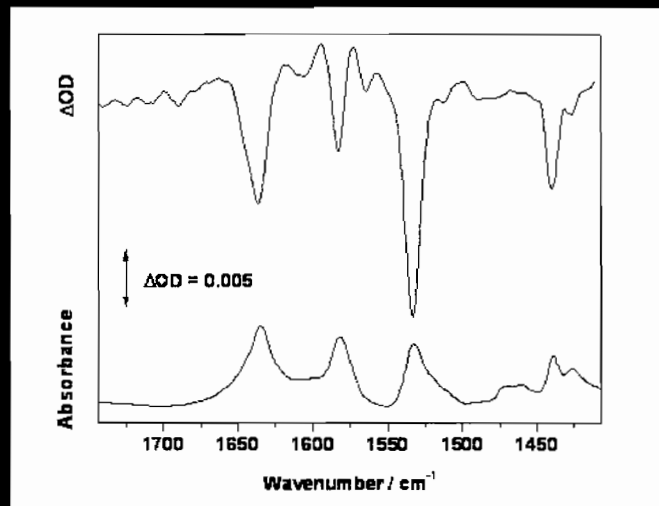
- 2-Aminopurine is Adenine analogue



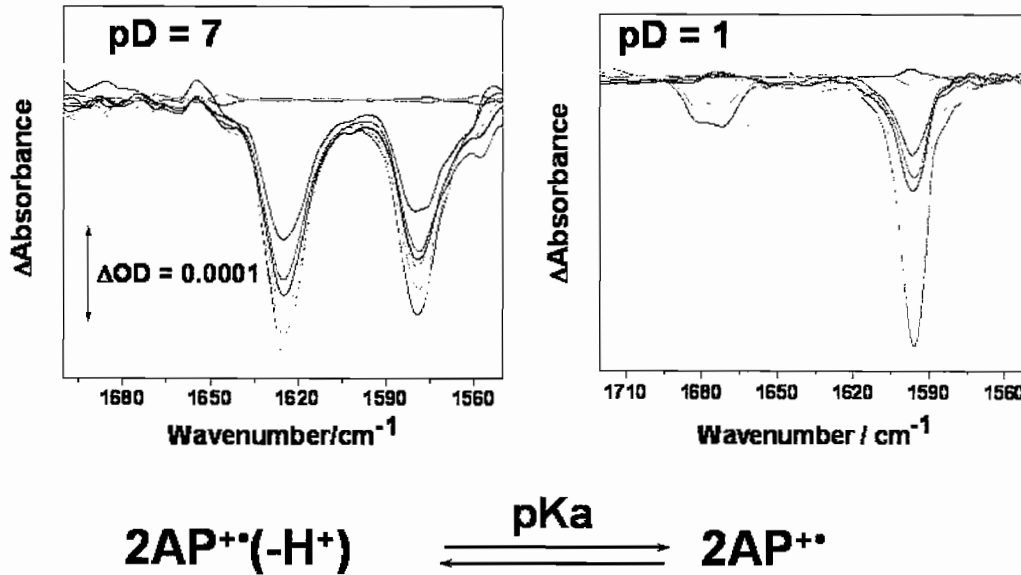
- 10 ns lifetime
- ionises at 308 nm
- participates in Watson-Crick base pairing

2-Aminopurine ionisation: 77K glass

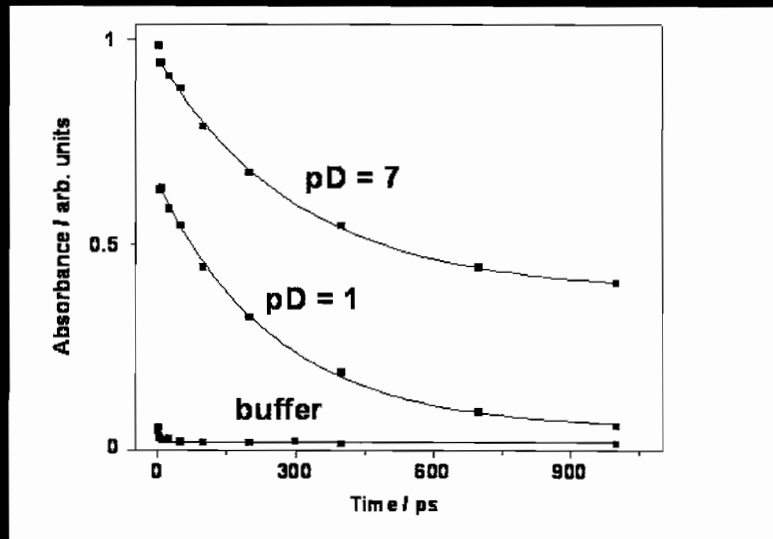
- use of 77K H₂O glass is established method for stabilising Base⁺ (EPR)



2-Aminopurine ionisation: solution

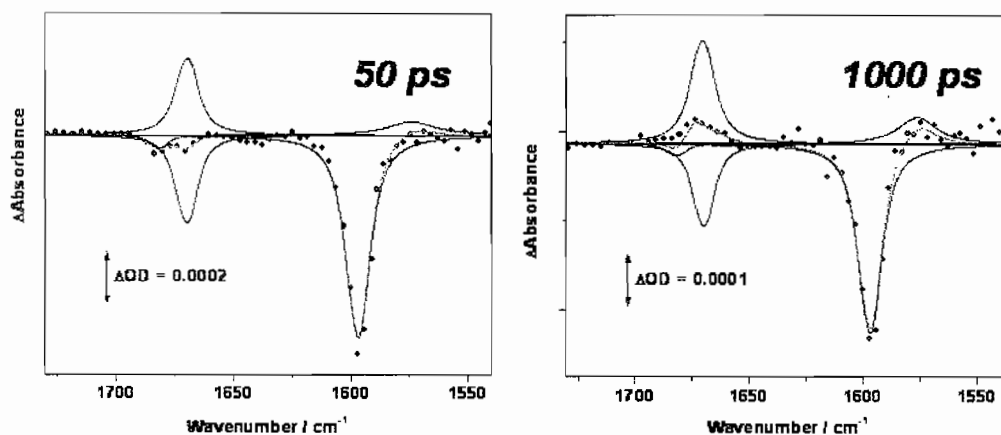


2-AP ionisation: monitoring e_{aq} @ 800 nm



- 2AP is ionised in biphotonic process at pD=7 and pD = 1

2-Aminopurine ionisation: pD = 1



- In neutral solution 2AP+• deprotonates in $< 2 \text{ ps}$
- Assignment supported by DFT calculations

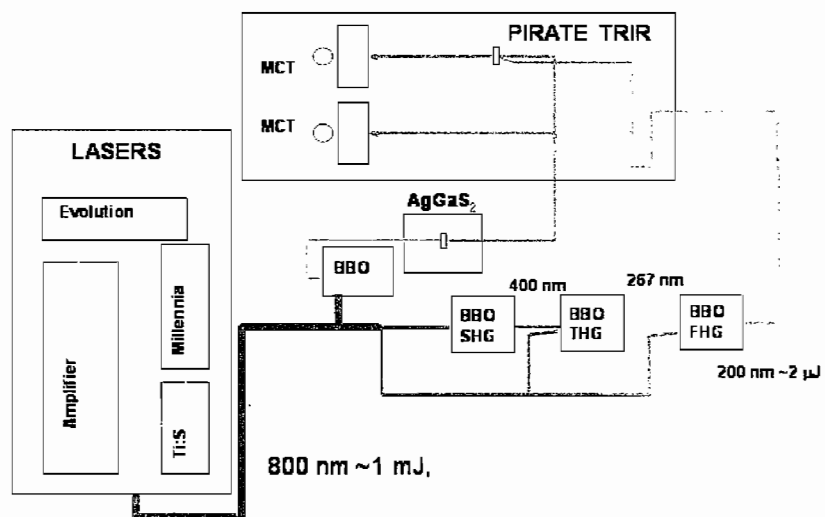
Natural DNA bases: ionisation

- G, A, C, T are ionised in one-photon process at 193 nm

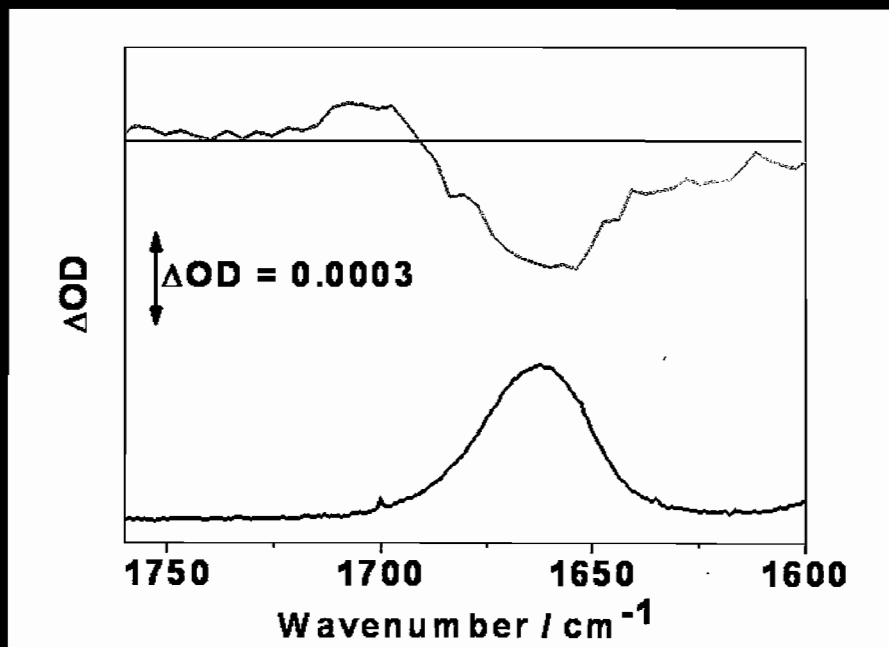


ps 200 nm excitation source was developed in RAL

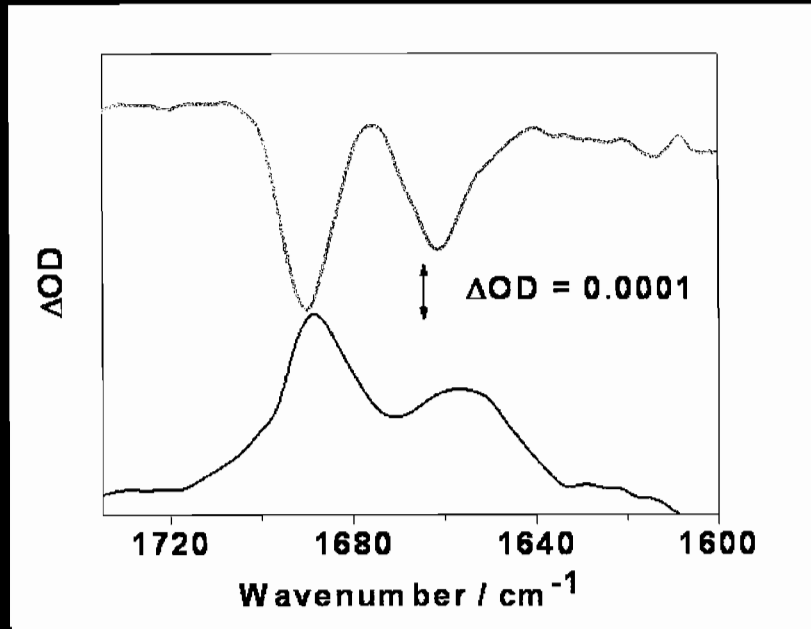
200 nm PUMP IR PROBE



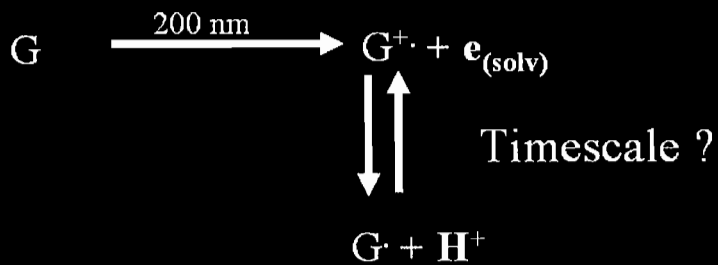
Guanine 200 nm ionisation: solution



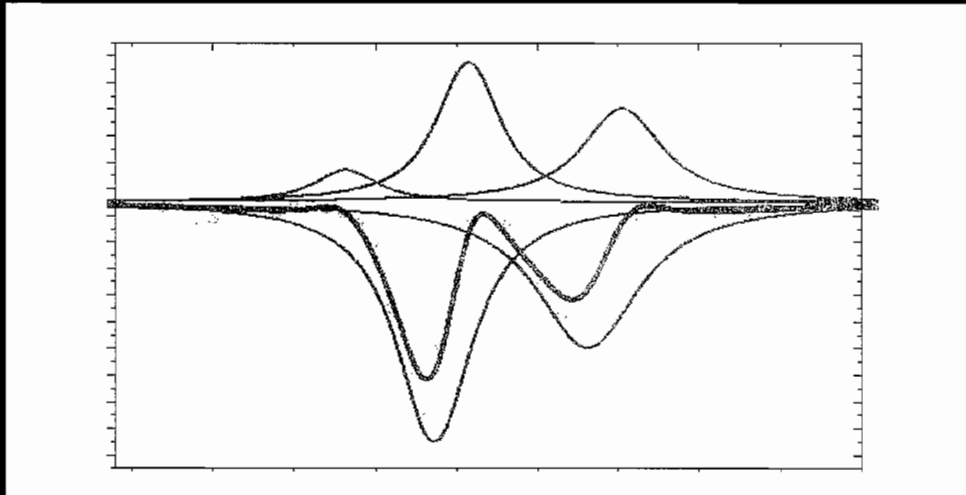
Poly(dGdC) ionisation: solution



Consequences of G Ionisation

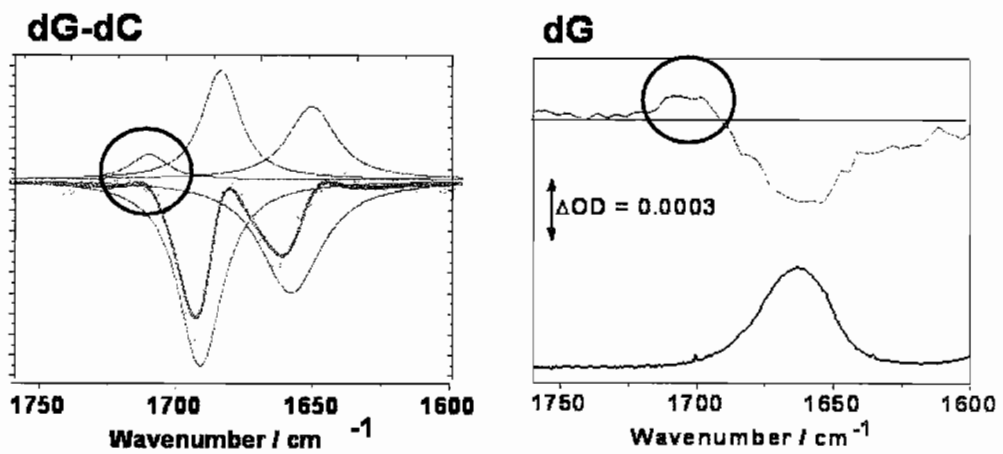


Poly(dGdC) ionisation: solution



Several transient bands are observed

DNA ionisation: solution



IR marker band of DNA damage

Ionisation yield monitoring e_{aq}

Substrate	Initial yield	Escape yield
NaCl	1	0.47
5'-GMP, pD = 7	0.03	0.03
5'-GMP, pD = 2	0.02	0.005
5'-GMP, pD = 13	0.04	0.03
5'-CMP	0.007	0.004
5'-AMP	0.005	0.003
5'-TMP	0.003	0.001
poly(dGdC)	0.05	0.03
CT DNA	0.05	0.03
50mM PO_4^{2-} buffer ^a	0.01	0.005

Photoionisation Conclusions

- 200 nm irradiation produces both excited states and photoionised species for G
- Excited states decay rapidly to vibrationally hot ground states analogous to 267 nm excitation
- C, A, T are not sufficiently photoionised
- Vibrational signature of G^{+*} is believed to be observed - characteristic of DNA damage
- Also, performed indirect studies using $[Co(NH_3)_4CO_3]NO_3$

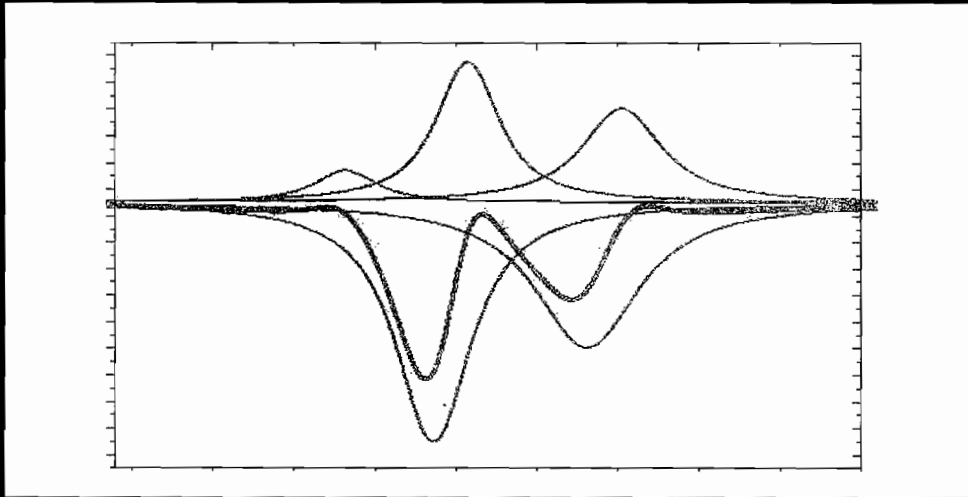
MK Kuimova, AJ. Cowan, P. Matousek, AW. Parker, XZ. Sun, M. Towrie, MW. George. PNAS 2006 103: 2150-2153

mjw23

\\server\name

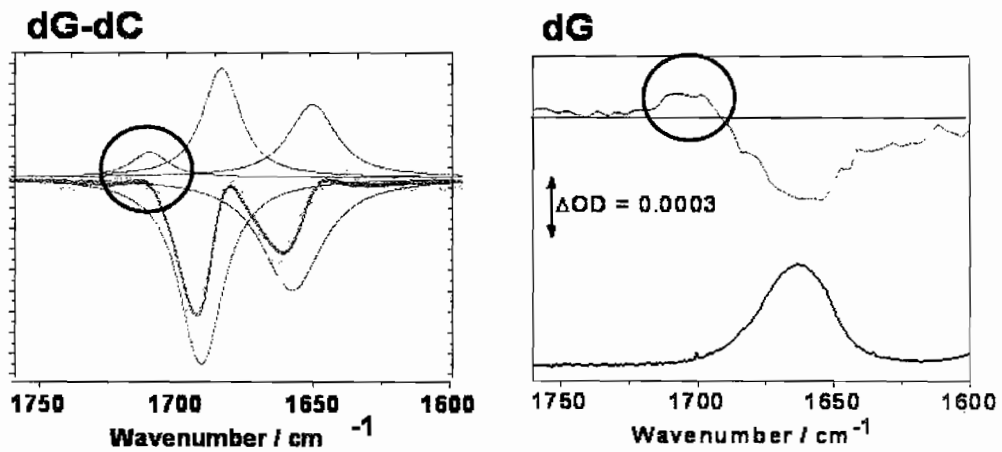
PSCRIPT Page Separator

Poly(dGdC) ionisation: solution



Several transient bands are observed

DNA ionisation: solution



IR marker band of DNA damage

Ionisation yield monitoring e_{aq}^-

Substrate	Initial yield	Escape yield
NaCl	1	0.47
5'-GMP, pD = 7	0.03	0.03
5'-GMP, pD = 2	0.02	0.005
5'-GMP, pD = 13	0.04	0.03
5'-CMP	0.007	0.004
5'-AMP	0.005	0.003
5'-TMP	0.003	0.001
poly(dGdC)	0.05	0.03
CT DNA	0.05	0.03
50mM PO_4^{2-} buffer ^a	0.01	0.005

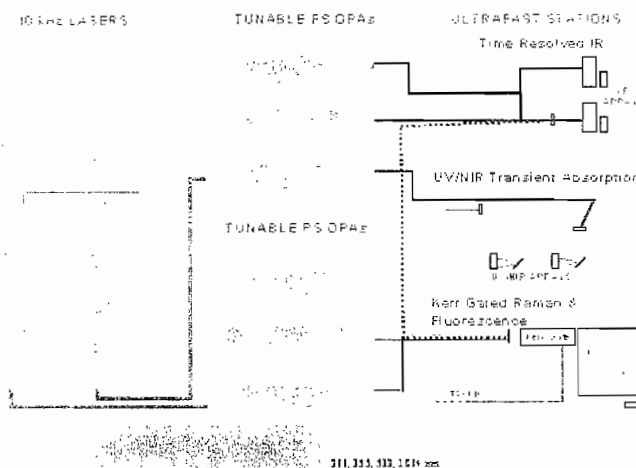
Photoionisation Conclusions

- 200 nm irradiation produces both excited states and photoionised species for G
- Excited states decay rapidly to vibrationally hot ground states analogous to 267 nm excitation
- C, A, T are not sufficiently photoionised
- Vibrational signature of G^{+*} is believed to be observed - characteristic of DNA damage
- Also, performed indirect studies using $[Co(NH_3)_4CO_3]NO_3$

MK Kuimova, AJ. Cowan, P. Matousek, AW. Parker, XZ. Sun, M. Towrie, MW. George. PNAS 2006 103: 2150-2153

ULTRA - details

A New Generation of High Repetition Rate Spectrometer



Time resolution
50 fs – 100 μ s

Spectral coverage
200 – 16000 nm

Techniques

- Infrared Absorption
- Raman
- 2D-IR
- TR - Absorption
- UV-NIR (50 fs)
- TR-Fluorescence < 1 ps

>60 fold faster acquisition than current state of the art - unsurpassed sensitivity.

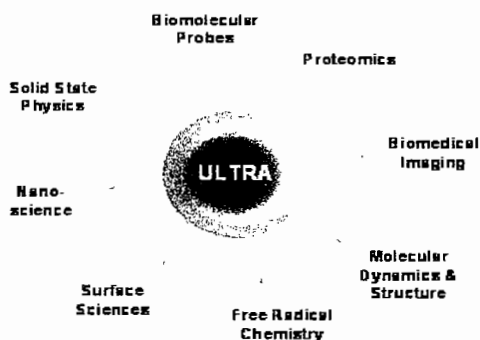
New LSF facility : ULTRA

Next Generation Laser Facility for Biological & Physical Sciences

World's most sensitive time-resolved vibrational spectrometer

Cross-disciplinary & Cross-departmental development
Leading edge technology (lasers, detectors)
Complementary to SRS, Diamond & 4GLS

Joint CCLRC/BBSRC funding (£1.78M/3yrs)



Examples of scientific applications

- **DNA Damage-**
What are the initial steps in cell mutation and repair mechanisms?
- **Protein function-**
Protein folding via time-resolved vibrational circular dichroism
- **Disease recognition-**
Novel non-invasive approaches to cancer and osteoporosis diagnosis

CCLRC, Nottingham, Cambridge, MRC, Leicester, Cranfield

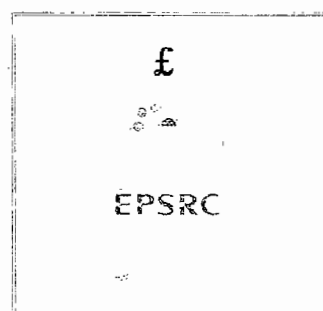
BIG Thanks to.....

F. Matusek, M. Towrie, Kate Ronayne, S. Botchway (CCLRC, RAL)

M. W. George, J. Dyer, D C. Grills, X. Z. Sun, M. K. Kuimova (Nottingham)

M. Kelly A. M. Whelan (Trinity, Dublin)

P. O'Neil, N. Melvin, S. Cunniffe, T. Roldan-Arjona (MRC, Harwell)



DFT analysis of Vibrational Spectra

Keith Refson
CCLRC Rutherford Appleton Laboratory

31 August 2000

RSC 2000 Vibrational Spectroscopy at Central Facilities



Contents

Contents

Experimental spectroscopies
Ab-initio lattice dynamics
Modelling of Neutron Inelastic Spectra
Modelling of IR and Raman Spectra

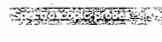
Experimental spectroscopies
Ab-initio lattice dynamics
Modelling of Neutron Inelastic Spectra
Modelling of IR and Raman Spectra

RSC 2000 Vibrational Spectroscopy at Central Facilities



Experimental spectroscopies

Spectroscopic probes



IR and Raman

- Laboratory scale equipment
- Sensitive to molecules in most many modes and frequencies
- Instrumental limitations on frequency range
- Only Zee selection phenomena are totally prohibited
- Anharmonicities contaminate spectra with multi-phonon peaks


INS

- Inelastic neutron scattering source
- Can probe large Q values in crystals or powder samples
- Can probe long scattering times
- Can complement Brillouin-Zone
- Not selection rule dependent

IXS

- X-ray photon source can sample entire BZ
- X-ray scattering sources have capability to probe spin waves
- Can probe high pressure cells
- X-ray scattering probe has long scattering time
- Inelastic I-V

IR provides general information on mode assignment can be used


 Home
 About
 News
Ab-initio spectroscopy
 Theory
 Software
 Publications
 Contact

Ab-initio lattice dynamics


Ab-initio spectroscopic calculations

- ☑ has no adjustable parameters
- ☑ can model the entire vibrational spectrum
- ☑ can perform mode assignments for vibrational (and electronic) spectra
- ☑ can fill in the missing step of *structure-property* relationship
- ☑ can help to understand *structure-process* relationships
- ☑ can provide *insight* into bonding

but

- ☑ accuracy of frequencies is usually a few percent
- ☑ usually limited to *harmonic* approximation (anharmonicity is possible, but not yet routinely)
- ☑ calculations can be computationally expensive for large or low-symmetry unit cells
- ☑ Prediction of IR intensities is easy, but peak shape hard
- ☑ Prediction of Raman intensities harder (but coming)
- ☑ Prediction of INS spectra already straightforward

RSC ©2016. V. Lational Spectroscopy at Central Facilities


 Home
 About
 News
Ab-initio lattice dynamics
 Theory
 Software
 Publications
 Contact

Ab-initio lattice dynamics

RSC ©2016. Vibration + Spectroscopy at Central Facilities



Ab-initio modelling

- Complete description of materials chemistry and physics given in principle by quantum mechanics of electrons and nuclei
- No adjustable or empirical parameters
- **All ab-initio methods are approximate**
- **Born-Oppenheimer Approximation** - Treat nuclei classically and assume motions are *adiabatically* in field of fixed ions.
- **Density Functional Theory** with local density or generalised gradient approximations (LDA, GGA) is method of choice for many atom/molecules
- Choice of pseudopotential (crystaline) or *cluster* (molecular) boundary conditions
- Many observables related to *charge* in T_0 when system is at T_0

Phase stability → phase with lowest T_0 is most stable at T_0
 Crystal Structure → given by the positions which minimise T_0
 Elastic Constants → $c_{ijkl} = \partial^2 T_0 / \partial \epsilon_{ij} \partial \epsilon_{kl}$
 Forces → on ions given by $\nabla_i T_0$
 Frequencies → of vibrational modes given by $\frac{\partial^2 T_0}{\partial Q^2}$

- Also have electronic properties → e.g. band-structures, densities of states



The CASTEP code

Full *ab-initio* density simulation code. Authors: M. Segall, J. A. Joannopoulos, D. J. Chadi, K. F. Hubert, P. J. Hasnip, K. Refson, J. Yates

- Plane-wave basis set and pseudopotential method
- Parallelised over FFT grid and k-points using MPI
- Optimised for maximum parallel scaling on HPC resources
- Ab-initio molecular dynamics using plane-wave functionals → LDA, PW91, PBE, PBE, HFX hybrid
- Electronic band structure
- Pseudopotential generation
- Equilibrium geometry (NVE, NVL and HPC) methods
- HPC optimisation of ions and cell
- Internal coordinates optimisation
- Linear scaling
- Geometry optimisation FID
- Transition State searching
- DFT and supercell calculations
- Quasiharmonic treatment
- IR intensities, Raman cross
- Dielectric Functions
- Born Effective Charges
- FWH for spectroscopic properties
- NMR Chemical shift
- Electric Field gradient tensor
- Mulliken population analysis
- Wannier functions
- Born-Oppenheimer DFT

Availability - Can be downloaded from Argonne National Materials Studio (URL: <http://www.ornl.gov/pub/castep>) or UK academic institutions (contact: castep@uk.fhfr.cam.ac.uk)



Phonons from density-functional theory

- 1. Phonons
- 2. Phonons from density-functional theory
- 3. Phonons from the Born-Huang theory
- 4. Phonons from the lattice dynamics
- 5. Phonons from the density-functional perturbation theory
- 6. Phonons from the density-functional perturbation theory
- 7. Phonons from the density-functional perturbation theory
- 8. Phonons from the density-functional perturbation theory
- 9. Phonons from the density-functional perturbation theory
- 10. Phonons from the density-functional perturbation theory

The *dynamical matrix* of lattice dynamics is given by

$$D^{\alpha\beta}(q) = \frac{1}{\sqrt{M^{\alpha}M^{\beta}}} \sum_{\mathbf{R}} \Phi_{\alpha\beta}(\mathbf{R}; q) e^{i\mathbf{q} \cdot \mathbf{R}}$$

$\Phi_{\alpha\beta}(\mathbf{R}; q)$ is the matrix of *force constants* of the lattice.

Several approaches to lattice dynamics

- ❑ **Frozen phonon method:** Create a structure perturbed by $2\pi/a$ (1D), $2\pi/a\sqrt{2}$ (2D) and evaluate energy as function of amplitude. Need supercell of size $\sim 1/a$ with q .
- ❑ **Finite Displacement method:** Perturb single ion $\pm 2\pi/a$ (1D), $\pm 2\pi/a\sqrt{2}$ (2D) gives row of dynamical matrix at q .
- ❑ **Supercell/Finite Displacement:** Use fact that $D^{\alpha\beta}(q)$ is periodic in q . Periodic replication of force constant matrix $\Phi_{\alpha\beta}(\mathbf{R}; q)$ in q -space. In large enough supercell, $D^{\alpha\beta}(q)$ can be extracted from q to $q + 2\pi/a$ above.
- ❑ **Density Functional Perturbation Theory**



Advantages of Density-Functional Perturbation Theory

- 1. Phonons
- 2. Phonons from density-functional theory
- 3. Phonons from the Born-Huang theory
- 4. Phonons from the lattice dynamics
- 5. Phonons from the density-functional perturbation theory
- 6. Advantages of Density-Functional Perturbation Theory
- 7. Advantages of Density-Functional Perturbation Theory
- 8. Advantages of Density-Functional Perturbation Theory
- 9. Advantages of Density-Functional Perturbation Theory
- 10. Advantages of Density-Functional Perturbation Theory

DFPT formalism gives $D^{\alpha\beta}(q)$ directly from perturbation theory (no linear response).

DFPT computes *first-order* KS orbitals (not the linear response) to the displacement of atoms with wavevector q in an electric field E . DFPT can calculate

- ❑ Born Effective Charges (aka atomic polar tensors)
- ❑ polarisability/dielectric permittivity
- ❑ LO-TO splitting
- ❑ infra-red reflectivity/absorption coefficients
- ❑ Raman tensor

LO-TO splitting and Born effective charges

- 1. LO-TO system LO and TO mode displacements indistinguishable in frequency in non-polar crystals LO mode freq higher than TO mode
- 2. Cause is additional restoring force due to macroscopic polarisation
- 3. Landau Lifshitz relation for cubic case $\frac{1}{\epsilon_0} = \frac{1}{\epsilon_\infty} + \frac{4\pi}{3} \frac{N}{\omega^2}$
- 4. Born effective charges using DFPT with $\epsilon_{\alpha\beta}$ representing electric field
- 5. Born effective charges also needs Born effective charges defined by

$$Z_{\alpha\beta}^* = \frac{1}{\omega^2} \left(\frac{\partial^2 \epsilon_{\alpha\beta}}{\partial u_\alpha \partial u_\beta} - \frac{\partial \epsilon_{\alpha\beta}}{\partial u_\alpha} \right)$$

- 6. LO-TO splitting per unit cell caused by displacement of atoms in direction of electric field on atom by microscopic electric field

Lattice dynamics in CASTEP

- 1. CASTEP uses Gougeon's variational formulation of DFPT
- 2. Collaborators S. J. Clark and P. R. Tulip, University of Exeter (s.j.clark@ex.ac.uk, p.r.tulip@ex.ac.uk)
- 3. Fully automated space-group symmetry of crystal cell
 - ◆ Only independent elements of $\epsilon_{\alpha\beta}$ calculated using LR summation and propagated to dependent elements
 - ◆ k-point sampling of Brillouin-zone performed using k-point set irreducible under symmetry of perturbation
- 4. Almost identical approach yields ϵ^{-1} , ϵ^{∞} and ϵ^0
 - ◆ Currently restricted to insulators and normal-conducting s -band semiconductors
- 5. ϵ^0 splitting calculated
- 6. Phonon masses
- 7. DFPT model for thermal expansion programs (a.c. 1998)
- 8. Phonon mass ratios under development
- 9. Phonon dispersion coefficients dispersion or LOOS
- 10. Phonon self-diffusion - supercell method for metals



- 1. Introduction
- 2. TOSCA spectrometer
- 3. Neutron diffraction
- 4. Modelling of Neutron Inelastic Spectra**
- 5. Ammonium Fluoride
- 6. Ammonium Fluoride
- 7. Ammonium Fluoride
- 8. Ammonium Fluoride
- 9. Ammonium Fluoride
- 10. Ammonium Fluoride
- 11. Ammonium Fluoride
- 12. Ammonium Fluoride
- 13. Ammonium Fluoride
- 14. Ammonium Fluoride
- 15. Ammonium Fluoride
- 16. Ammonium Fluoride
- 17. Ammonium Fluoride
- 18. Ammonium Fluoride
- 19. Ammonium Fluoride
- 20. Ammonium Fluoride

Modelling of Neutron Inelastic Spectra

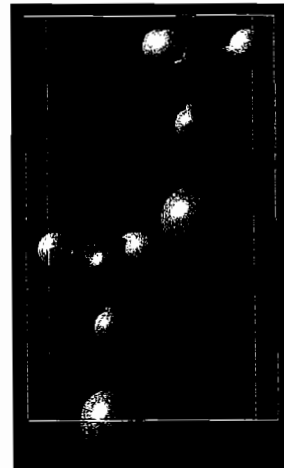
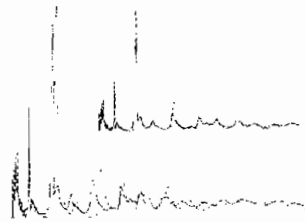
RSC, 2006. Virtual Spectroscopy at Central Facilities



Ammonium Fluoride

- 1. Introduction
- 2. TOSCA spectrometer
- 3. Neutron diffraction
- 4. Modelling of Neutron Inelastic Spectra
- 5. Ammonium Fluoride**
- 6. Ammonium Fluoride
- 7. Ammonium Fluoride
- 8. Ammonium Fluoride
- 9. Ammonium Fluoride
- 10. Ammonium Fluoride
- 11. Ammonium Fluoride
- 12. Ammonium Fluoride
- 13. Ammonium Fluoride
- 14. Ammonium Fluoride
- 15. Ammonium Fluoride
- 16. Ammonium Fluoride
- 17. Ammonium Fluoride
- 18. Ammonium Fluoride
- 19. Ammonium Fluoride
- 20. Ammonium Fluoride

- ❑ NH_4F is one of a series of ammonium halides studied in the TOSCA spectrometer (Collab Mark Adams (ISIS))
- ❑ Structurally isomorphic with ice Ih
- ❑ INS spectrum modelled using A-CLIMAX software (A. J. Ramirez Cuesta, ISIS)
- ❑ Predicted INS spectrum in mostly excellent agreement with experiment
- ❑ NH_4 libration modes in error by $\pm 5\%$
- ❑ Complete mode assignment achieved

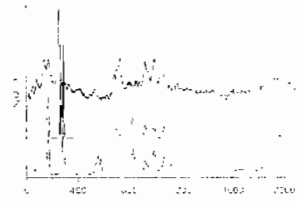
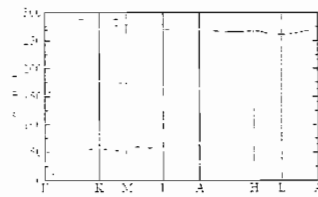
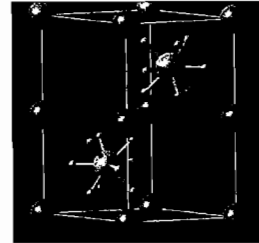


RSC, 2006. Virtual Spectroscopy at Central Facilities

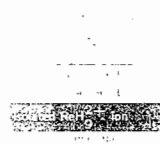
Bismuth Rhenium Hydride



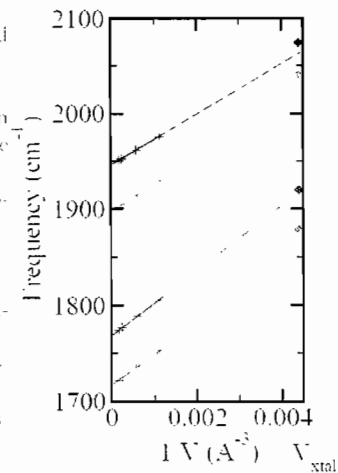
- with S. F. Parker, ISIS facility, KAL
- BiReH₆ with unusual ReH₆³⁺ ion has very high molar hydrogen content
- INS spectrum modelled using A-CLIMAX software (A. J. Ramirez-Cuesta, ISIS)
- Predicted INS spectrum in mostly excellent agreement with experiment
- LO-TO splitting essential to model INS
- Librational modes in error (c.f. NH₃F)
- Complete mode assignment achieved



Isolated ReH₆³⁺ ion



- Re ions in cubic coordination on isolated ReH₆³⁺ ion give point to INS
- Repeat isolated ion using CASTEP
- CASTEP model periodic array of ions in charged lattice. Exp. V scaling and take $V_{\text{ion}} \rightarrow V$ limit
- $V_{\text{ion}} \rightarrow V$ frequencies in agreement with isolated ion modes
- Large c.f. (~150 cm⁻¹) crystal field shift
- Can also extrapolate down to V_{xtal}
- Extrapolated ion freqs are very close to A-point crystal freqs
- Crystal field shift is directly \propto periodic volume error
- Anion modes completely insensitive to presence of cation



H-Storage materials MgH₂

- MgH₂ is one of highest wt % candidate hydrogen storage materials
- H₂ desorption reaction only at high T in bulk MgH₂, but ball mill-d and then microstructured material promising
- Spectroscopy will be key tool investigating microstructured material.
- INS spectra measured on TOSCA by A. J. Ramirez Cueto.
- Light materials have large thermal expansivity and athermal limit magnitude → need *quasi-harmonic free energy* minimum
- F evaluated using phonon DOS calculation at range of volumes
- LDA lattice parameter in better agreement with expt than GGA

LDA	4.55Å	GGA	4.60Å
Expt	4.517Å		

MgH₂ Energy and QH Free energy

RSC 2006, Vibration Spectroscopy at Central Facilities

MgH₂ INS and lattice dynamics

AB Predicted spectrum computed from *AB* adjusted frequencies

RSC 2006, Vibration Spectroscopy at Central Facilities

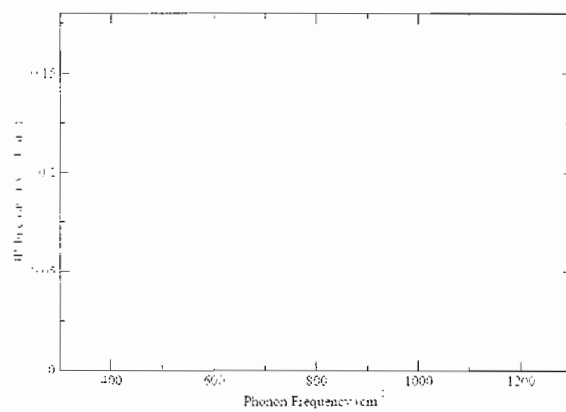
Modelling of IR and Raman Spectra

Research in Spectroscopy and Crystallography

2013

16

IR spectrum of α -quartz



- Straight line fit to compute peak areas
- Peak shape modelling depends on sample and experimental variables
- Multiphonon and overtone terms less straightforward

Research in Spectroscopy and Crystallography

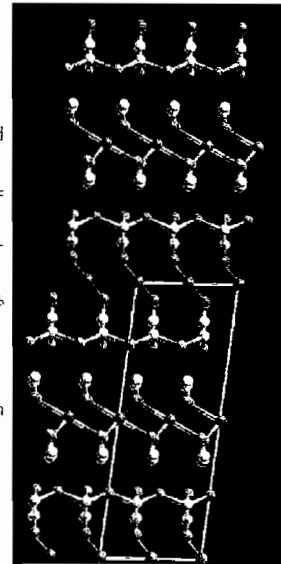
2013



High-pressure phase transition in clinocllore

- 1. Introduction
- 2. Background
- 3. Methods
- 4. Results
- 5. Discussion
- 6. Conclusions
- 7. Acknowledgements
- 8. References
- 9. Appendix
- 10. High-pressure phase transition in clinocllore

- Collaborators Dr Andrew Jephcoat (DLS) and Dr Annette Klepepe (Oxford)
- Clinocllore is H-rich chlorite which may be water-bearer in subduction zones
- Structure is mixed-layers of mica-like phyllosilicate and (Mg, Al) brucite
- Crystal structure of synthetic clinocllore is monoclinic $C2/m$
- X-ray powder diffraction and Raman spectroscopy show a phase transition at 10GPa
- X-ray powder data for high-pressure phase can not be indexed for structure determination.



RSC 2006 Vibrational Spectroscopy at Central Facilities

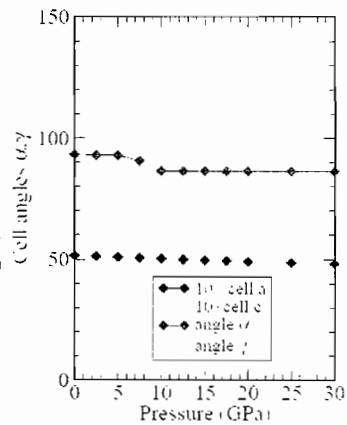


Ab-initio DFT results for Clinocllore

- 1. Introduction
- 2. Background
- 3. Methods
- 4. Results
- 5. Discussion
- 6. Conclusions
- 7. Acknowledgements
- 8. References
- 9. Appendix
- 10. Ab-initio DFT results for Clinocllore

- Model Al/Si disorder using either fully ordered or all-Si approximations
- Optimize co-ordinates and simulation cell under applied pressure
- Both models show a phase transition at ~10GPa.
- Characterised by shear and compression along c-axis; change in inter-layer registration from Type IIIb stacking.
- new phase is still monoclinic
- *ab-initio* prediction of new high pressure crystal structure

DFT lattice parameters of clinocllore

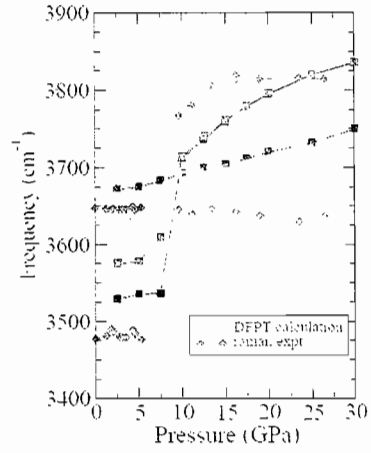


RSC 2006 Vibrational Spectroscopy at Central Facilities

Vibrational Spectroscopy

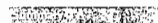


- 33 Experiment and calculated OH stretch frequencies show spread of 200 cm^{-1} in 3700 cm^{-1} range. Need resolution of order 1% for meaningful comparison
- 37 Both calculations and expt show upward trend of order of 100 cm^{-1} and compression of range
- 38 Same pattern of frequency shifts across transition observed in calculation as experiment
 - 39 support for hypothesis that high-P phase predicted in calculation is true structure
- 38 Analysis of eigenvectors shows that highest freq in low-P phase becomes lowest in high-P. Mode is silicate layer OH stretch
- 38 Modes with a upshift are hydroxide layer OH stretch



Summary

- 39 Density functional dynamics is a powerful tool for modelling experimental vibrational spectra of all kinds
- 39 Accuracy is usually a few percent except where Harmonic approximation breaks down
- 39 Can treat molecules, metals, insulators and semiconductors
- 39 Crystal dispersion is essential for modelling INS spectra of molecular crystals
- 39 Eigenvector capability adds vital *structure-property* link
- 39 Combined DFT modelling and experiment gives better *understanding*





Rutherford Appleton Laboratory



Vibrational Spectroscopy with Neutrons: Catalysts, Hydrides and Polyethylene

Stewart F. Parker

ISIS Facility

Joint IRDG and RSC Molecular Spectroscopy meeting, 31st August 2006



Rutherford Appleton Laboratory

Menu

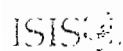
**Introduction: neutrons
vibrational spectroscopy with neutrons**

Catalysis: adsorbed states of hydrogen on platinum fuel cell catalysts

Hydrides and hydrogen storage: $\text{Rb}_2[\text{PtH}_6]$ and $\text{Ba}[\text{N}_2]$

Polyethylene

Conclusions



Neutrons: the subtle probe

Neutrons are **NEUTRAL particles**. They

- are highly penetrating
- can be used as non-destructive probes
- can be used to study sample in severe environments
- they cause little damage to the sample.

Neutrons have a **MAGNETIC moment and a SPIN**. They can be

- used to study microscopic magnetic structures and fluctuations
- polarised, thereby enhancing their selective power to magnetic features
- used to develop magnetic materials

The **ENERGIES and WAVELENGTHS** of thermal neutron are "just right"

- molecular vibrations and lattice modes.
- magnetic fluctuations.
- dynamic of atomic motion (e.g., diffusion)

Neutrons "see" **NUCLEI**, so they

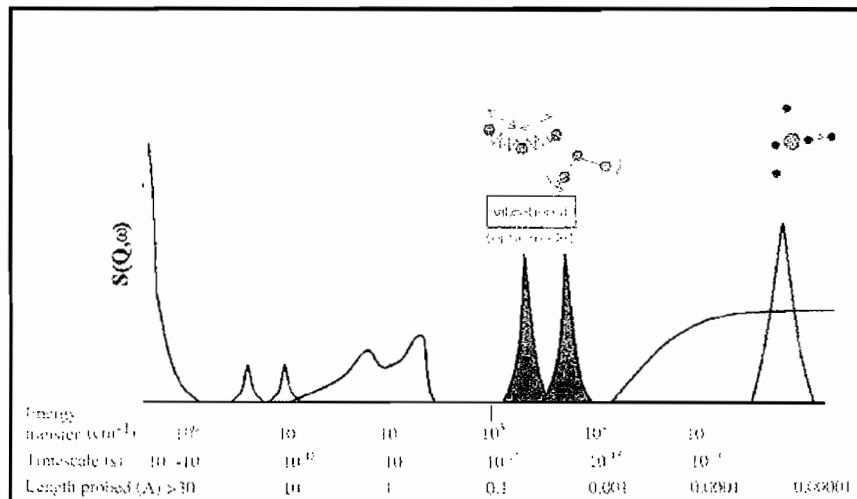
- are sensitive to light atoms.
- can be exploited for **ISOTOPIC SUBSTITUTIONS**. In particular
- the neutron contrast can be varied selectively for important species such as **HYDROGEN**).



Neutrons tell you where atoms are and how they are moving!

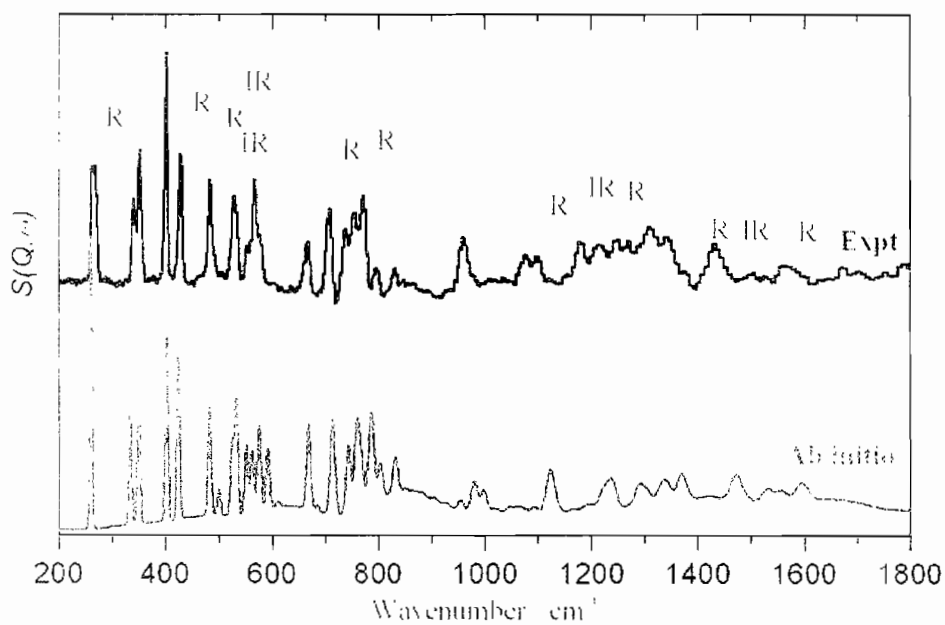
ISIS

Inelastic neutron scattering



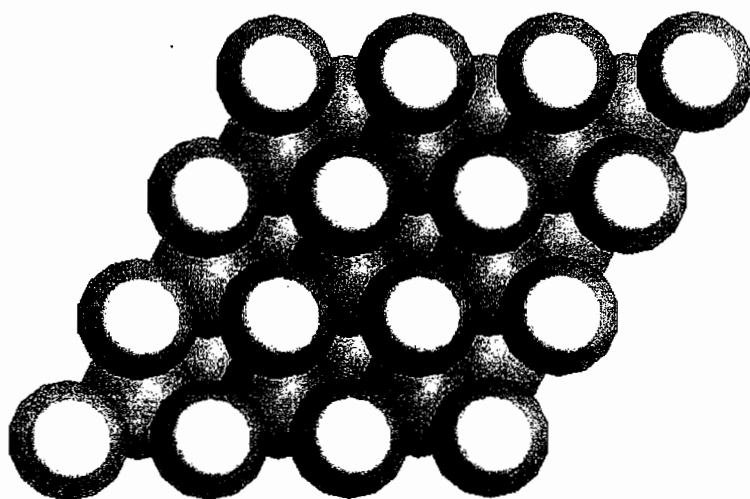
ISIS

C₆₀



ISIS

Adsorbed states of hydrogen

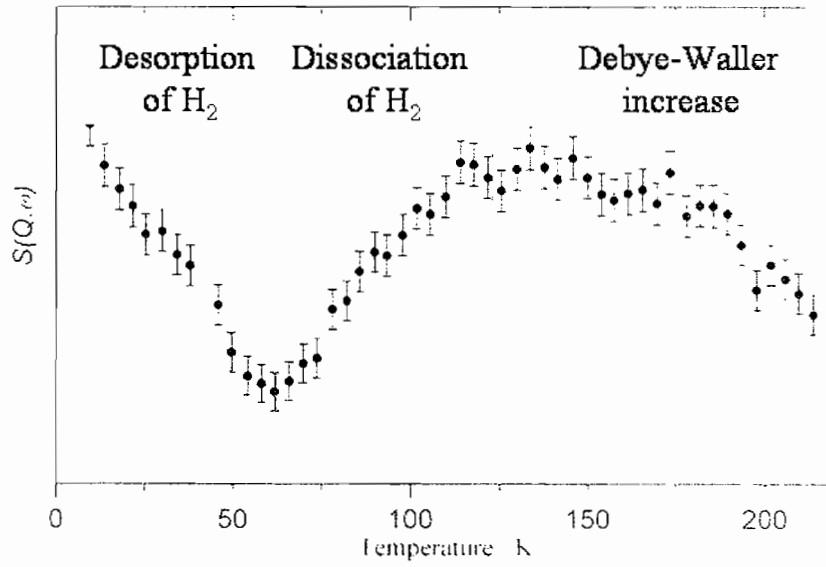


S.F. Parker, C.D. Frost, M. Telling, P. Albers, M. Lopez and K. Seitz
Characterisation of the adsorption sites of hydrogen on Pt/C fuel cell catalysts
Catalysis Today, 114 (2006) 418-421.

ISIS

Dissociation of H₂ on a Pt(50%)/C fuel cell catalyst by QENS

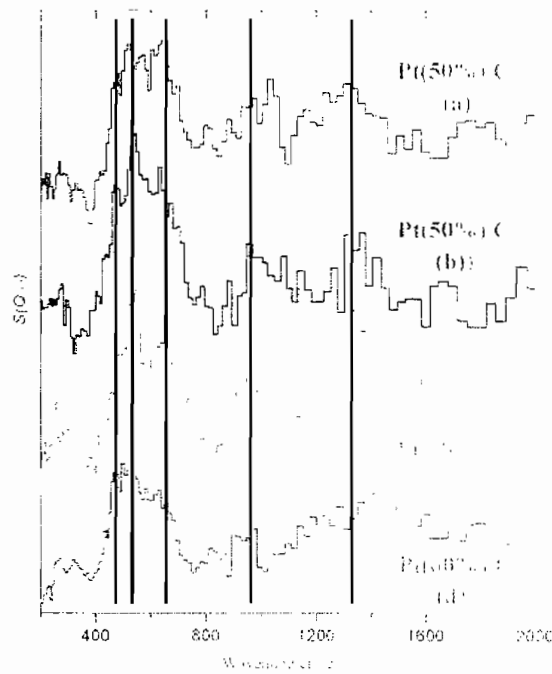
ISIS Muon Application Laboratory



ISIS

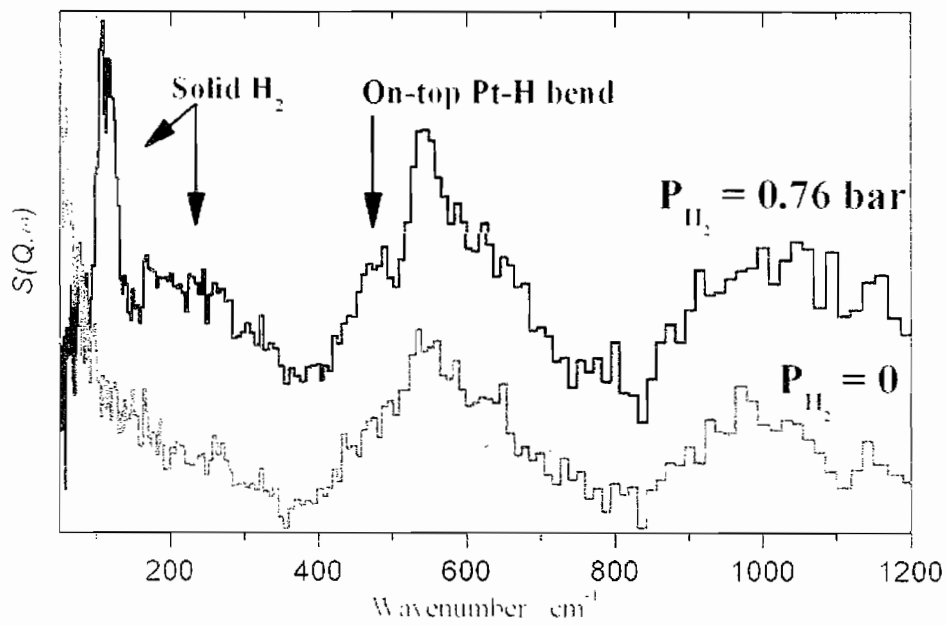
Adsorbed hydrogen on Pt/C fuel cell catalysts

ISIS Muon Application Laboratory



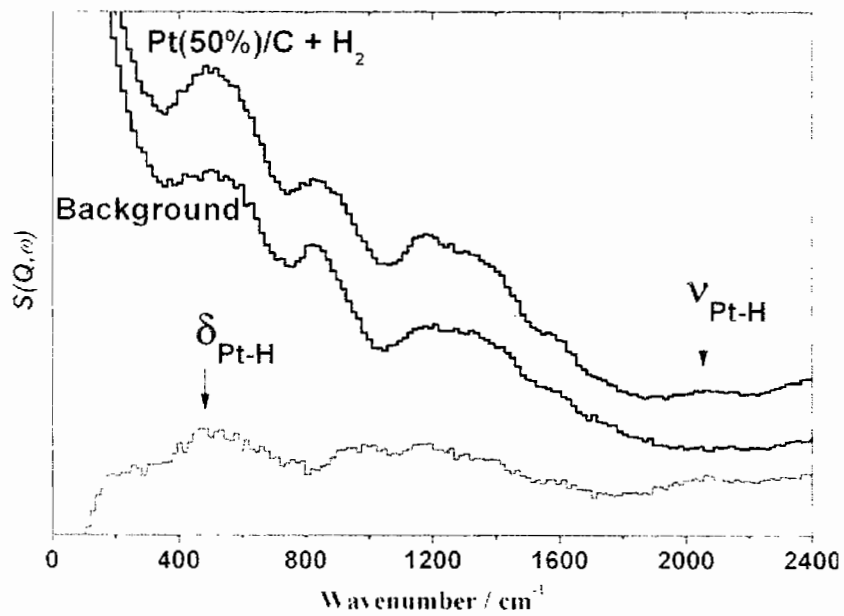
ISIS

Fuel cell catalyst: Pt(58%)/C



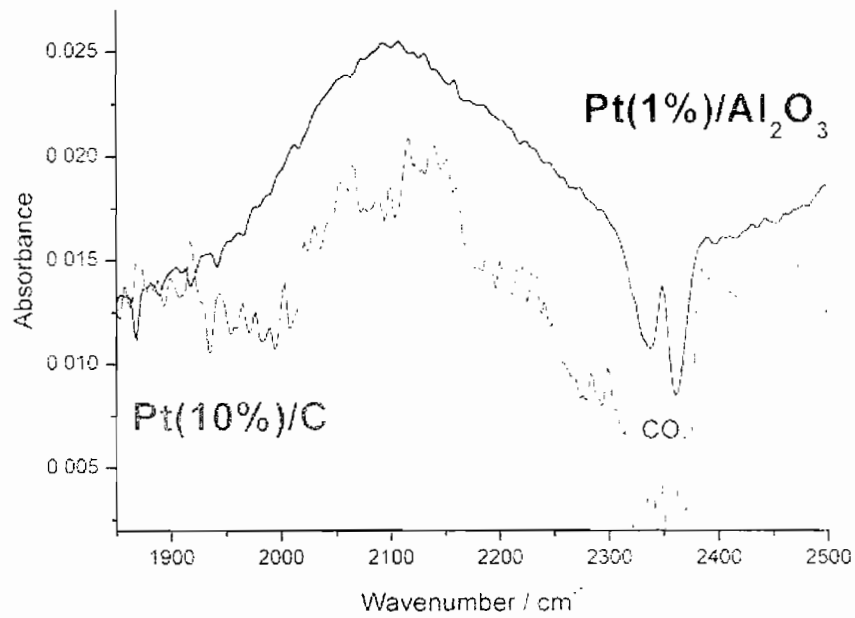
ISIS

The on-top hydrogen

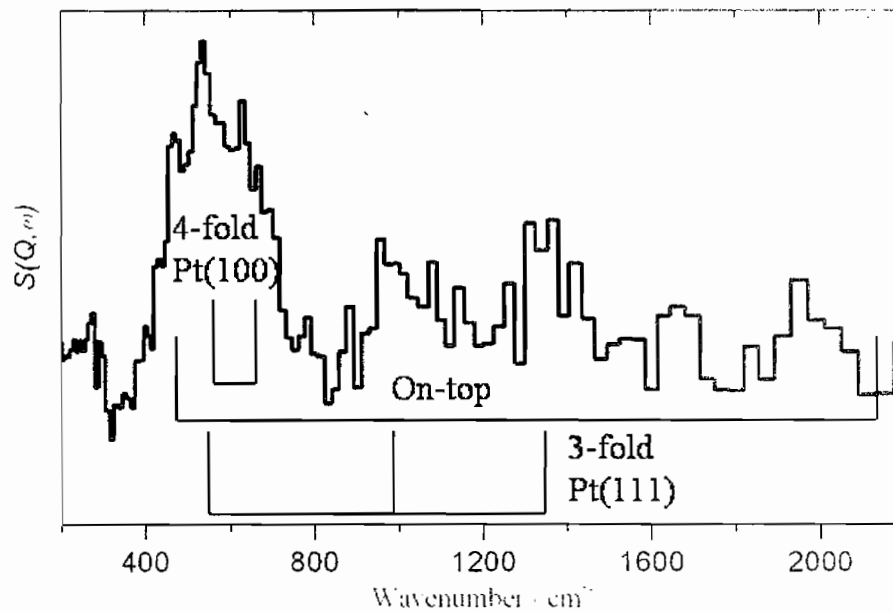


ISIS

IR of Pt-H stretch of on-top



Summary of assignments



Hydrides and hydrogen storage

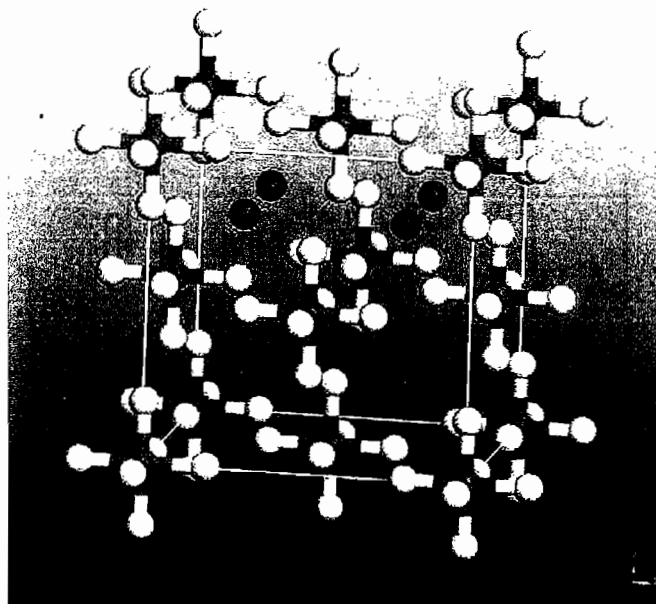
S. F. Parker, S. M. Bennington, A. J. Ramirez-Cuesta, G. Auffermann, W. Bronger, H. Herman, K. P. J. Williams and T. Smith

Inelastic neutron scattering, Raman spectroscopy and periodic-DFT studies of Rb_2PtH_6 and Rb_2PtD_6

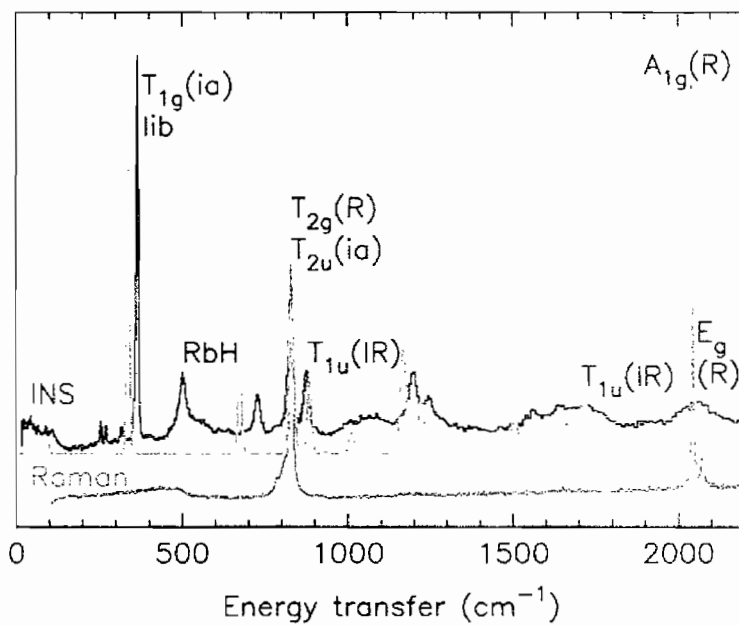
J. Am. Chem. Soc., 125 (2003) 11656-11661.

Stewart F. Parker, Jon W. Taylor, Keith Refson and Gudrun Auffermann

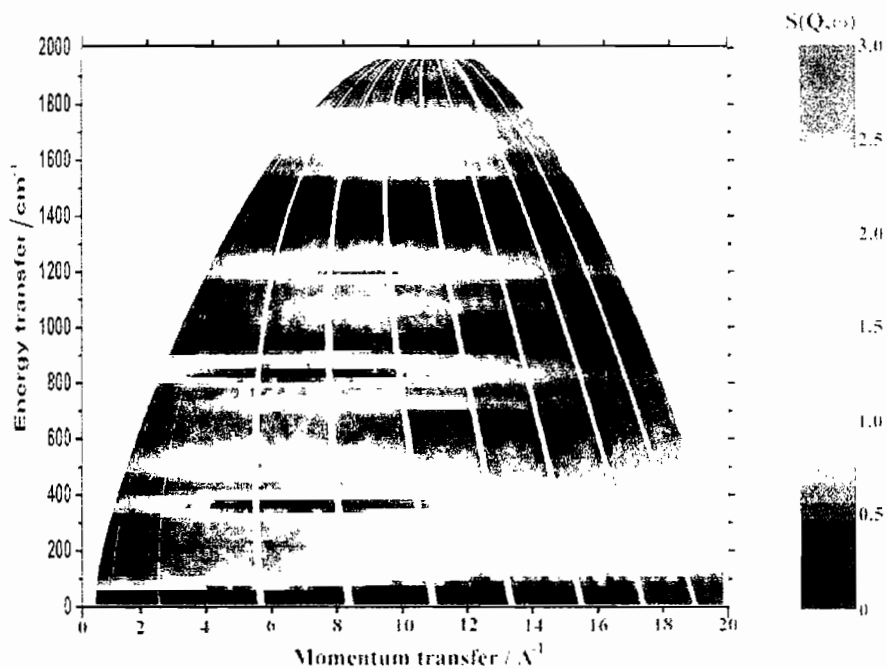
Spectroscopic and ab initio characterisation of alkaline earth nitrides and diazenides: detection of the N=N stretch



INS and Raman spectra of O_h $[\text{PtH}_6]^{2-}$



$\text{Rb}_2[\text{PtH}_6]$ on MARI



**Comparison of properties of M_2PtH_6 . (M = Li, Na, K, Rb, Cs).
Experimental values in parentheses.**



ISIS - The neutron source

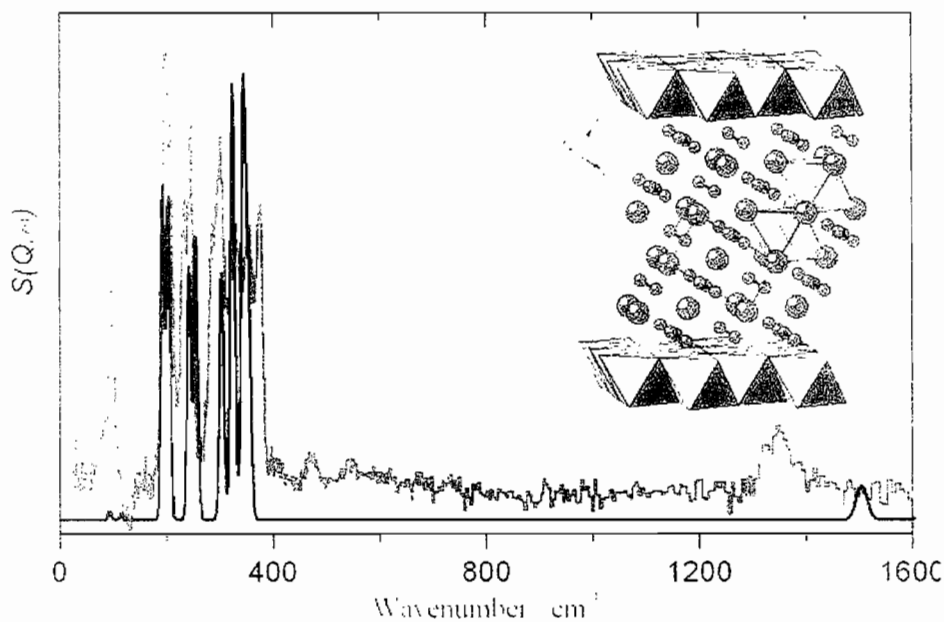
Property	Li	Na	K	Rb	Cs	Gas phase
Lattice parameter (Å)	6.564 (6.55)†	7.1716 (7.3410)	8.2002 (8.1399)	8.6222 (8.5369)	8.9503 (8.9681)	
Pauling ionic radius M (Å)	(0.60)	(0.95)	(1.33)	(1.48)	(1.69)	
Lattice energy (kJ mol ⁻¹)	2223	1966	1755	1665	1577	
Pt-H / (Å)	1.639	1.641 (1.615)	1.644 (1.640)	1.646 (1.629)	1.647 (1.641)	1.678
M-H / (Å)	2.354	2.540 (2.74)	2.927 (3.12)	3.091 (3.06)	3.219 (3.52)	
ν_1 Pt-D stretch A_{1g} (cm ⁻¹)	1673	1651 (1491)	1604 (1471)	1588 (1466)	1577	1387
Charge on Pt	-1.718	-1.777	-1.601	-1.511	-1.422	-1.860
Charge on M	+0.370	+0.598	+0.698	+0.703	+0.536	
Charge on H	+0.163	+0.097	+0.034	+0.018	+0.058	-0.232

ISIS

Ba[N₂] - metallic

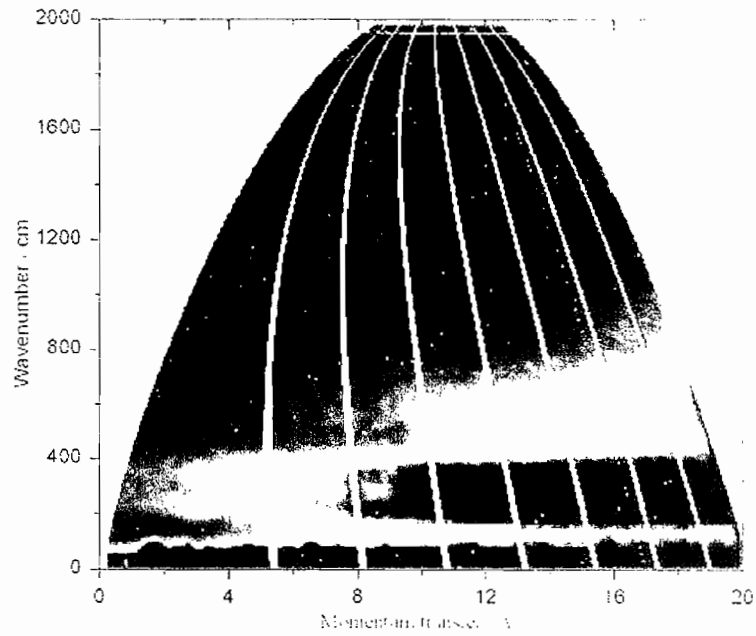


ISIS - The neutron source



ISIS

Ba[N₂] on MARI

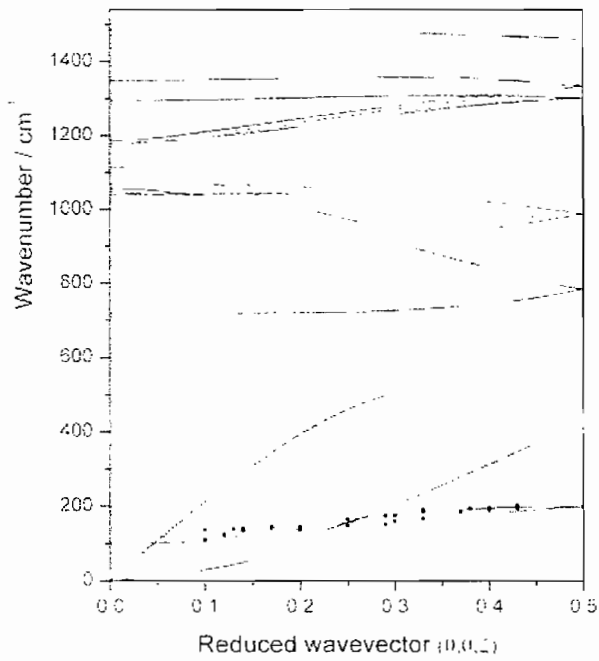


Polyethylene

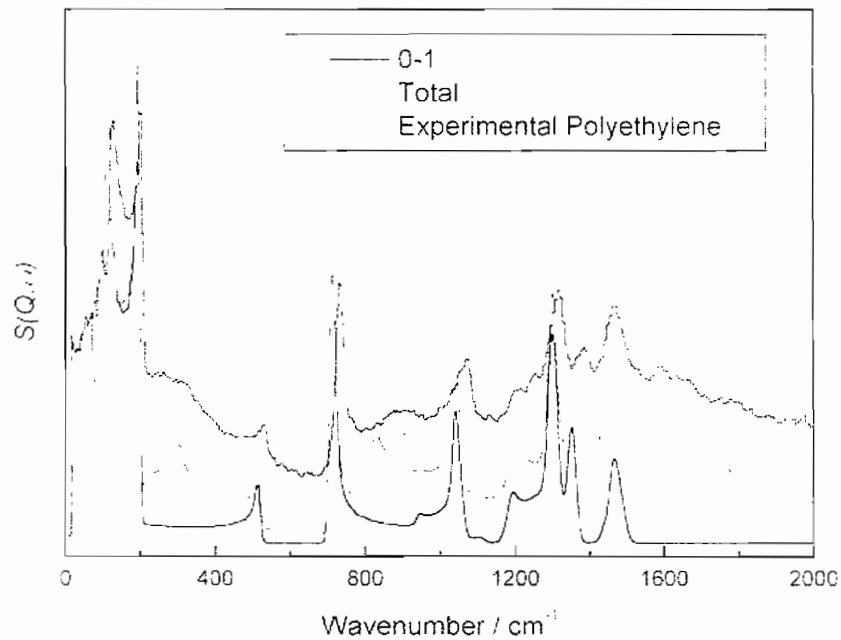


G.D. Barrera, S.F. Parker, A.J. Ramirez-Cuesta, and P.C.H. Mitchell
The vibrational spectrum and ultimate modulus of polyethylene
Macromolecules, **39** (2006) 2683-2690.

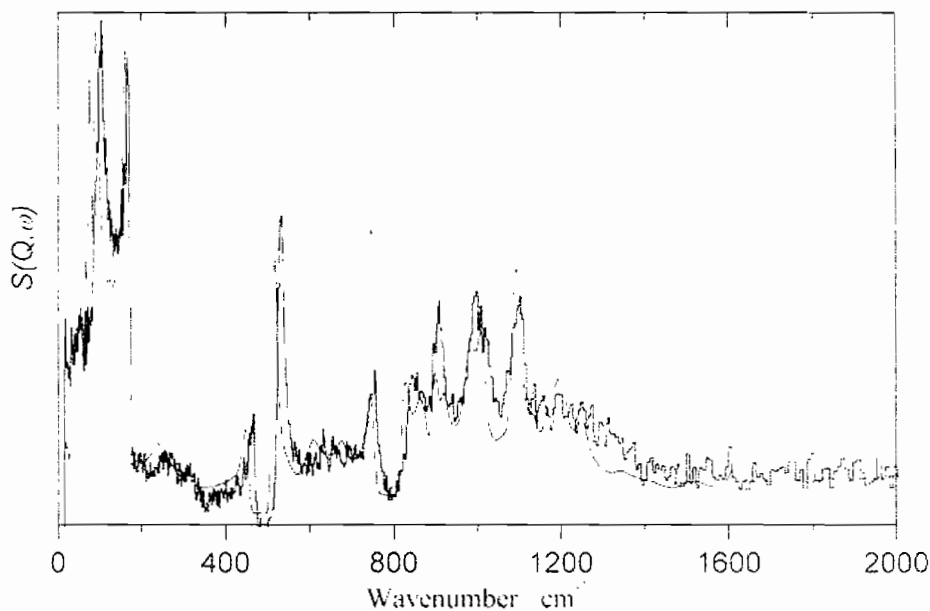
Polyethylene dispersion along chain (c) axis



INS spectrum of polyethylene



INS spectrum of polyethylene-D₄



Observed and Calculated Young's Moduli (GPa) of Polyethylene

Modulus / GPa	Experimental				Theoretical			
	Mechanical	X-ray	Raman	Coherent INS	<i>Ab initio</i>	Molecular dynamics	Force field	This work
Y_{cc}	288	235-255	280-358	329	350-400	334	286-386	360.20
Y_{bb}		2.5-5.0					9.4	12.92
Y_{aa}		1.9-3.9					9.0	13.34

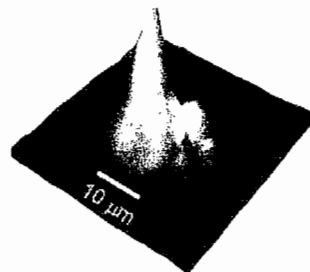
Conclusions

Vibrational spectroscopy with neutrons provides a different view of materials
it allows access to forbidden modes
metallic systems and catalyst supports are transparent

Combination with *ab initio* results is mutually beneficial
enables unambiguous assignments of vibrational spectra
provides stringent test of *ab initio* results

Photons and neutrons are complementary
best science results from use of both
co-location of sources (ILL/ESRF, ISIS/Diamond) promising

S LEIL
SYNCHROTRON



Synchrotron Infrared Microspectroscopy

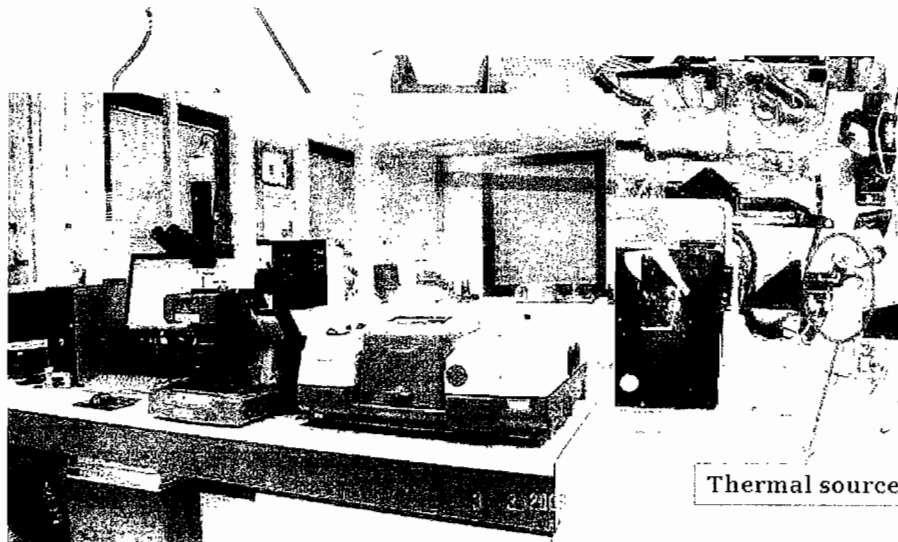
Paul Dumas
Synchrotron SOLEIL
paul.dumas@synchrotron-soleil.fr

Infrared Spectroscopy at Central Facilities - August 21st, 2006 - P. Dumas

5

S LEIL
SYNCHROTRON

Infrared microspectroscopy with a blackbody source

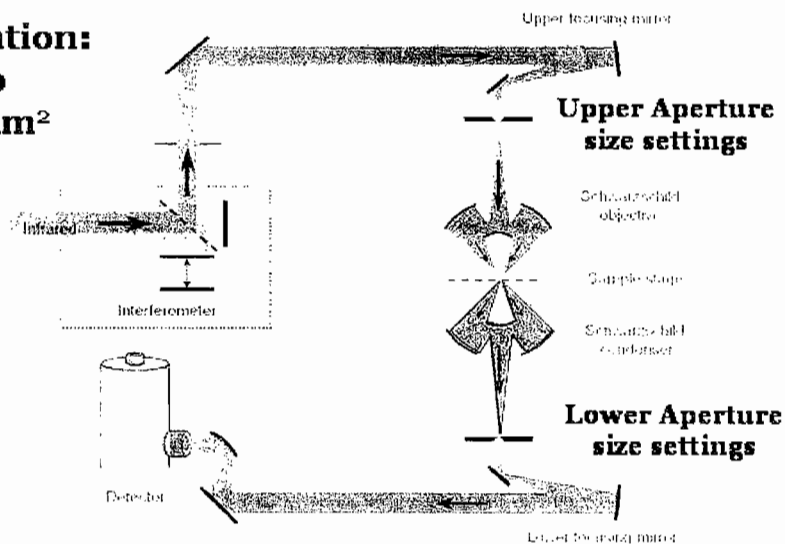


Infrared Spectroscopy at Central Facilities - August 21st, 2006 - P. Dumas

2

Infrared microscope with blackbody : limitations

**Confocal
configuration:
limited to
~20x20 μm^2
aperture**



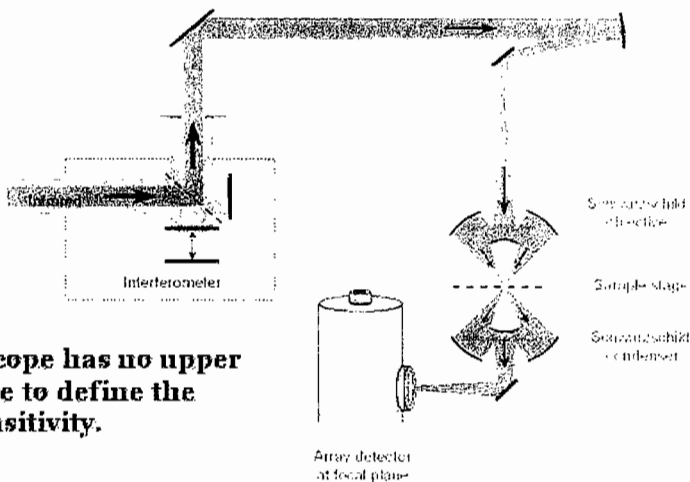
The limitation arises from the low brightness of the source

3

Infrared microscope with blackbody : limitations

**Non-confocal
configuration:
Focal Plane
Array Detector**

Optical arrangement for detector array , or FPA



**The FPA microscope has no upper
or lower aperture to define the
instrument's sensitivity.**

Instead, each detector pixel serves as an aperture for this purpose

4

The need of a brighter source

In order to achieve:

- Diffraction limited domain size analysis ($\lambda/2$)
- High spectral quality (High S/N)
- Confocal configuration (contrast fidelity)

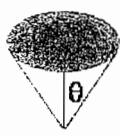
There is a need for a different infrared photon source, much brighter than the blackbody.

Confocal versus non-confocal

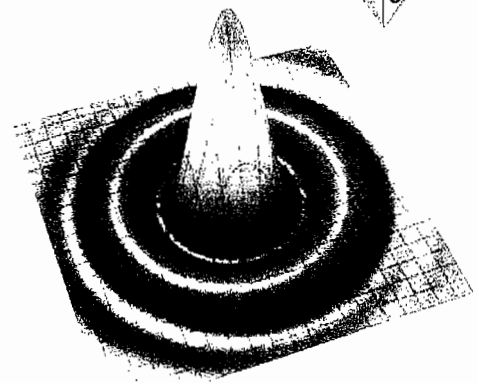
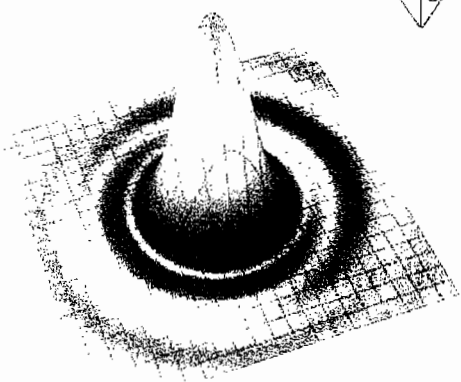
Preserving the contrast fidelity

S LEIL SYNCHROTRON **Diffraction-limited Point Spread Functions**

"Normal" (circular aperture)
 $d = 1.22\lambda / (n \sin\theta)$



Schwarzschild
 $d \approx \lambda / (n \sin\theta)$



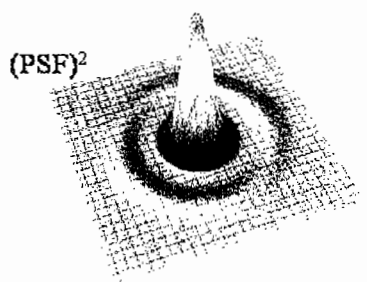
$\lambda = 6 \mu\text{m}, 1 \mu\text{m}$ grid spacing

"fat" 1st order diffraction ring for Schwarzschild

7

S LEIL SYNCHROTRON **Confocal versus non-confocal**

G.L. Carr



Confocal results in narrower central peaks, and also reduces effect of 1st order diffraction ring.

8

Example of an imaging artifact

G.L.Carr, O. Chubar and P. Dumas
Spectrochemical Analysis using multichannel infrared detectors,
Analytical Chemistry Series, Blackwell Publishing (2005)

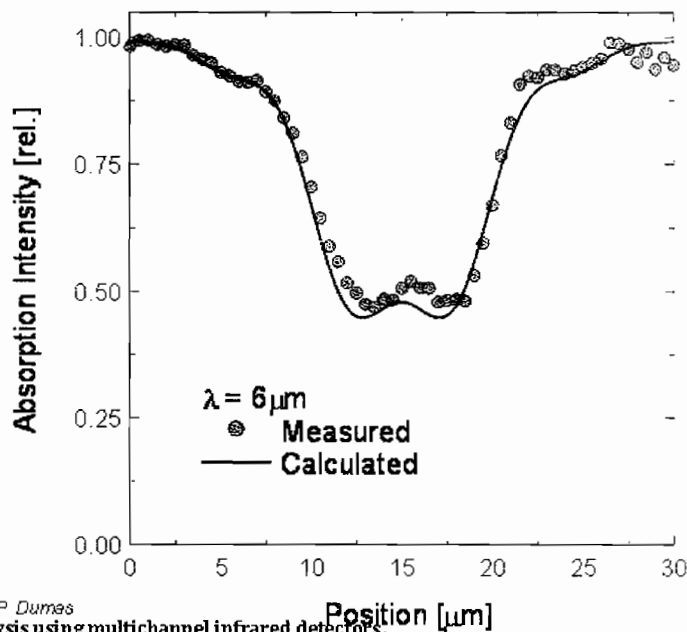


Left: object consisting of an opaque specimen except for a $12\ \mu\text{m}$ diameter circular aperture
Right: calculated transmission image for a single (non-confocal) Schwarzschild objective with $\text{NA}=0.65$ and for $\lambda=6\ \mu\text{m}$.

1-Note the dark patch in the center, suggesting the presence of absorbing material inside the hole

2-Note that the dimension of the hole is not preserved!

Artifact verified experimentally



G.L.Carr, O. Chubar and P. Dumas
Spectrochemical Analysis using multichannel infrared detectors,
Analytical Chemistry Series (2005)

S LEIL **Chemical imaging: FPA versus Synchrotron**
SYNCHROTRON

Lipids profile across and hair cut

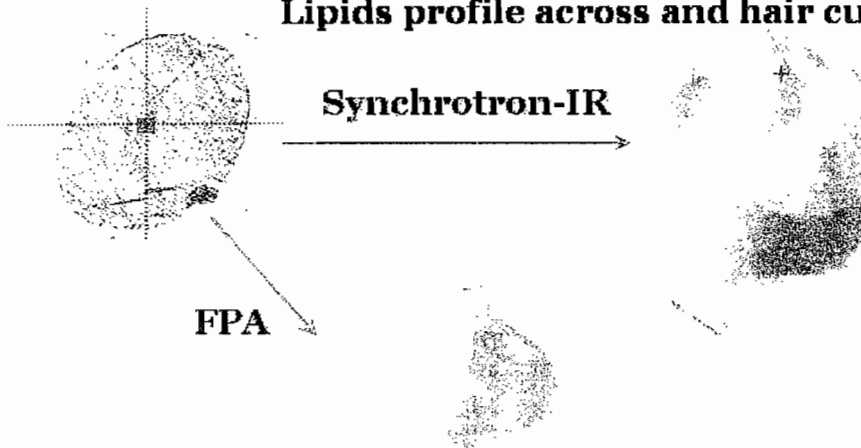


Image contrast fidelity with synchrotron!!

...and detection facilities August 2006 P. Dumas

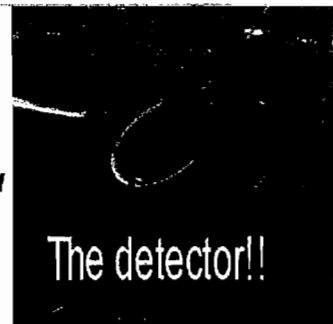
11

Brightness, or brilliance, or spectral radiance

S LEIL
SYNCHROTRON



Low brightness source



**Synchrotron source is a
broadband and bright
source.**

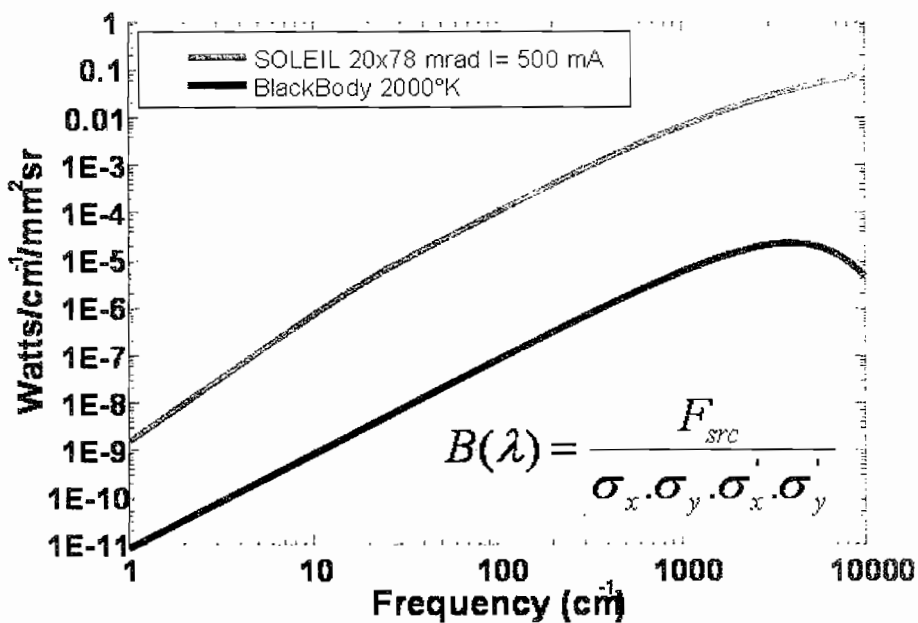


High brightness source

...and detection facilities August 2006 P. Dumas

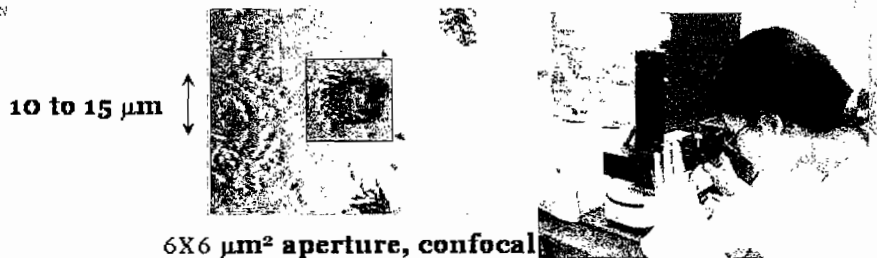
12

Synchrotron source: advantages



SOLEIL Synchrotron at Central Facilities - August 2006 - P. Lott

Exploiting the source brightness

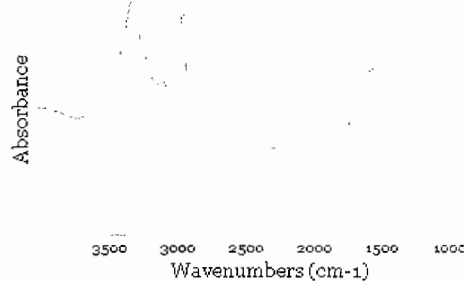
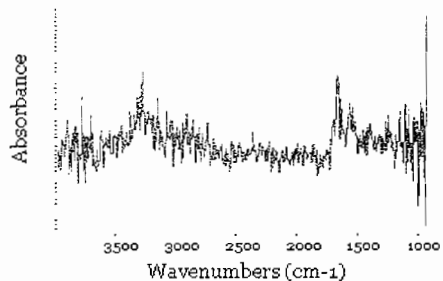


With the global source

With the synchrotron source

1000 scans = 500s

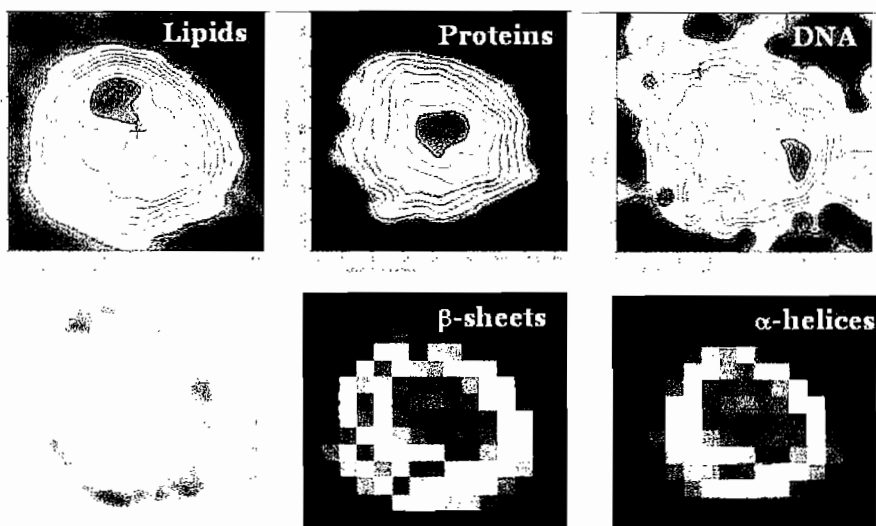
32 scans = 16 s



SOLEIL Synchrotron at Central Facilities - August 2006 - P. Lott

Imaging at sub-cellular spatial resolution

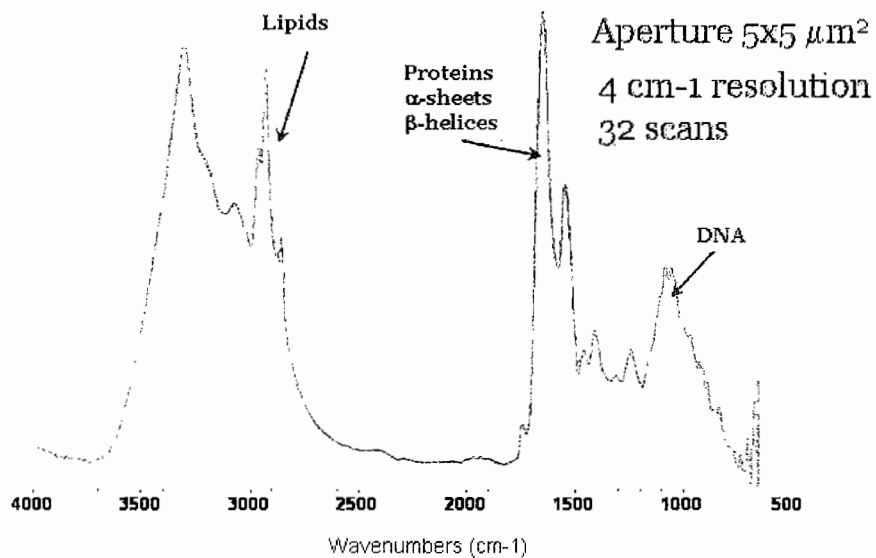
HL60 cell, after 24 hours induction of differentiation (PMA)



Dumas, Sockalingum, Sulé-Suso Trends in Biotechnology

15

Infrared spectrum



Dumas, Sockalingum, Sulé-Suso Trends in Biotechnology

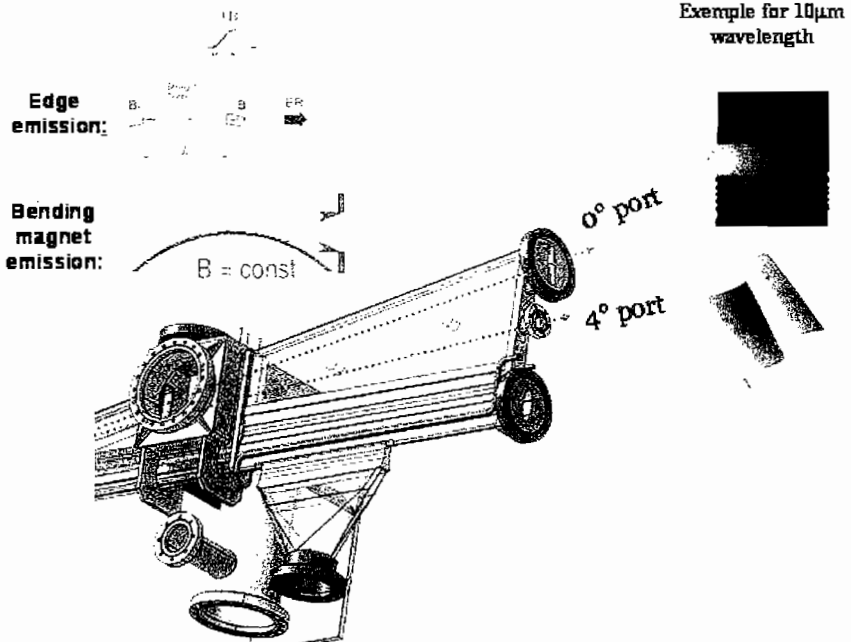
16

Design and Challenges

International Synchrotron Consortium Central Facility August 13-17, 2006 - P. Dumas

17

Synchrotron radiation and infrared emission

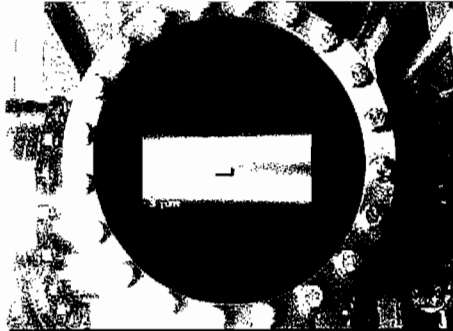


International Synchrotron Consortium Central Facility August 13-17, 2006 - P. Dumas

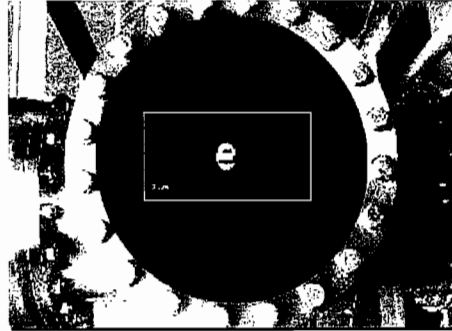
18

History of synchrotron IR ?

It takes much longer before being recognized as a potential source for spectroscopy



Bending magnet radiation



Edge radiation

*: calculated using the SRW code for E=2.75 GeV, 1.56 T, 7 meters straight section

Formulas for calculating infrared flux

(Non-coherent) Synchrotron Radiation from Constant Field of Bending Magnet

$$\left(\frac{dW}{d(l/\lambda)} \right)_{SR} \left[\frac{W}{cm^{-1}} \right] \approx 4.88 \cdot 10^{-7} E[GeV] I[A] \theta_x[mrad] G(\lambda_c / \lambda)$$

$$G(x) \equiv x \int_x^{+\infty} K_{5/3}(x') dx'$$

$\gamma = E / m_0 c^2$ = electron relativistic mass enhancement factor

θ_y = aperture

$\lambda_c = 4\pi\rho / (3\gamma^3)$ = critical synchrotron radiation wavelength for the bending magnet

$K_{5/3}$ = modified Bessel function

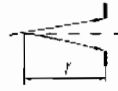
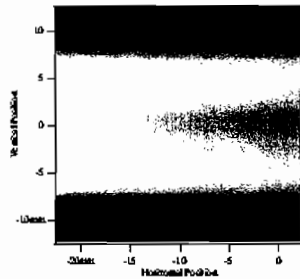
For a storage ring with parameters E = 2.75 GeV, I = 0.5 A, $\lambda_c = 1.43 \text{ \AA}$,
horizontal angular aperture $\theta_x = 40 \text{ mrad}$, at the wavelength $\lambda = 10 \text{ \mu m}$

$$\left(\frac{dW}{d(l/\lambda)} \right)_{SR} \left[\frac{W}{cm^{-1}} \right] \approx 2 \cdot 10^{-20} \frac{dN}{dt (d\lambda/l \lambda)} \left[\frac{\text{Photons}}{s (0.1\%bw)} \right] \left(\frac{dW}{d(l/\lambda)} \right)_{SR} \approx 1.40 \cdot 10^{-6} \frac{W}{cm^{-1}}$$

Multi-channel Detection with a Synchrotron Light Source GL Carr, O. Chubar and P. Dumas

Infrared Synchrotron Radiation from Bending Magnet

Intensity Distribution in transverse plane close to the source



Natural Opening Angle:

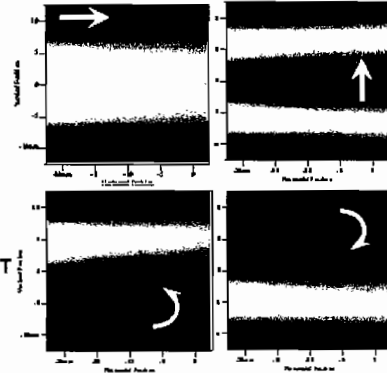
$$\psi \sim (\lambda/\rho)^{1/3}$$

$$(\lambda \gg \lambda_c)$$

$E = 3.0 \text{ GeV}; B = 1.30 \text{ T}$
 $\rho = 7.89 \text{ m}$
 $I = 200 \text{ mA}$
 $\lambda = 10 \mu\text{m}, r = 1.23 \text{ m}$

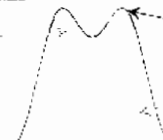


Intensity Distributions at Various Polarizations



Circular right
H-pol.

total
Circular left
V-pol.



Practical Formulas for calculating infrared flux

(Non-coherent) Edge Radiation from Extremities of Bending Magnet

$$\left(\frac{dW}{d(l/\lambda)} \right)_{ER} \left[\frac{W}{\text{cm}^{-1}} \right] \approx 5.76 \cdot 10^{-7} I[A] H \left[\frac{\pi \cdot \theta_c^2 [\text{mrad}]}{\lambda [\mu\text{m}]} \frac{zL}{z+L} [m] \right]$$

where $H(x) \equiv \ln(x) - \text{ci}(x) + C$,

$\text{ci}(x) \equiv - \int_0^x \cos(t) t^{-1} dt$ is the cosine integral function

$C \approx 0.577216$ is the Euler constant

L is the distance between bending magnet edges

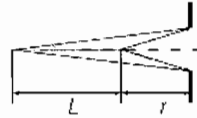
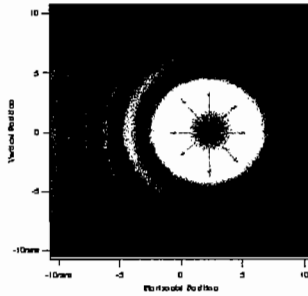
z is distance from downstream bending magnet edge to observation plane

Taking the following realistic parameters: $I = 0.5 \text{ A}$, $L = 10 \text{ m}$, $z = 5 \text{ m}$, $\theta_c = 10 \text{ mrad}$
 $\lambda = 10 \mu\text{m}$

$$\left(\frac{dW}{d(l/\lambda)} \right)_{ER} \approx 1.5 \cdot 10^{-6} \frac{W}{\text{cm}^{-1}}$$

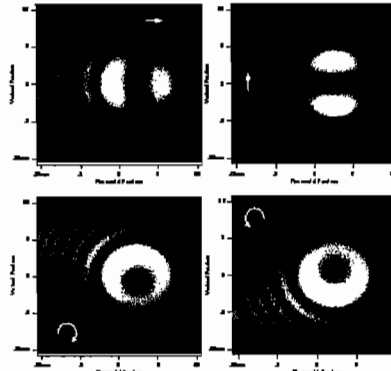
Infrared Synchrotron Radiation from Edge of bending magnet

"Pure ER" is polarized "Radially"



$E = 3.0 \text{ GeV}$ $L = 5 \text{ m}$
 $B_{max} = 1.30 \text{ T}$ $r = 1.23 \text{ m}$
 $I = 200 \text{ mA}$ $\lambda = 10 \mu\text{m}$

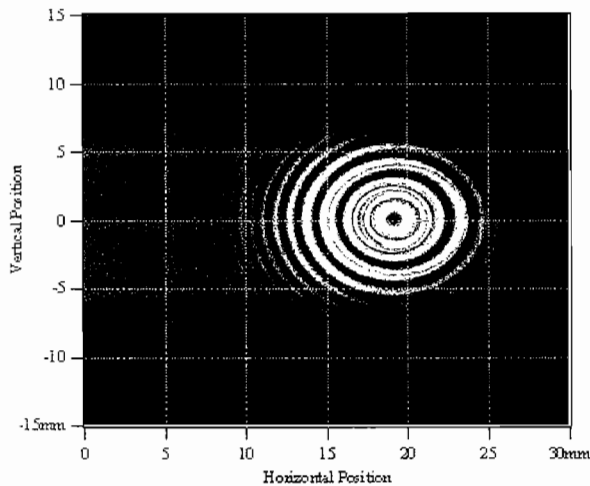
Intensity Distributions at Various Polarizations



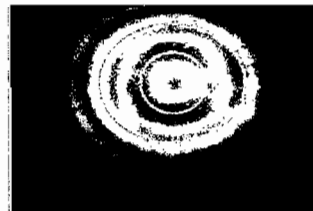
Are we confident with the simulations?

Calculated intensity profile
at 6.2 meters from source
 $\lambda = 0.52 \text{ microns}$

Measured at the ESRF
beamline



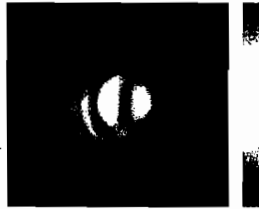
Recorded with a CCD camera
at 6.2 meters from source
 $\lambda = 0.52 \text{ microns}$



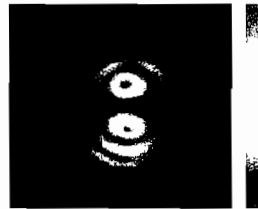
S LEIL SYNCHROTRON

Edge radiation observed at IR beamline ESRF

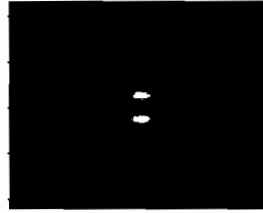
Measurements done with a CCD camera, 10m from source, filter=700nm



H-polarized

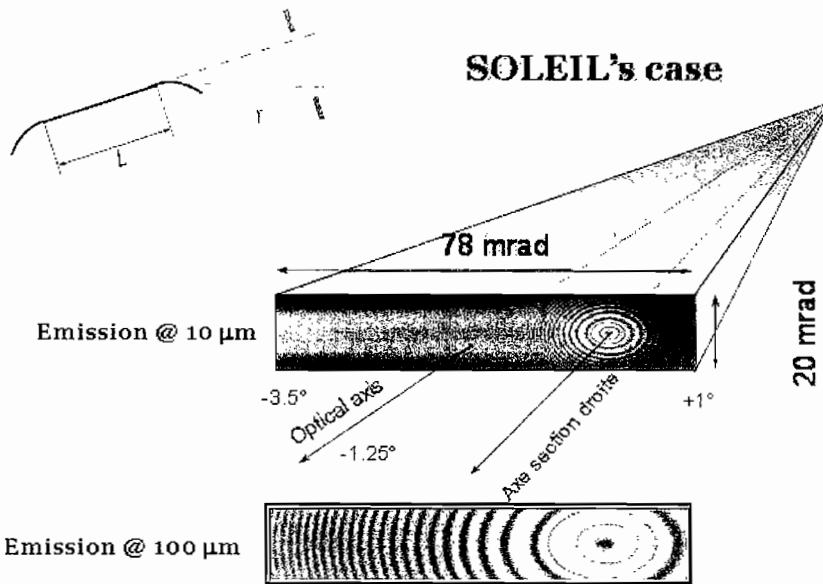


V-polarized



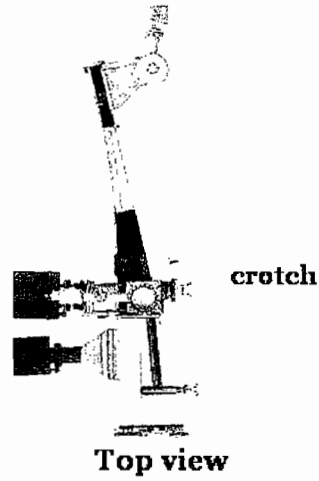
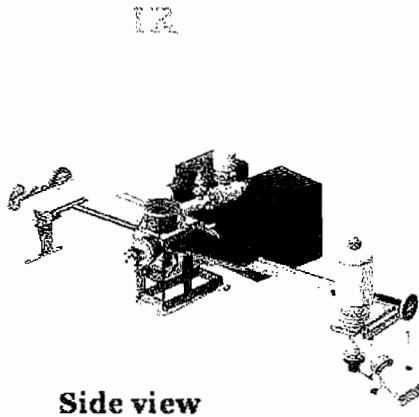
Collecting the two sources

SOLEIL's case

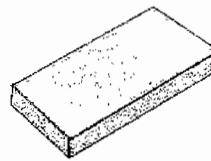
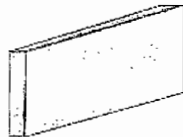


Extraction optics

Allows to collect 20 mrad vertical and 78 mrad horizontal



Extracting the beam



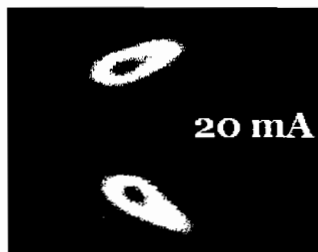
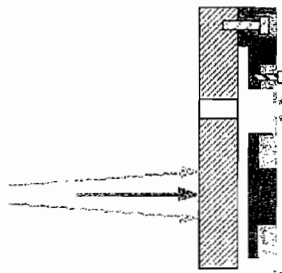
High power density on the mirror!

Extraction optics



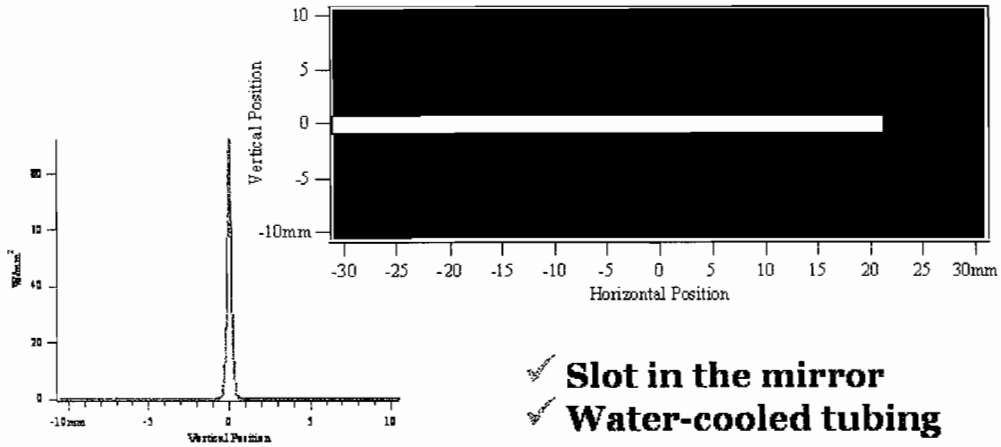
Dealing with high incident power

Recorded at ESRF IR-beamline



Calculating power on the first mirror

SRW- O. Chubar



- ✓ Slot in the mirror
- ✓ Water-cooled tubing

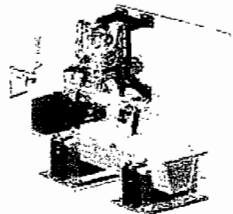
Beamline schematic

Tunnel wall



Experimental hall

M1=extracting mirror
M2= Ellipsoid
W1=Diamond Window

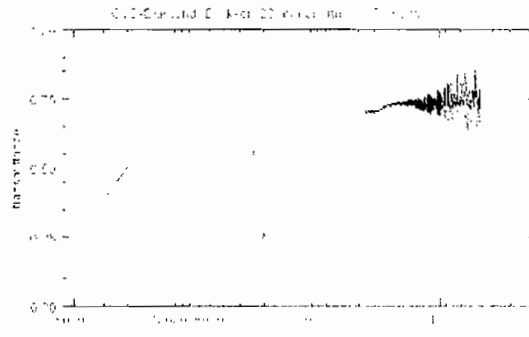


W1

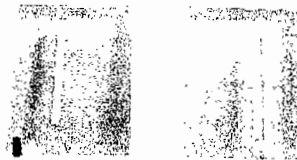


To spectrometer

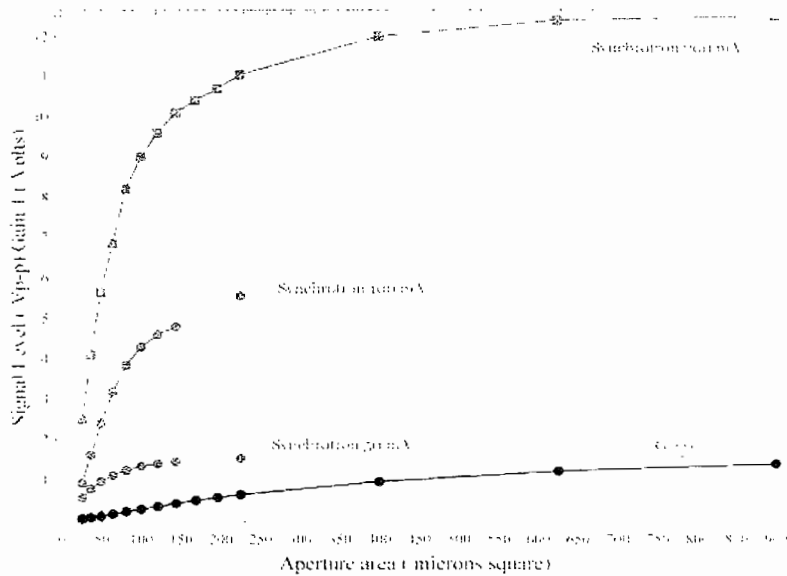
CVD diamond window@ ESRF

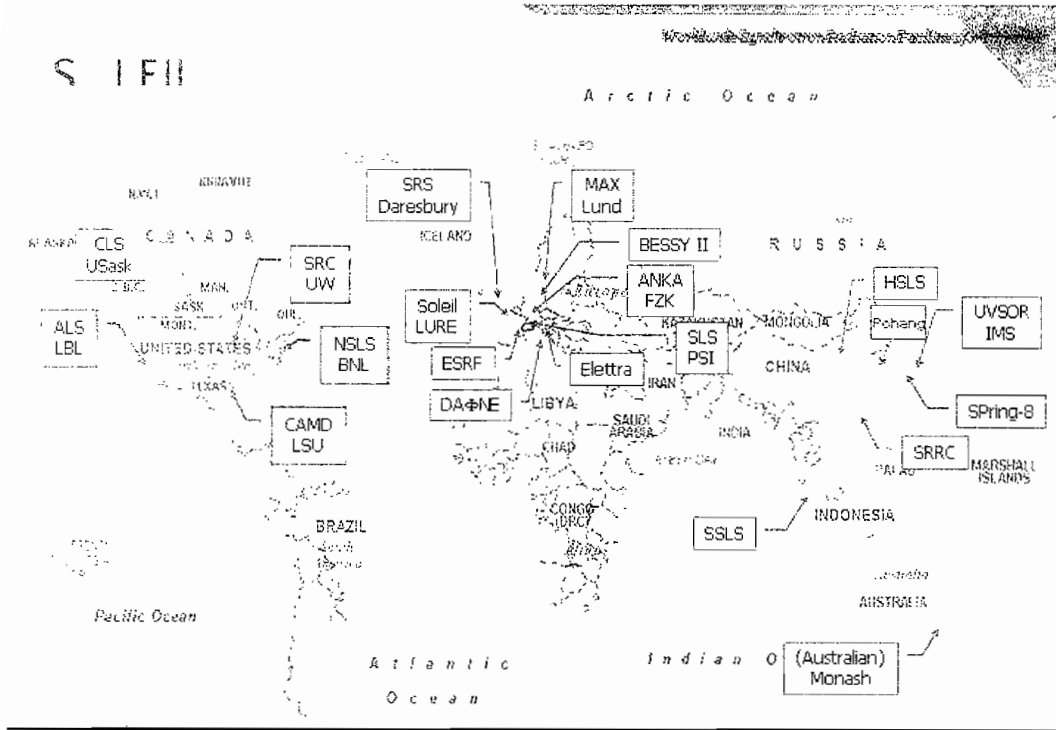


First mirror - slotted

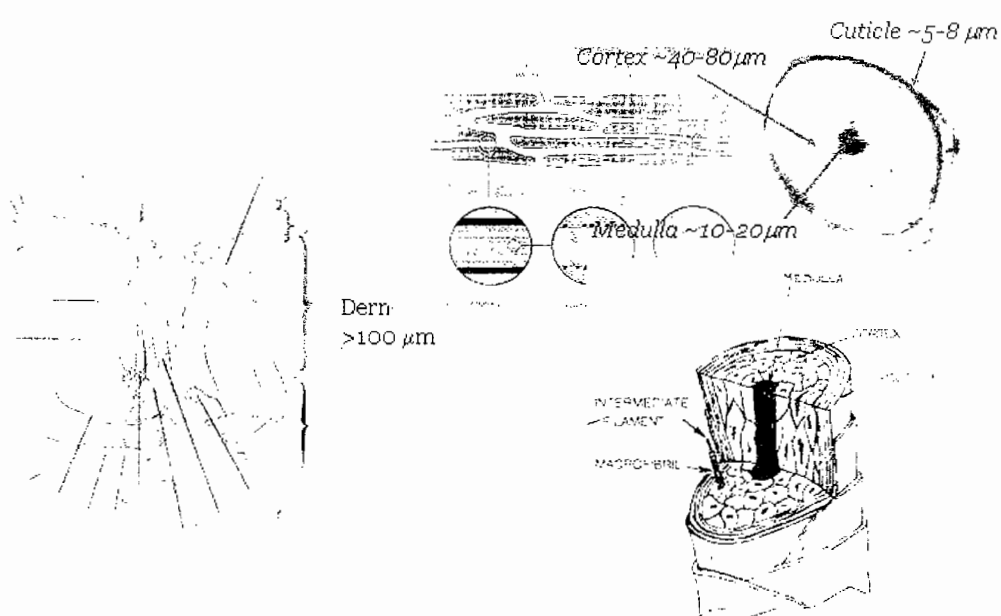


Performances achieved at ESRF



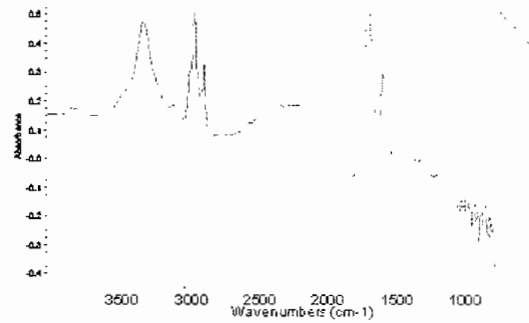
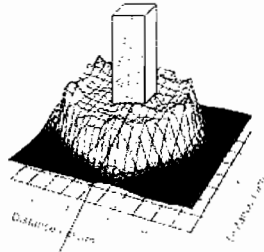


Biological applications: human tissues

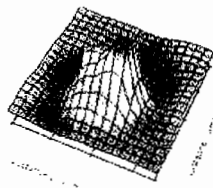


S LEIL
SYNCHROTRON

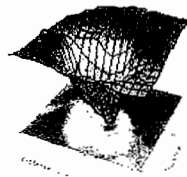
Lipid profile



3x3 μm^2 aperture
1 μm step



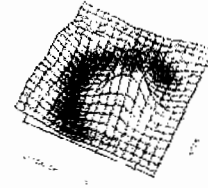
CH₂



Amide I



C=O



carboxylate

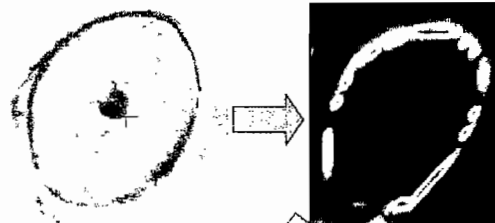
Intern.J. of Cosmetics Science **23** 1-6 (2001) 369-374

Journal of Synchrotron Radiation Control Facilities - August 2006 - E. Dumas

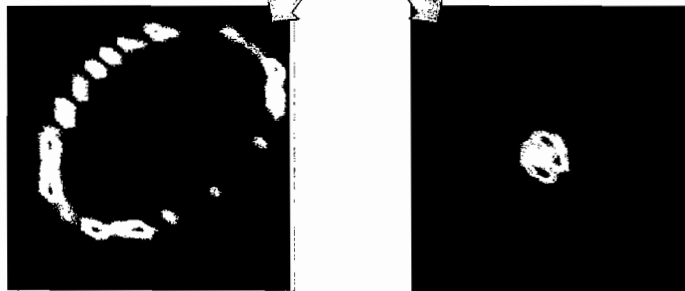
37

S LEIL
SYNCHROTRON

Beside chemical imaging: multivariate...



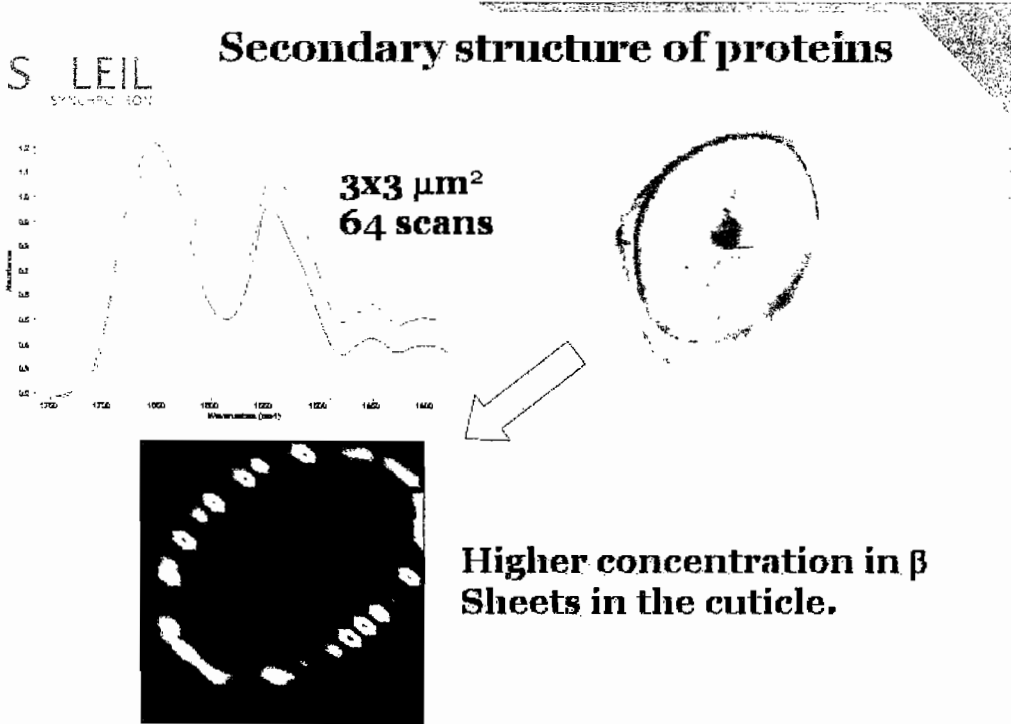
**Two types of lipids
identified across hair
section**



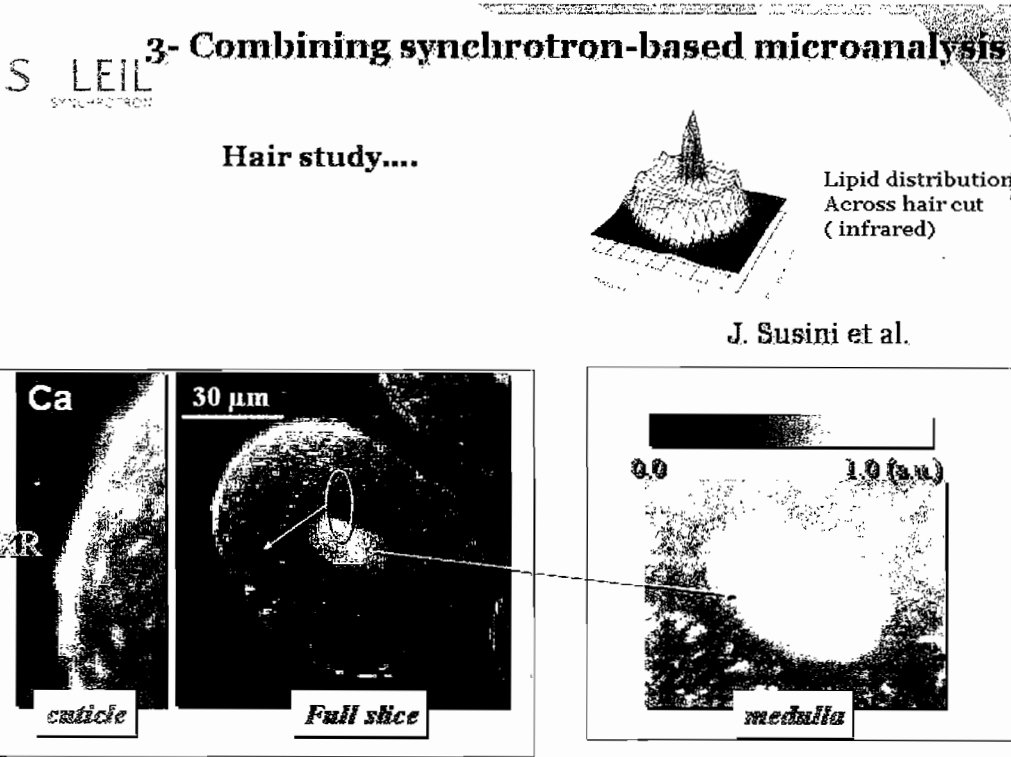
Two types of lipids identified by HCA (Hierarchical Cluster Analysis)

Journal of Synchrotron Radiation Control Facilities - August 2006 - E. Dumas

38

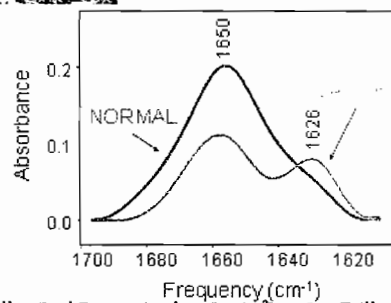
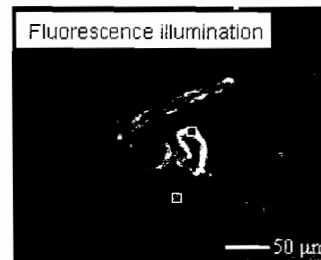
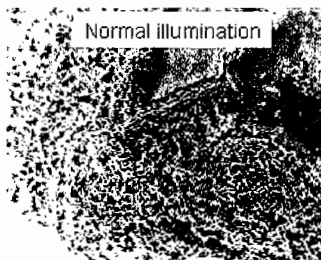
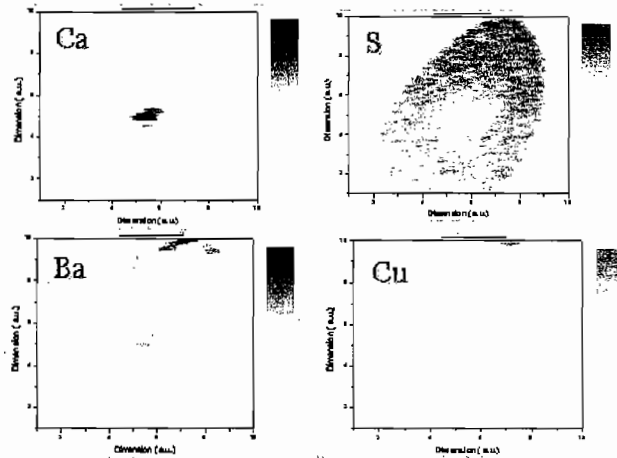


Journal of Microencapsulation, 2006, 23(1), 1-10



Journal of Microencapsulation, 2006, 23(1), 1-10

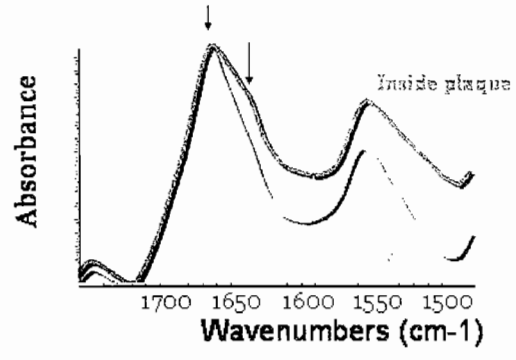
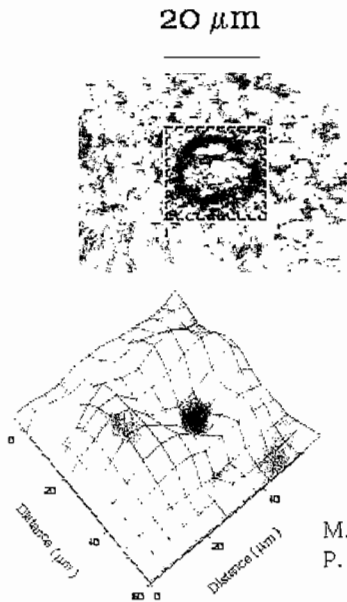
X-ray fluorescence microscopy at ID 22 (ESRF)
S. Bohic, A. Somogyi, A. Simionivici, J. Susini, P. Dumas



Lisa M. Miller, Paul Dumas, Nadege Jamin,³Jean-Luc Teillaud, Judit Miklossy, and Laszlo Forro
Rev. Sci. Instrum. (2003)

Alzheimer's disease

Imaging beta misfolding



M. Lankosz, M. Boruchowska, J. Chwiez Cracow (Poland)
P. Dumas (SOLEIL/LURE)

Cell differentiation

Induced by Phorbol Myristate Acetate (PMA)
(morphology and activity changes)

HL-60 few minutes after « activation »



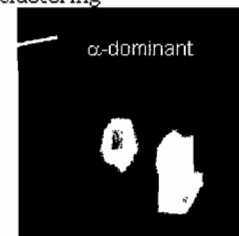
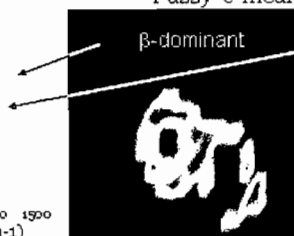
Lipids profile



Protein profile
(Amide I)

20 μm

Fuzzy-c-means clustering



1750 1700 1650 1600 1550 1500
Wavenumbers (cm-1)

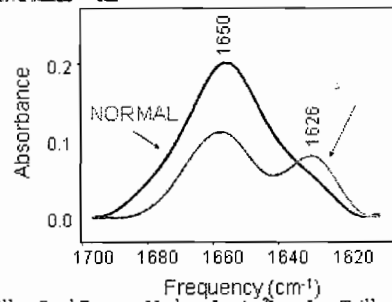
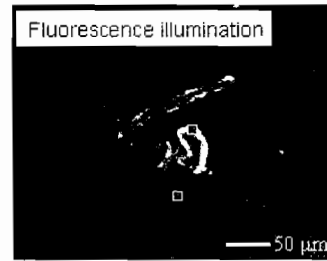
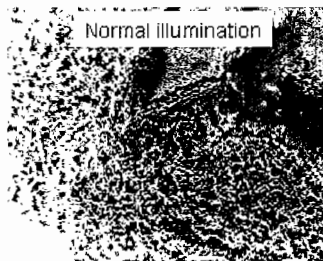
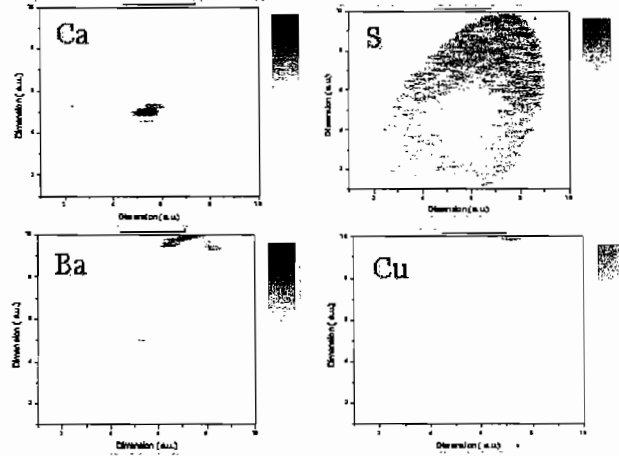
J.L. Teillaud, N. Jamin, L. Miller and P. Dumas

mjw23

\\server\name

PSCRIPT Page Separator

X-ray fluorescence microscopy at ID 22 (ESRF)
S. Bohic, A. Somogyi, A. Simionivici, J. Susini, P. Dumas

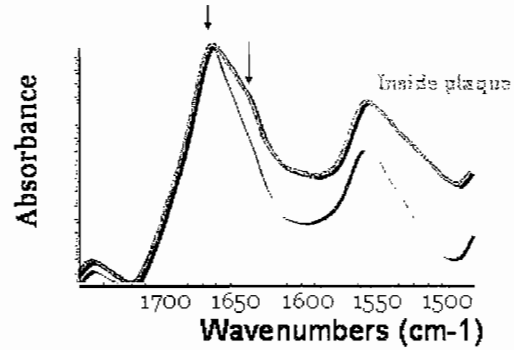
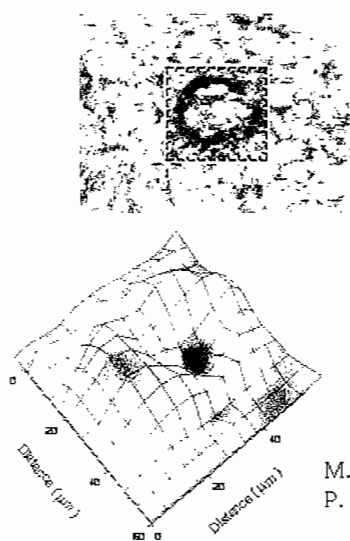


Lisa M. Miller, Paul Dumas, Nadege Jamin, Jean-Luc Teillaud, Judit Miklossy, and Laszlo Forro
Rev. Sci. Instrum. (2003)

Alzheimer's disease

20 μm

Imaging beta misfolding

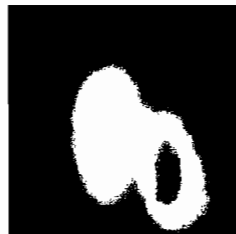


M. Lankosz, M. Boruchowska, J. Chwiez Cracow (Poland)
P. Dumas (SOLEIL/LURE)

Cell differentiation

Induced by Phorbol Myristate Acetate (PMA)
(morphology and activity changes)

HL-60 few minutes after « activation »



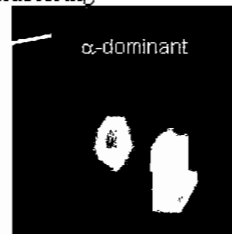
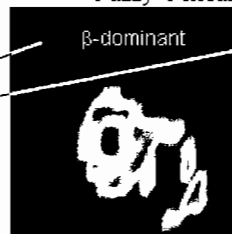
Lipids profile



Protein profile
(Amide I)

20 μm

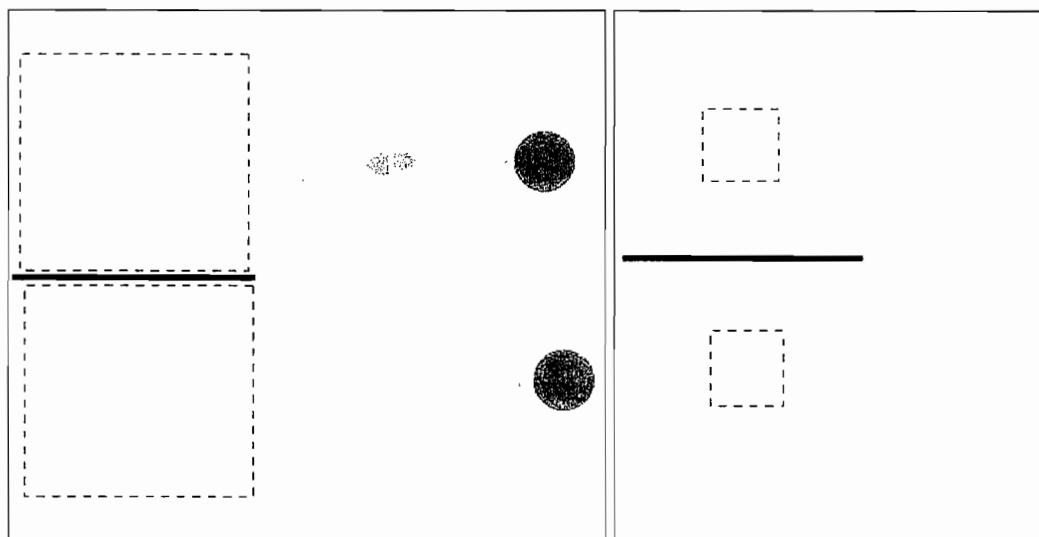
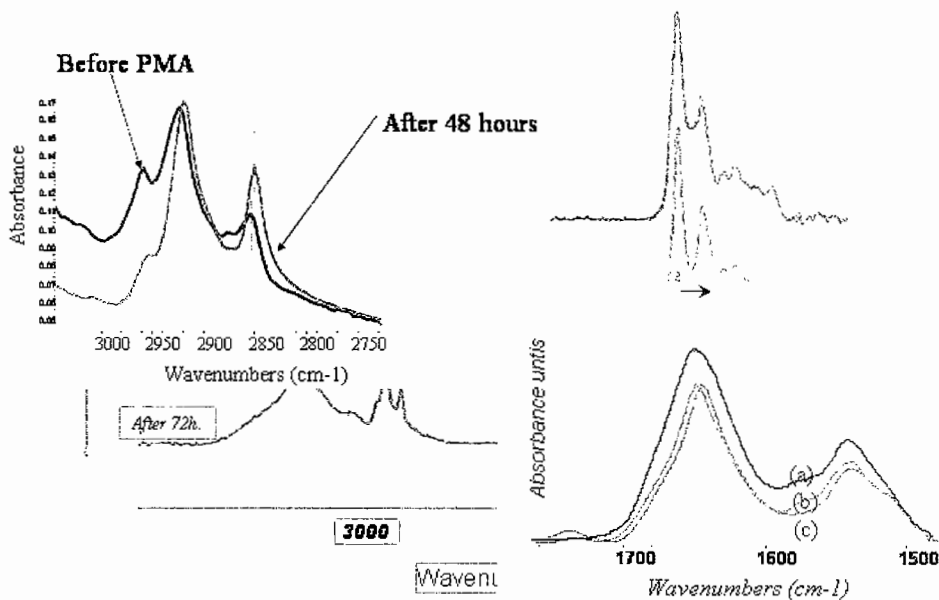
Fuzzy-c-means clustering



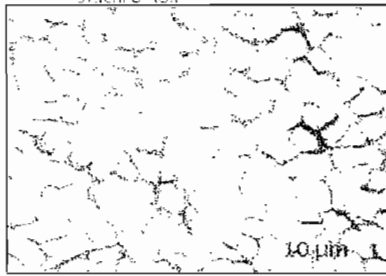
1750 1700 1650 1600 1550 1500
Wavenumbers (cm-1)

J.L. Teillaud, N. Jamin, L. Miller and P. Dumas

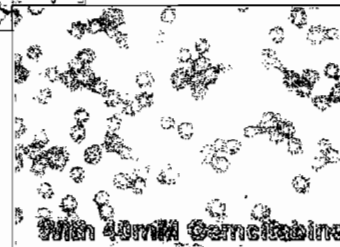
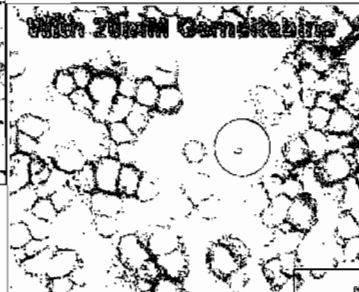
Spectra recorded with a $3 \times 3 \mu\text{m}^2$ aperture
in the nucleus



SKMES lung cancel cells line



Gemcitabine= a chemotherapeutic drug



Are these cells sensitive to the drug?

From Dr. Josep Sulé-Suso

SKMES lung cancel cells line



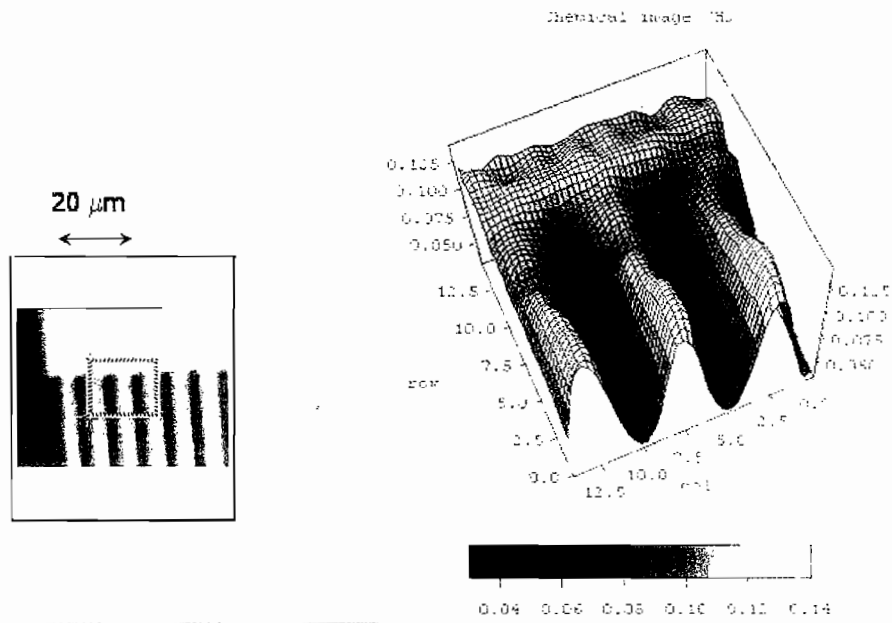
From Dr. Josep Sulé-Suso

Absorbance (a. u.)

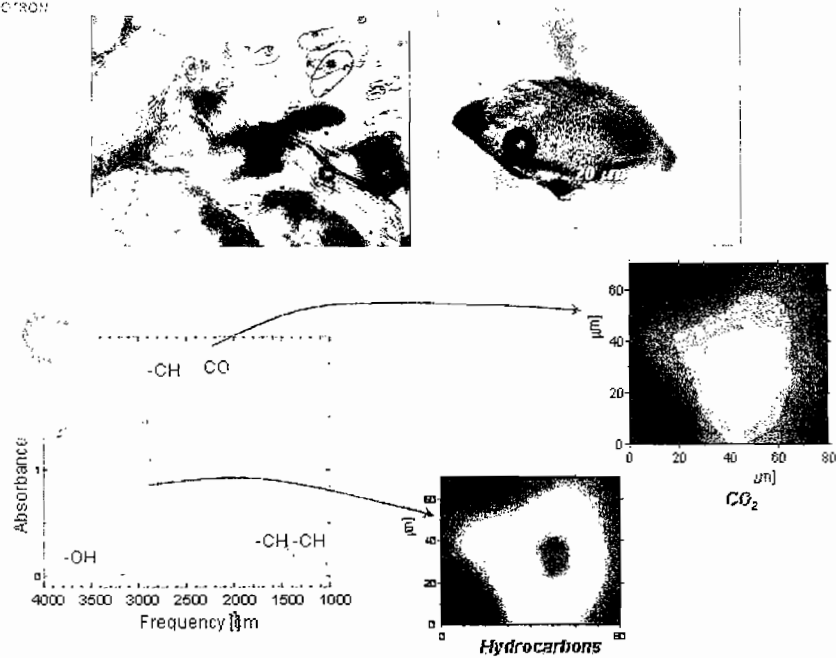
the biochemical changes in these cells measured with synchrotron IR micro-spectroscopy could help us to better clarify the state of a single cell, i. e.,

- **alive without damage,**
- **alive with damage but able to recover,**
- **alive but entering a death pathway and unable to recover, or**
- **dead.**

Gold grid deposited on silicon wafer imaging the protective layer on top of the gold grid

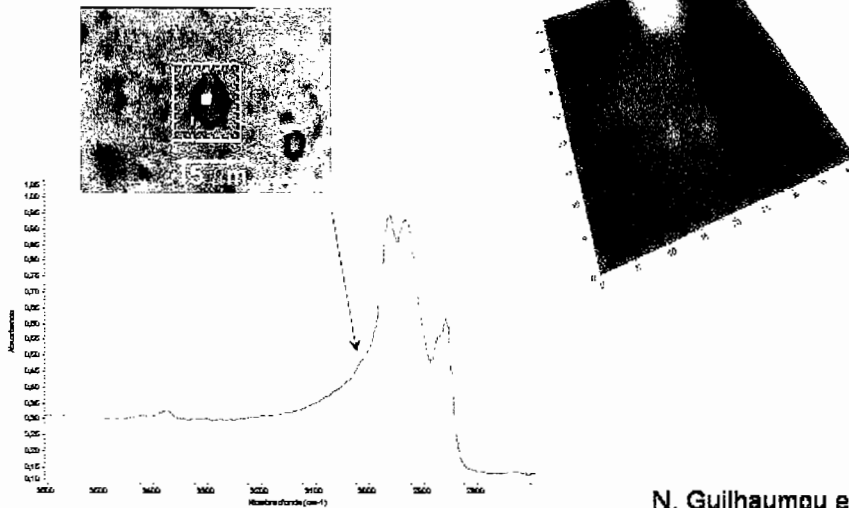


Inclusions in rocks



Small inclusions in rocks

Inclusion in calcite



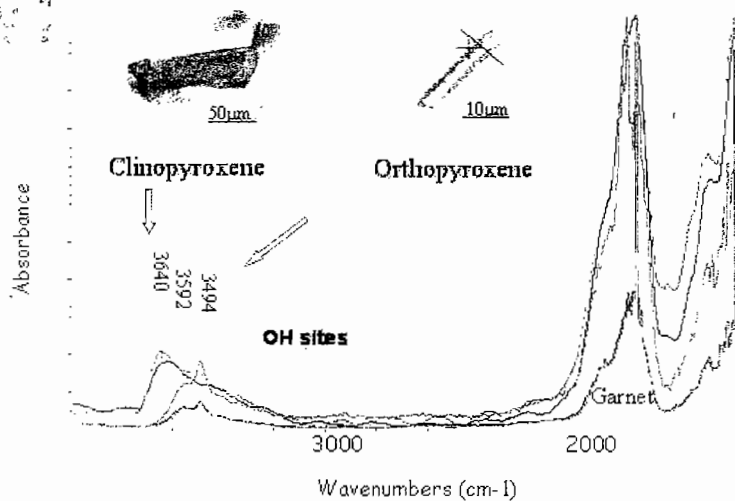
Aperture= 3x3 μm²

N. Guilhaumou et coll.

Water in deep seated minerals (200-400 kms)



N. Guilhaumou et al.



Summary

- **Synchrotron IR microscopy has become an important analytical tool in synchrotron facilities**
- **Such facilities are of high ratio scientific/cost**
- **Association with fluorescence is desirable**
- **Good S/N and higher spatial resolution.... Statistical treatment (unsupervised or supervised)**
- **Complementarities with other synchrotron based techniques are very potential especially if combined studies are performed on the same sample.**

53

Acknowledgments

Special thanks to my long term collaborators:



- G. Larry Carr (NSLS)
- Gwyn P. Williams (JLab)
- Lisa M. Miller (NSLS)
- O. Chubar (SOLEIL)
- F. Polack (SOLEIL)



And

- J. Susini (ESRF)
- P. Elleaume (ESRF)
- K. Scheidt (ESRF)

54

Synchrotron Reflection Absorption Infrared Spectroscopy

Peter Gardner
The University of Manchester

RSC-IRDG Rutherford Appleton Laboratory – 31 August 2006

Outline of Talk

Reflection absorption Infrared Spectroscopy (RAIRS)

Why do we need a synchrotron

What can we do with it

(Surface dynamics CO on metal surfaces)

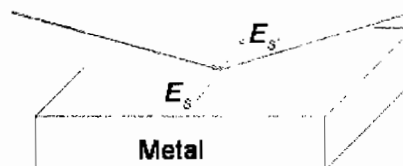
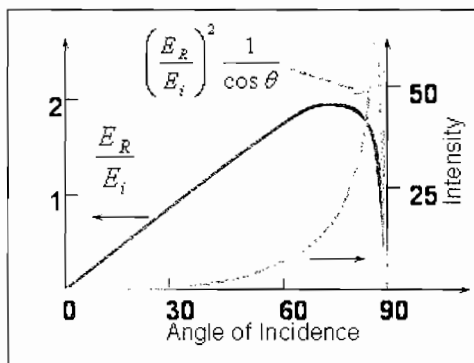
CVD growth of SnO₂

Model Z-N catalysts

Outlook

RSC-IRDG Rutherford Appleton Laboratory – 31 August 2006

Reflection-Absorption Infrared Spectroscopy RAIRS



This is the basis of the "Metal Surface Selection Rule"

RSC-IRDG Rutherford Appleton Laboratory – 31 August 2006

Reflection Absorption Infrared Spectroscopy RAIRS

An experimental technique that enables IR spectra to be obtained from molecules or thin films on highly reflecting metal surface

Highly sensitive – fractions of a monolayer

Metal Surface Selection Rule – simple spectra, orientation information

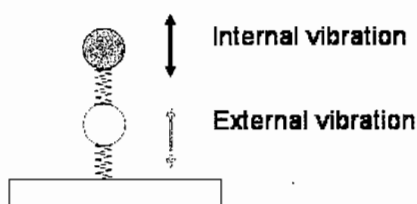
Particularly relevant to adsorbates on model catalytic systems

RSC-IRDG Rutherford Appleton Laboratory – 31 August 2006

The method was used extensively in the late 1980s and early 1990s to study adsorbates on metal surfaces

In the mid 1990s there was an explosion of interest in using RAIRS for the study of SAMs on Au and Ag surfaces

However the standard RAIRS set-up using an LN₂ cooled MCT detector is limited to monitoring internal vibrations of the molecules



RSC-IRDG Rutherford Appleton Laboratory – 31 August 2006

Why do we want to use a synchrotron?

Above 800 cm⁻¹ a conventional lab based RAIRS system easily outperforms the synchrotron

Below 500 cm⁻¹ the synchrotron starts to have an advantage and below 300 cm⁻¹ this advantage is significant

Most metal-adsorbate stretches are in this low frequency region of the spectrum

RSC-IRDG Rutherford Appleton Laboratory – 31 August 2006

Early days of far IR-RAIRS

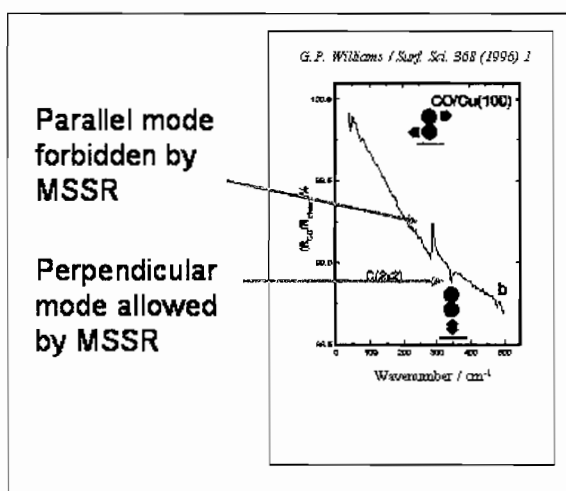
Preliminary data by Bradshaw and Schweizer taken at BESSY in 1986 did not look promising

Gwyn Williams at Brookhaven pioneered the Far IR RAIRS method in 1990 with the completion of U4IR. *Nucl. Instrum. Methods A291 (1990)*

Collaborations with P. Dumas, F. Hoffman Y. Chabal B. Persson A. Volokitin, C. Hirschmugl and others resulted in a series of seminal papers mainly on low frequency vibrations of CO on low index faces of metal surfaces.

RSC-IRDG Rutherford Appleton Laboratory – 31 August 2006

First observation of dipole forbidden modes



At the same time M. Chester, P. Hollins M. Surman started to build station 13.3 on the SRS.

Initial source instability slowed progress

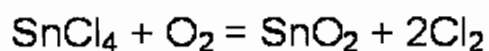
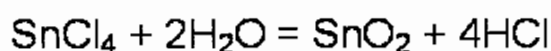
In the late 1990s we started to look at adsorbates on oxide surfaces

RSC-IRDG Rutherford Appleton Laboratory – 31 August 2006

Infrared Studies of CVD Precursor Molecules on Thin-film Oxide Surfaces

RSC-IRDG Rutherford Appleton Laboratory – 31 August 2006

CVD Growth of SnO₂ on Float Glass



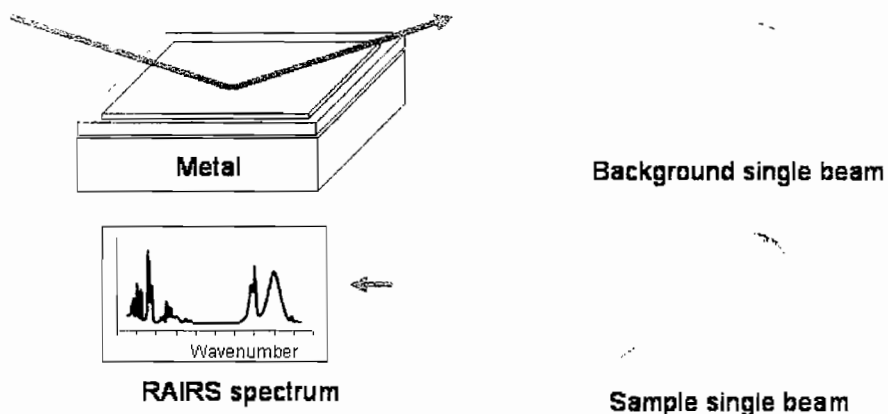
We want to study the formation of SnO₂ on SiO₂

RAIRS is straight-forward on a metal surfaces but, it is difficult to do on oxide surfaces due to poor

change in reflectivity

RSC-IRDG Rutherford Appleton Laboratory – 31 August 2006

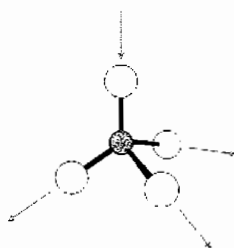
The Buried Metal Layer Method



If the thickness of the oxide is $\ll \lambda$ then the reflection will be dominated by the metal but the surface chemistry being probed will be that of the oxide

RSC-IRDG Rutherford Appleton Laboratory – 31 August 2006

Why work at Daresbury?



ν_3 Sn-Cl (asym)
408 cm^{-1}

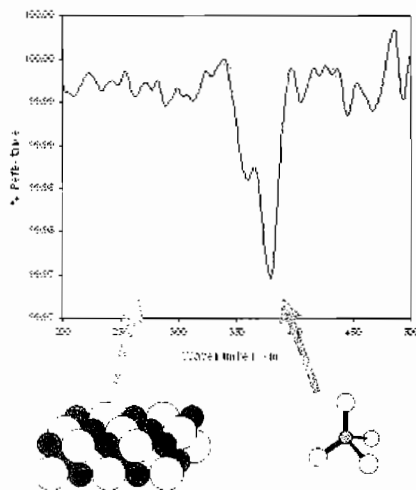
Sn-Cl stretching modes in the region 300 – 450 cm^{-1}

Conventional RAIRS shows poor sensitivity below 800 cm^{-1}

Low intensity of conventional source necessitates the use of synchrotron radiation

RSC-IRDG Rutherford Appleton Laboratory – 31 August 2006

RAIRS spectrum of tin tetrachloride on thin-film (100 nm) silica / W sample at 291K



At 291 K spectra are consistent with molecular adsorption

On Na doped SiO₂ spectra are consistent with the formation of small NaCl clusters

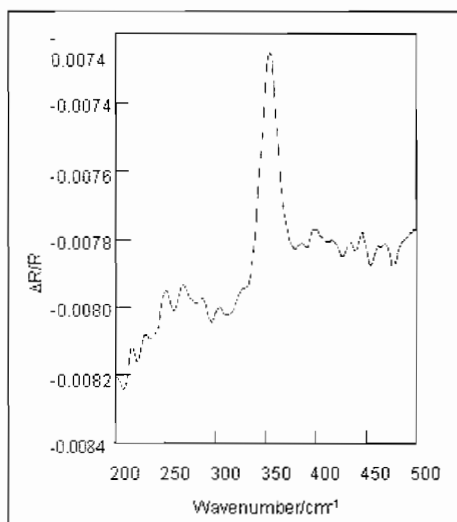
M. J. Pilling, P. Gardner, M. E. Pemble and M. Surman, *Surface Science Letters*, 418, (1998), 1-7

M. J. Pilling, P. Gardner, R. Kausar, M. E. Pemble and M. Surman, *Surface Science*, 433-435, (1999), 22-26,

M. J. Pilling, Nurhayti, P. Gardner, A. Awalludin, M. E. Pemble, and M. Surman, *Accelerator-based Sources of Infrared and Spectroscopic Applications*, Eds. G. Lawrence Carr, Paul Dumas, *Proceedings of SPIE Vol 3775*, page 192-200 (1999)

RSC-IRDG Rutherford Appleton Laboratory – 31 August 2006

RAIRS spectrum of 25L tin tetrachloride on SnO₂ at 291K



On a thin film SnO₂ surface adsorption results in an inverse adsorption band

Is this due to the SnCl₄?



Need to revisit the theory of the RAIRS experiment

RSC-IRDG Rutherford Appleton Laboratory – 31 August 2006

Greenler Calculations

The Greenler equations are extensions of the well know Fresnel relationships, which define the reflectivity at the interface between two isotropic materials.



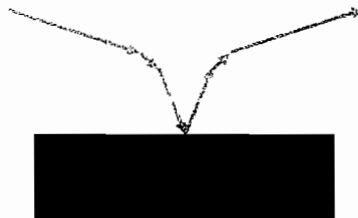
- n_1-ik_1 Vacuum (fixed)
- n_2-ik_2 Adsorbate (fixed)
- n_3-ik_3 Metal (fixed)

The reflectivity R' for a particular thickness of adsorbate layer is compared with the reflectivity R in the absence of the adsorbate

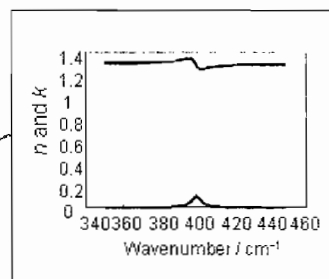
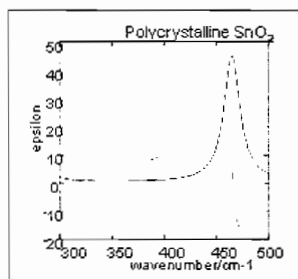
$$\Delta R / R = (R' - R) / R$$

RSC-IRDG Rutherford Appleton Laboratory – 31 August 2006

Greenler-Buried metal layer

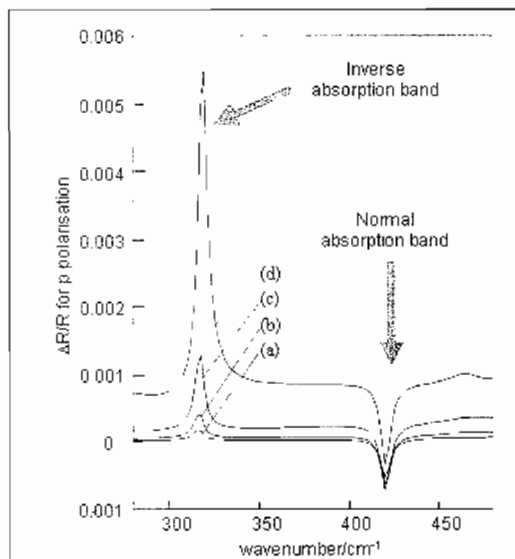


- n_1-ik_1 Vacuum (fixed)
- n_2-ik_2 Adsorbate (variable)
- n_3-ik_3 Oxide (variable)
- n_4-ik_4 Metal (fixed)



RSC-IRDG Rutherford Appleton Laboratory – 31 August 2006

Typical wavenumber-dependent 4-layer Greenler calculation for a adsorbate with k maximum at 420 cm^{-1}



Calculations can qualitatively reproduce the inverse absorption band

They suggest that the inverse absorption band is induced by the adsorbate but is not related to the vibrational properties of the adsorbate

This is confirmed by experiments with SnBr_4

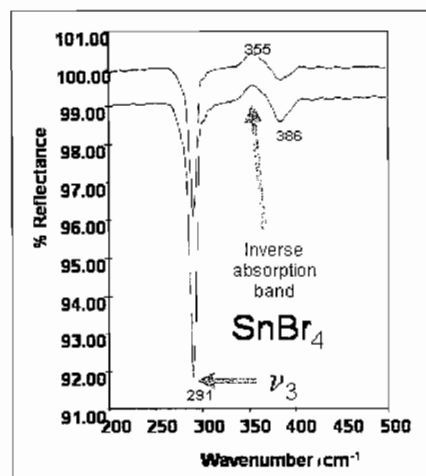
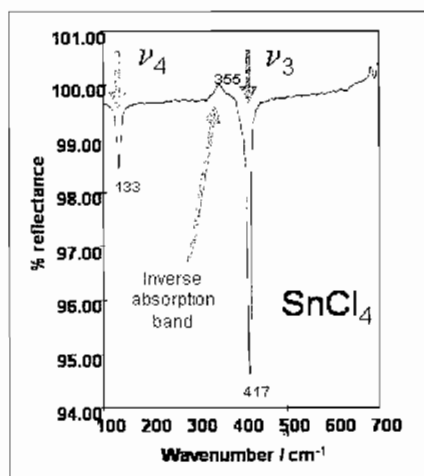
A. Awaluddin, M. J. Pilling, P. L. Wincott, S. Le Vent, M. Surman, M. E. Pemble and P. Gardner, Surface Science 505 (2002) 63-69

RSC-IRDG Rutherford Appleton Laboratory – 31 August 2006

Confirmation using SnBr_4

	ν_1	ν_2	ν_3	ν_4
SnCl_4	369	95	408	126
SnBr_4	222	59	284	86

The SnBr_4 has no vibrational modes above 300 cm^{-1}



M. J. Pilling, S. Le Vent P. Gardner, A. Awaluddin, P. L. Wincott, M. E. Pemble and M. Surman, Anomalous inverse absorption features in the far infrared RAIRS spectra of SnCl_4 on thin-film SnO_2 , J. Chem Phys 117 (2002) 6780-6788

The calculations show that the band is related to the optical properties of the bulk oxide film

This stimulated additional theory work related to Far IR RAIRS on non-metallic surface

P. Gardner, S. LeVent, M. J. Pilling
A theoretical investigation of the far-infrared RAIRS experiment applied to a buried metal layer substrate
Surface Science 559 (2004) 186 – 200

M J Pilling, P Gardner, S Le Vent
Considerations of Optical Anisotropy in the Simulation of Reflection Absorption Infrared Spectra
Surface Science 582 (2005) 1

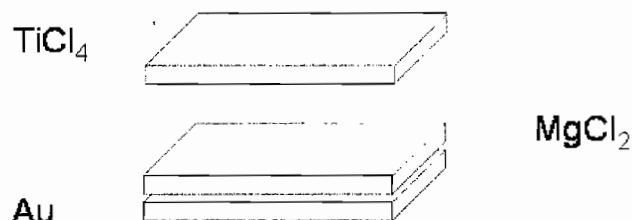
S. LeVent, M. J. Pilling, P Gardner
A theoretical study of inverse features in far-infrared RAIRS spectra from non-metallic substrates
Surface Science 587 (2005) 150

RSC-IRDG Rutherford Appleton Laboratory – 31 August 2006

Far infrared RAIRS studies of MgCl_x/TiCl_y thin-films related to model Ziegler-Natta catalysts

RSC-IRDG Rutherford Appleton Laboratory – 31 August 2006

Preliminary work by Somorjai et al have shown that model Z-N catalysts can be prepared under UHV conditions but the exact nature of the surfaces produced is still open to question



The ideal method of producing the model catalyst would be to deposit TiCl_4 on top of the MgCl_2 on a suitable substrate e.g. Au

TiCl_4 will not stick on MgCl_2

RSC-IRDG Rutherford Appleton Laboratory – 31 August 2006

In order to get TiCl_4 to adsorb we need reduced Mg sites

This may be achieved in a number of ways

Adsorb on pure Mg

Electron beam irradiation of MgCl_2

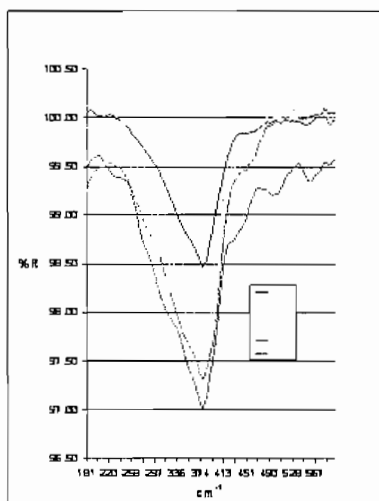
Pre adsorption of TiCl_4

During adsorption of TiCl_4

These different methods produce different types of films that may have different surfaces.

RSC-IRDG Rutherford Appleton Laboratory – 31 August 2006

RAIRS spectra following exposure of a thin-film of Mg on Au, to varying amounts of TiCl_4



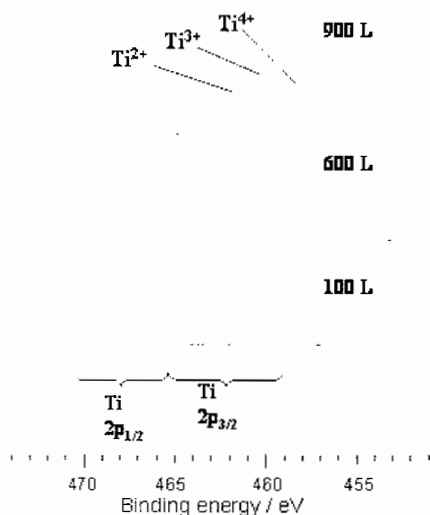
TiCl_4 does stick at 300 K to the Au/Mg surface but the resulting RAIRS spectrum is very broad $\sim 200 \text{ cm}^{-1}$

The positions of these bands are consistent with transmission far infrared spectroscopy performed on $\alpha\text{-MgCl}_2$ and $\beta\text{-MgCl}_2$ [2] where absorption bands have been observed at 407cm^{-1} , 372cm^{-1} , 329cm^{-1} , 276cm^{-1} and 248cm^{-1} .

What about the Ti?

RSC-IRDG Rutherford Appleton Laboratory – 31 August 2006

XPS of Au/Mg/ TiCl_4



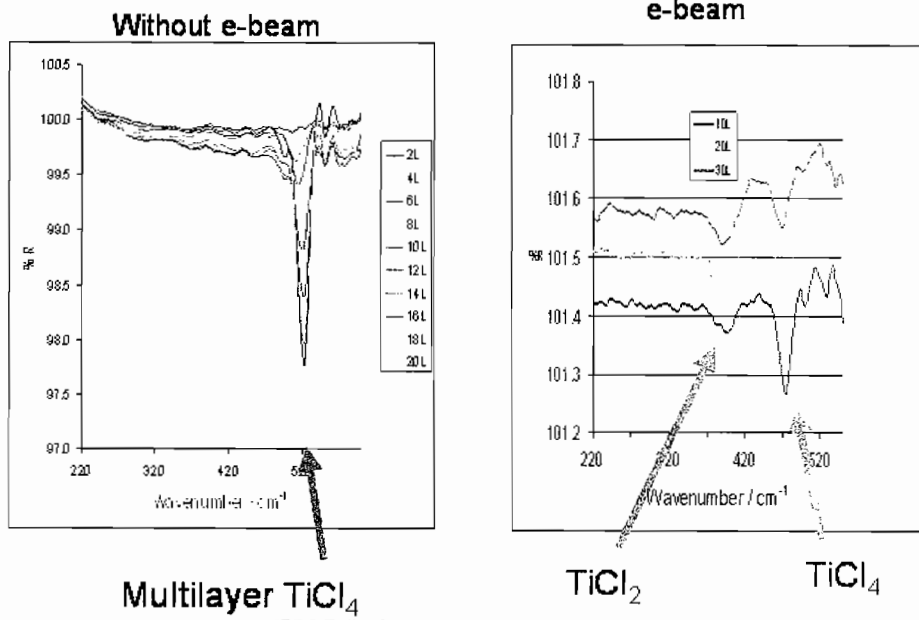
The XPS spectra clearly show three different oxidation state of Ti.

This is clearly very complex

We need to simplify the system

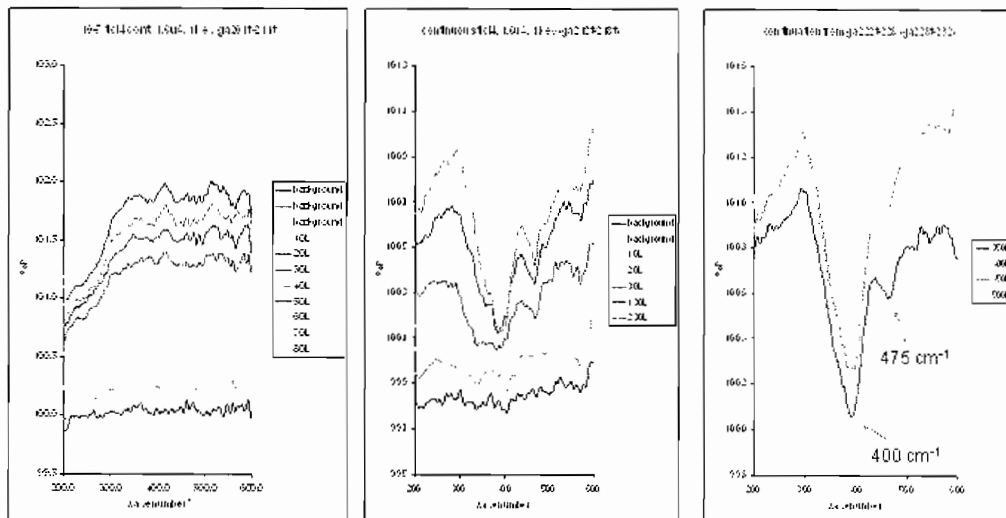
Laboratory – 31 August 2006

TiCl₄ on Au at 120 K



RSC-IRDG Rutherford Appleton Laboratory – 31 August 2006

TiCl₄ on Au at 300 K using e-beam

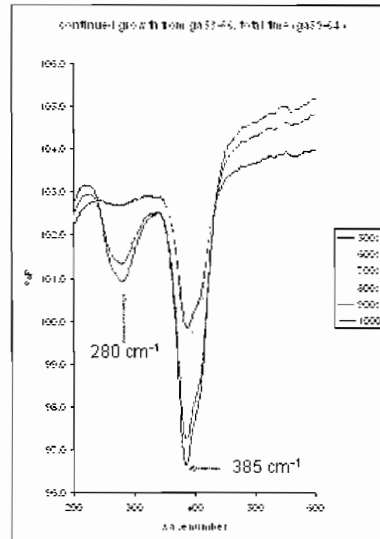
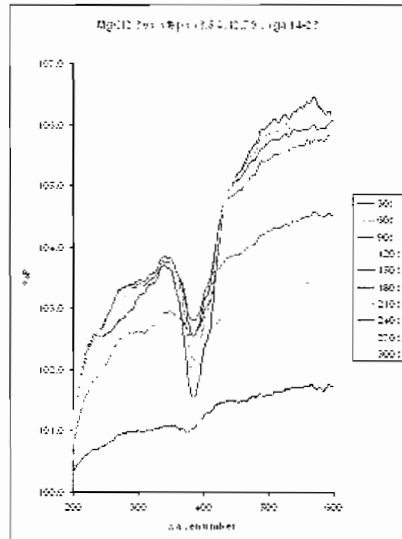


Little observed at low exposure

Two broad bands at high L consistent with TiCl₂ and TiCl₄

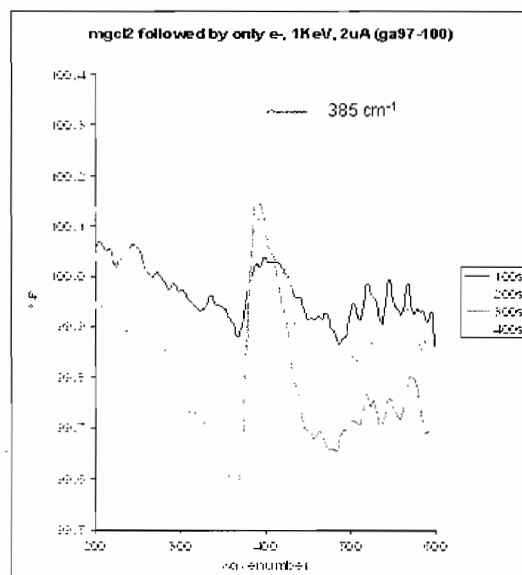
RSC-IRDG Rutherford Appleton Laboratory – 31 August 2006

MgCl₂ on Au at 300 K



RSC-IRDG Rutherford Appleton Laboratory - 31 August 2006

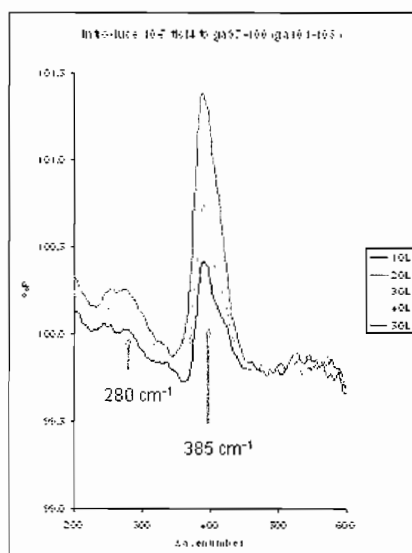
Au/MgCl₂ with e-beam only



Loss of MgCl₂

RSC-IRDG Rutherford Appleton Laboratory - 31 August 2006

Adsorption of TiCl_4 on Au/MgCl_2 with e-beam



Under these conditions all we observe is loss of MgCl_2 .

Where is the TiCl_x ?

M. J. Pilling, M. J. Cousins, A. Amiero Fonseca, K. C. Waugh, M. Surman, P. Gardner
Far Infrared RAIRS and XPS Studies of TiCl_4 Adsorption and Reaction on Mg Films.
Surface Science 587 (2005) 78

RSC-IRDG Rutherford Appleton Laboratory – 31 August 2006

Conclusions

The $\text{Au/MgCl}_2/\text{TiCl}_x$ system is a very complex one

Production of a film that is a good model of the catalyst is not straight forward

It is not at all clear that the model of the surface produced by Somorjai is correct

Far IR RAIRS alone is not going to solve this problem on its own

RSC-IRDG Rutherford Appleton Laboratory – 31 August 2006

Outlook

Far-IR RAIRS using synchrotrons has been carried out successfully only at Brookhaven and Daresbury. Both these station have now closed

Why?

**There was only a small user community
The technique is complicated and good results difficult to obtain.
Only a few systems worked.
Poor source stability on second generation machines**

New third generation sources should have better source stability

There is need for one good far IR RAIRS station.

Call it THz-RAIRS or RATZS and it might get funded!!!!

RSC-IRDG Rutherford Appleton Laboratory – 31 August 2006

Acknowledgements

**MSc Students
Danny Bird
Sarah Bickerstaff**

**PhD Students
Sunil Patel
Mike Pilling
Mrs Nurhayati**

**Post Docs
Mike Pilling**

S Le Vent

Mark Surman Daresbury

**Martyn Pemble Salford
Paul Wincott
Amir Awaluddin**

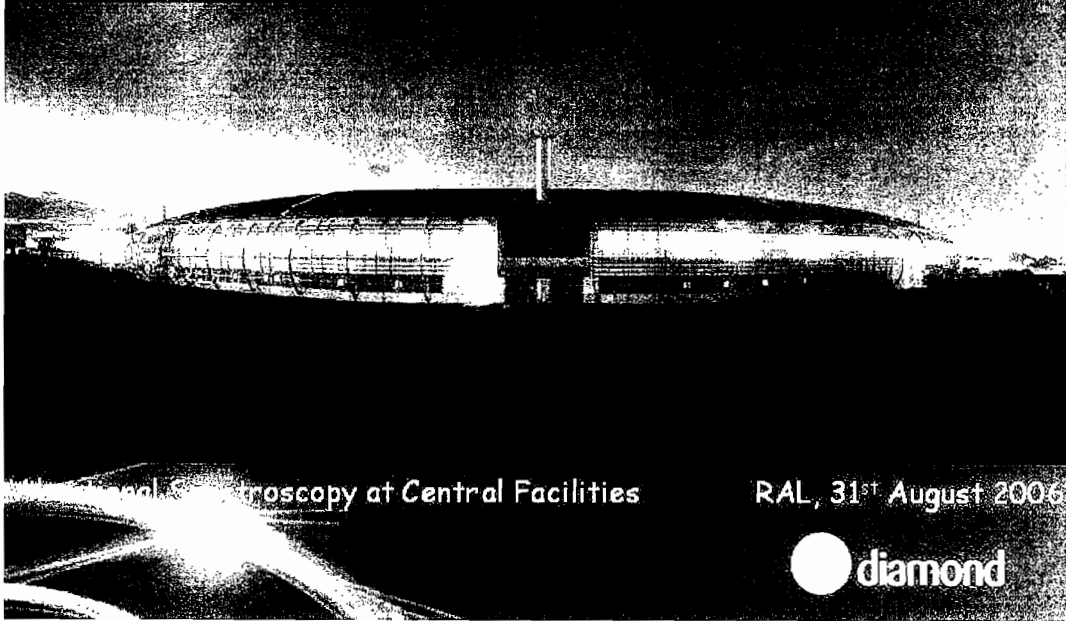
**Mike Chester, Nottingham
Peter Hollins, Reading**

EPSRC

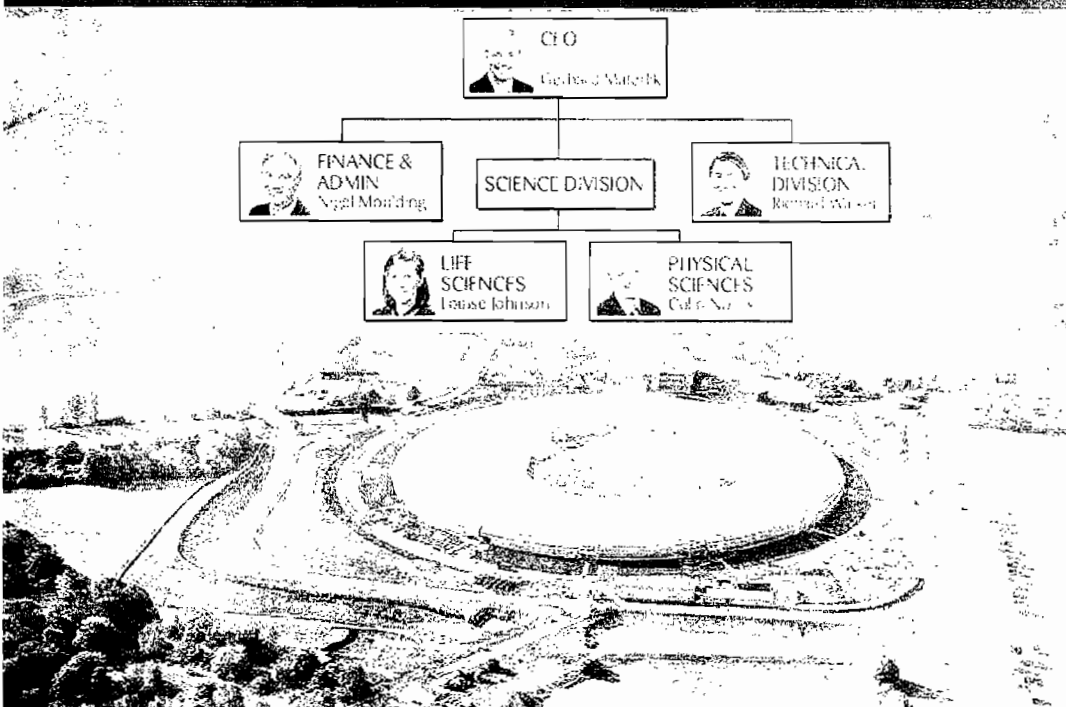
RSC-IRDG Rutherford Appleton Laboratory – 31 August 2006

The Infrared Beamline at the New Diamond Facility

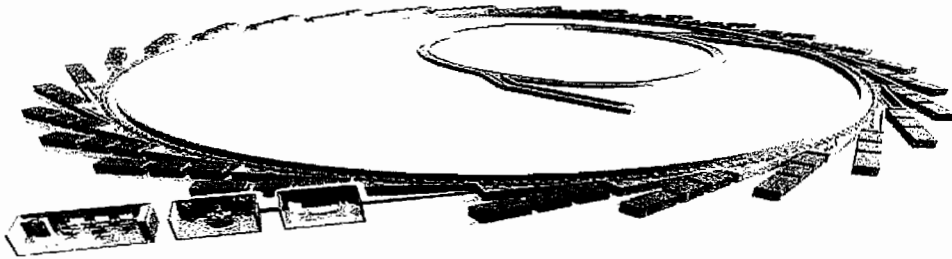
Gianfelice Cinque, B22 - IR microspectroscopy beamline



Diamond Light Source at RAL



Key Machine Parameters

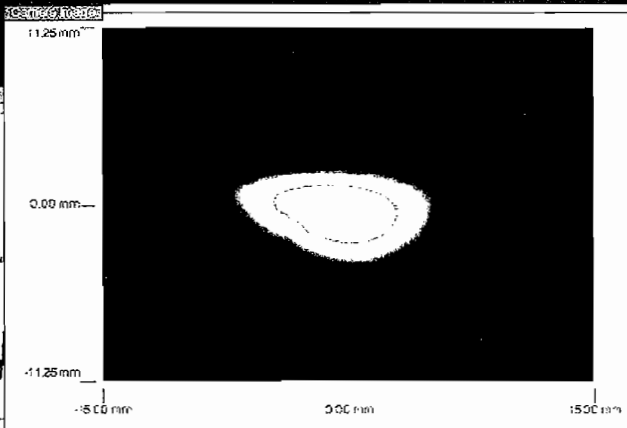
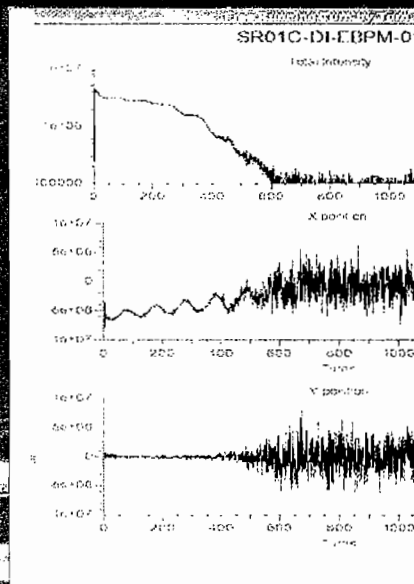


Electron Beam Energy	3 GeV
Circumference - Storage Ring	561.6 m
Number of cells	24 double-bend achromatic 6-fold symmetry
Insertion devices	4 x 8 m & 18 x 5 m
Dipole field	1.4 T
Beam current	300 mA (500 mA)
Beam emittance	2.74 nm rad (hor) 0.0274 nm rad (ver)
Beam life time	>10 h (20h)



Beam in the storage ring

First circulating beam
4th-5th May 2006



600 turns in the
storage ring
6th-7th May 2006



Diamond SAC 2003: proposal of an Infrared Beamline for Microspectroscopic Analysis

Mike Chesters, University of Nottingham
 Mark Tobin, Australian Synchrotron Project
 Peter Hollins, University of Reading
 Paul Dumas, Soleil
 Liane Benning, University of Leeds
 Andrea Russell, University of Southampton
 Neil Everall, ICI, Wilton
 Nick Terill, Diamond

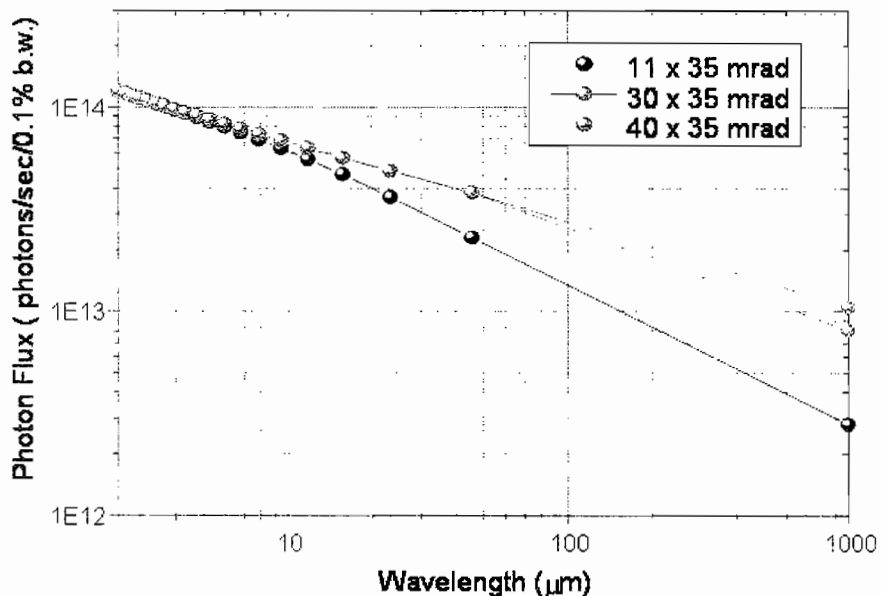
Conclusions:

- ❖ Performance in the mid-IR ($500\text{-}4000\text{ cm}^{-1}$) will not be compromised by restricting the vertical acceptance angle to 11 mrad. **Provision of a 30 mrad vertical opening angle is recommended.**
- ❖ Flux in to a $4\text{-}5\ \mu\text{m}^2$ spot at 2000 cm^{-1} compared to a conventional blackbody source:

(ex) SRS 13.3	x 20
(till 2008) SRS 11.1	x 200
Diamond IMS	> 1500
- ❖ Intense edge radiation to provide 2 beamlines at one bending magnet should be investigated.



Diamond SAC 2003 IMS beamline proposal

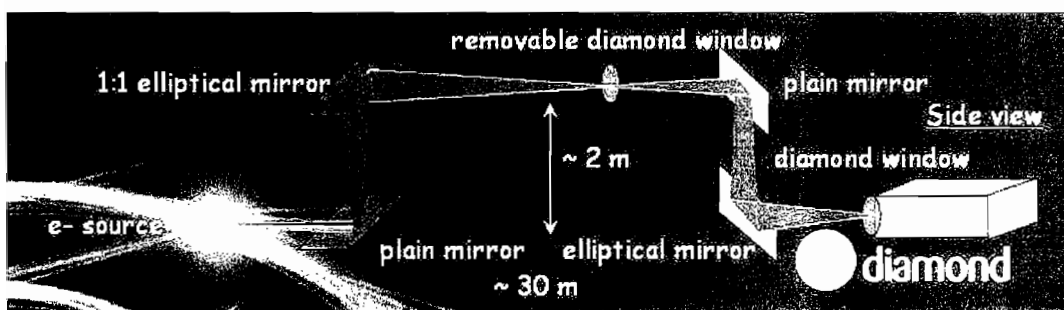
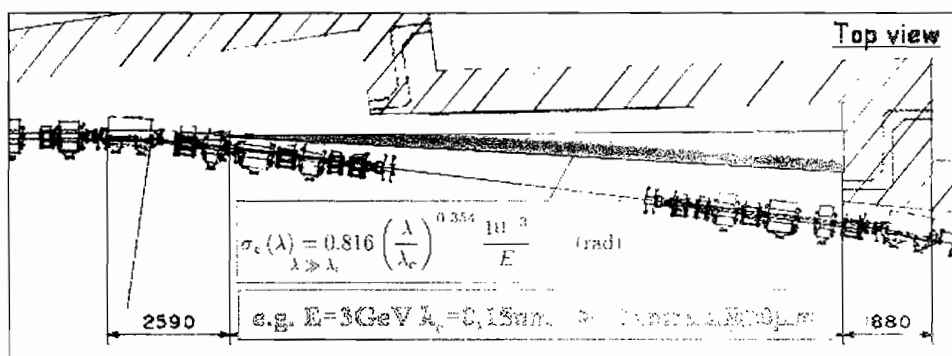


Scientific case for the IR microspectroscopy beamline at Diamond experienced UK community working on FTIR, IR microspectroscopy and SR in fields like:

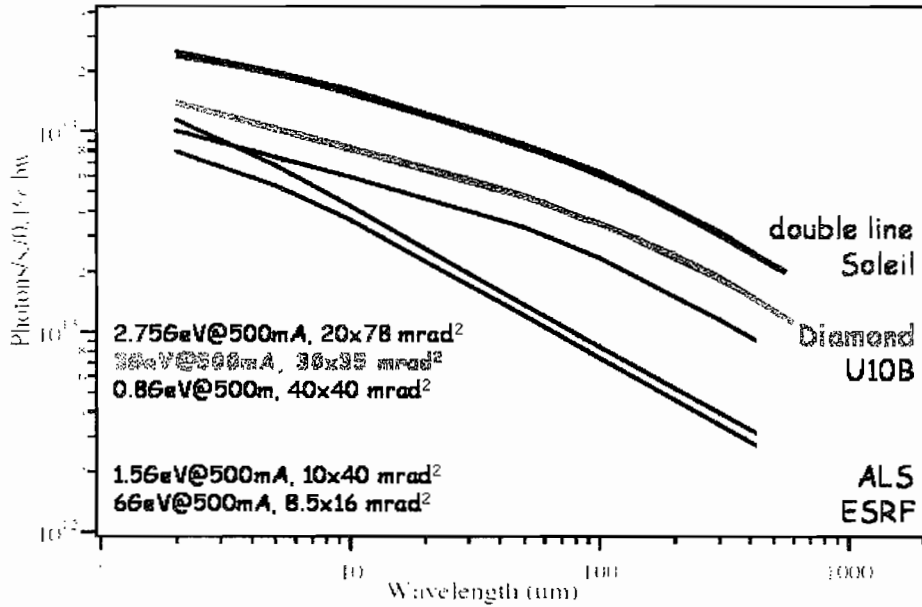
- Life Sciences and Biomedicine:
 - Single cell studies
 - Sub cellular analyses
 - Cancer diagnosis
- Solid state physical chemistry
 - Surfaces
 - Interfacial science
 - Catalysis
- *to be explored*
 - *High pressure and FTIR*
 - *Archaeology and Fine Arts*
 - *Food science*
 - *Planetary science*



Front end and optics sketch



Diamond IR source



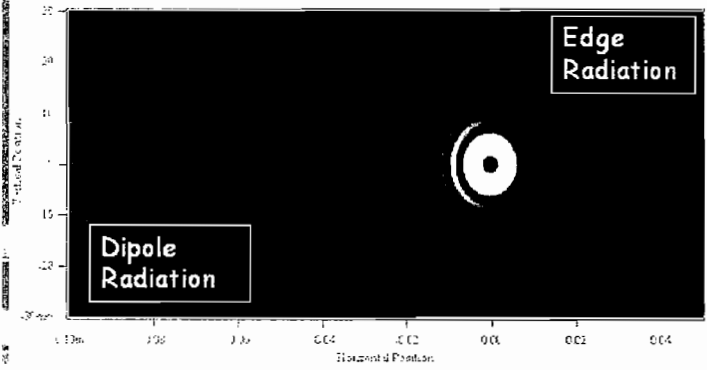
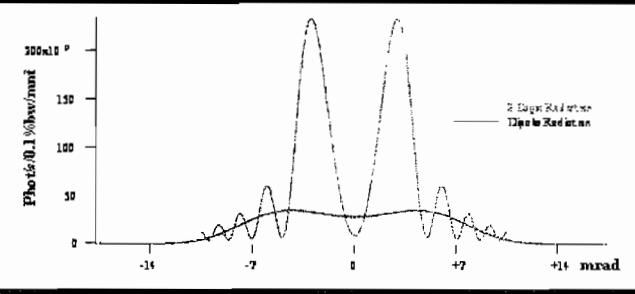
Pascal... ALLES Infrared Beamline on the Third Generation
...SOLEIL, WIRMS,
<http://www.synchrotron-soleil.fr/francals/vie-scientifique/experiences/alles/>
...SNEWS_01-06_img/WIRMS...?openement

Transition Edge Radiation as Far IR source

e.m. radiation by a relativistic charge in a rapidly changing magnetic field,
e.g. bending magnet ends

$$\lambda_{c}^{edge} \approx \frac{L_{edge}}{\gamma^2} (\approx 3nm)$$

$$\lambda_{c}^{BM} \approx \frac{R}{\gamma^3} (\approx 0.15nm)$$

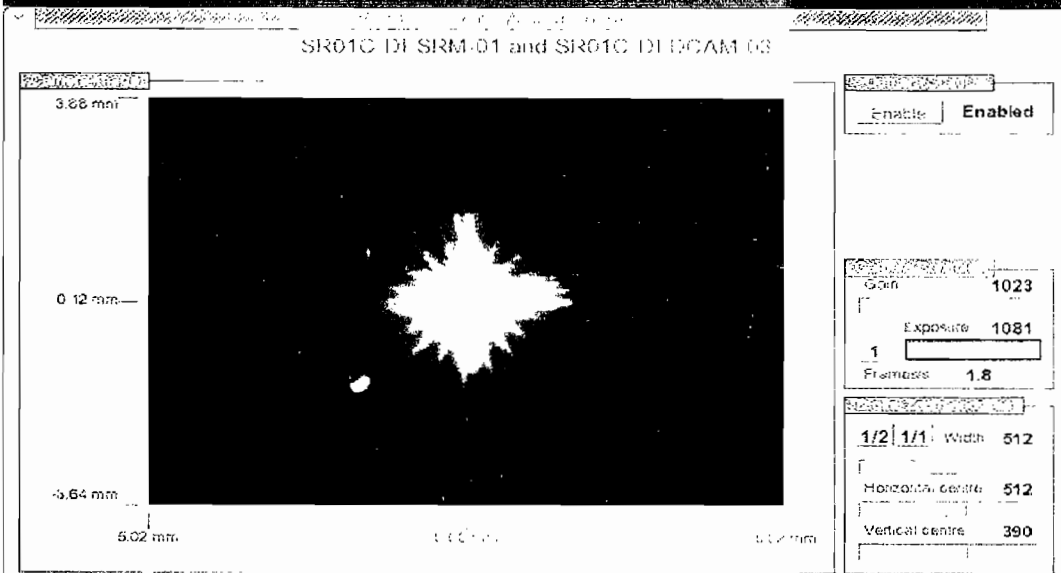


- Assuming $\lambda \gg \lambda_c$:
- no flux on axis
 - peak flux cone at $1/\gamma$
 - radially polarised

From J.A. Clarke,
Edge Radiation,
4th August 2000
CLRC Accelerator Physics
and New Sources Group

First Synchrotron Light at Diamond

2 mA and 0.7 GeV 6th-7th May 2006



IR light to users from April 2010

<http://www.diamond.ac.uk/Beamlines/Beamlineplan/B22/default.htm>

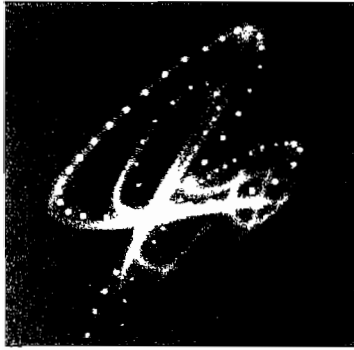
gianfelice.cinque@diamond.ac.uk

Thank you

Vibrational Spectroscopy at Central Facilities

RAL, 31st August 2006





4

The UK's energy recovery linac free electron laser facility

Vibrational Spectroscopy at Central Facilities

Elaine Seddon, August 2006



Acknowledgements

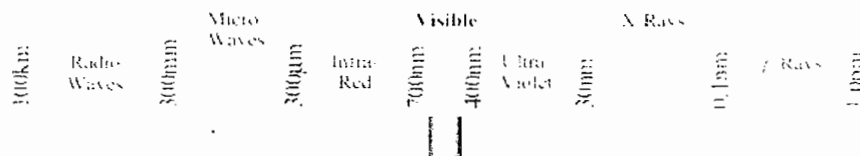
- The 4GLS Team
- The 4GLS International Advisory Committee
- The 4GLS Steering Committee
- National and international scientific community
- Funding: OST/DTI, CCLRC, NWDA and EU



information <http://www.4gls.ac.uk>



- ❖ **Milestones and hurdles**
- ❖ **4GLS machine update (focus on longer wavelength systems)**
- ❖ **Flavour of some of the science potential of 4GLS**



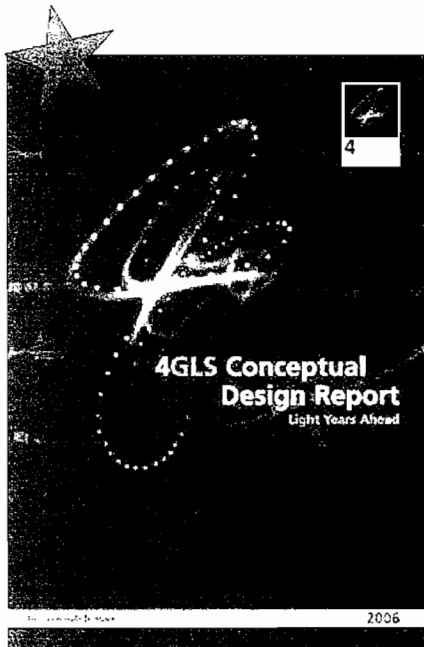
4GLS: timescales



- ✓ April 02 **Scientific case approved (Gateway 0)**
- ✓ Nov 02 **Business case approved (Gateway 1)**
- ✓ April 03 & 04 **£13.9 M funding for prototype accelerator (ERLP) and R&D (OST £8 M, CCLRC £5.9 M)**
- ✓ Feb 05 **EUROFEL R&D work funded (Euro 9M)**
- ✓ March 05 **Funding for 4GLS Technical Design (CCLRC £1.6 M)**
- ✓ Nov 05 **£3 M NWSF funding for ERLP science**
- ✓ Spring 06 **4GLS CDR**
- **late 06** **Prototype construction complete**
- **2007** **Report on 4GLS phase I, ERLP operational, 4GLS TDR**
- **2008/09 ??** **Approval for 4GLS procure and start build**
- **2012/13 ??** **Facility starts to become available to researchers**



4GLS: CDR April 2006



- 4GLS Conceptual Design Report launched
- Available as a CD or on the web at <http://www.4gls.ac.uk>

CDR launch



4GLS Phase I results:

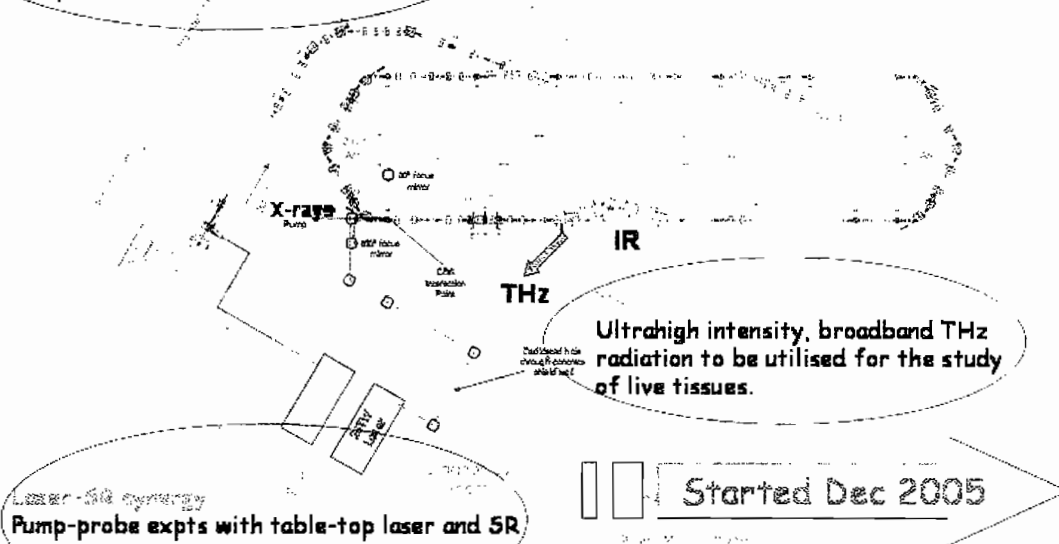
First Beam from the ERLP Photoinjector August 2006



ERLP photon science: NWSF £3M, 3 years



Time resolved X-ray diffraction studies probing shock compression of matter on sub picosecond timescales.



4GLS: timescales

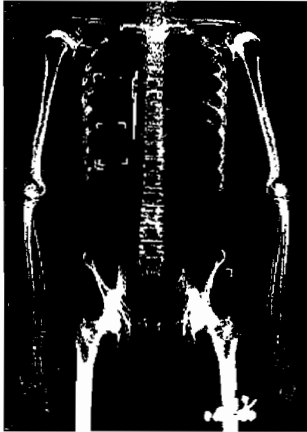


- | | |
|-----------------|---|
| ✓ April 02 | Scientific case approved (Gateway 0) |
| ✓ Nov 02 | Business case approved (Gateway 1) |
| ✓ April 03 & 04 | £13.9 M funding for prototype accelerator (ERLP) and R&D (OST £8 M, CCLRC £5.9 M) |
| ✓ Feb 05 | EUROFEL R&D work funded (Euro 9M) |
| ✓ March 05 | Funding for 4GLS Technical Design (CCLRC £1.6 M) |
| ✓ Nov 05 | £3 M NWSF funding for ERLP science |
| ✓ Spring 06 | 4GLS CDR |
| ▫ late 06 | Prototype construction complete |
| ▫ 2007 | Report on 4GLS phase I, ERLP operational, 4GLS TDR |
| ▫ 2008/09 ?? | Approval for 4GLS procure and start build |
| ▫ 2012/13 ?? | Facility starts to become available to researchers |

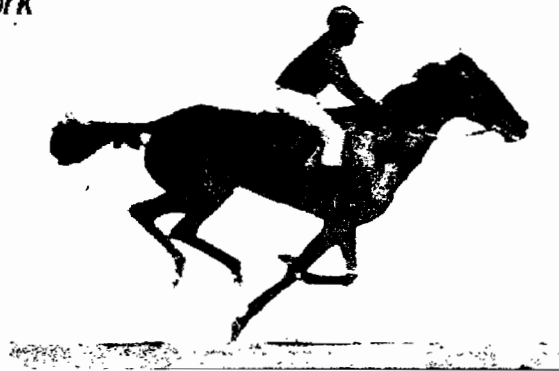
The Science Need...



Fundamental requirement to understand the *dynamic* behaviour of matter, often in very small (nm) units, on very fast (fs) timescales



Need not just to determine *structure* with high precision, but to understand *how these structures work*



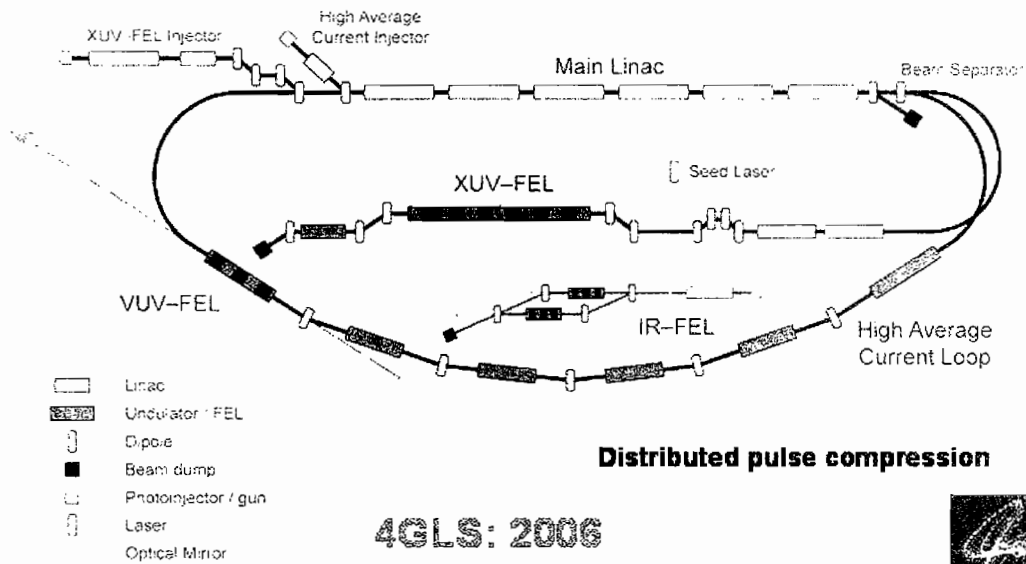
The Science Need...



Require an *ultra-high brightness low energy facility* that allows the use of *ultra-short pulsed sources* both individually and in combination

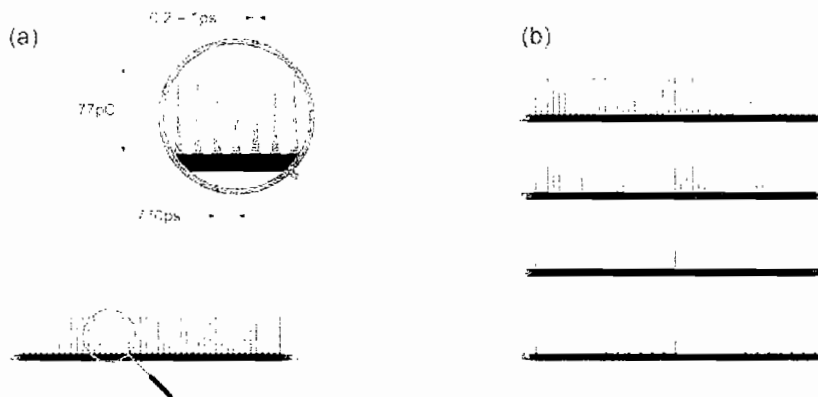
4GLS is being designed to meet this need

4GLS combines superconducting ERL, SR, laser and FEL technology in a fully integrated multi-source, multi-user facility



Pulse structures: High Average Current Loop

- Considerable flexibility in bunch patterns





CDR Layout

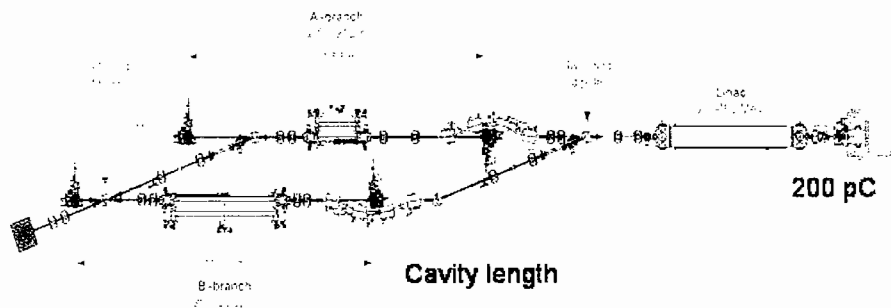


Multuser facility

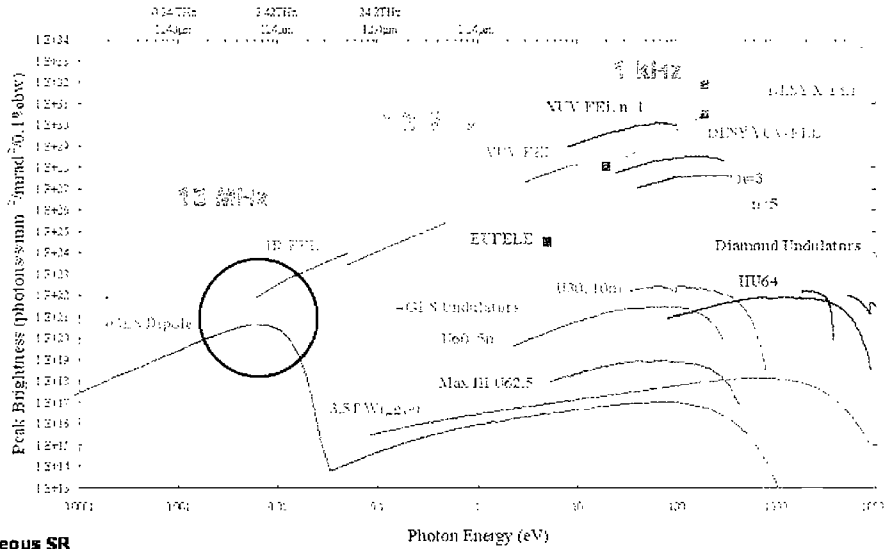
The IR-FEL



- 2.5 to 200 μm
- Bunch length 1-10ps rms
- Variable polarisation
- SC linac > stability
- CW or macropulse
- Tuning - JLAB lased at 20-100W over 0.7 to 4.8 μm in seconds
- Partial waveguiding to get to longer wavelengths?
- Max pulse energy $\sim 50 \mu\text{J}$

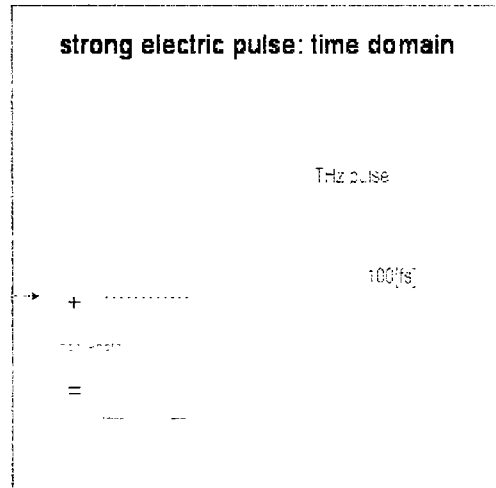
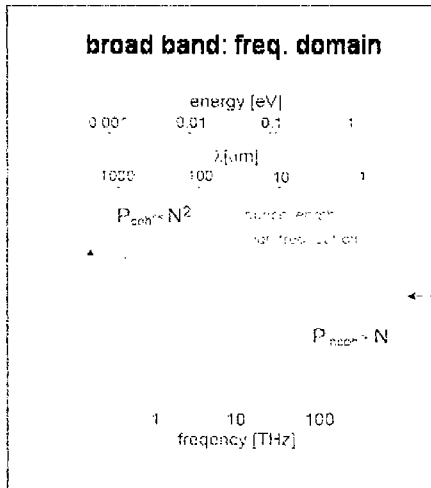


AGLS Photon Output



Spontaneous SR
Range: up to 1keV
Pulse length: few ps down to 100 fs
Repetition rate: 1.3GHz max

Broad band THz short pulse



**broad band photon source in frequency domain,
 strong electric field pulse in time domain**

Courtesy of A. Nilsson



Temporally coherent (transform limited) beams have:

$$\text{Spectral width} \times \text{pulse duration} \approx 2 \text{ eV fs}$$

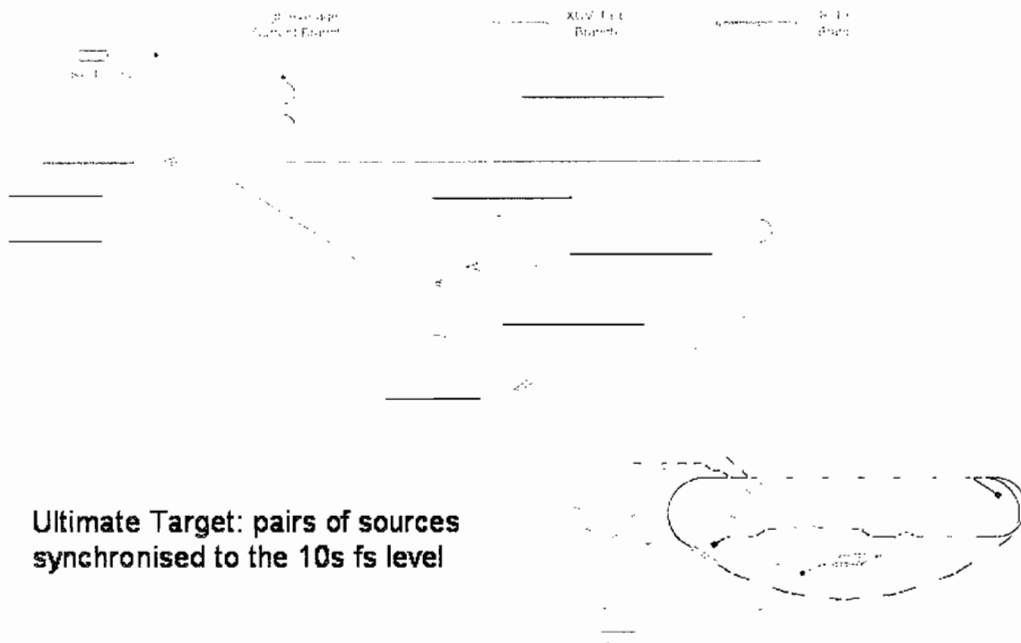
Spatially coherent (diffraction limited) beams have:

$$\text{Beam area} \times \text{divergence} \approx 1/(2E^2) \text{ mm}^2 \text{ mrad}^2$$

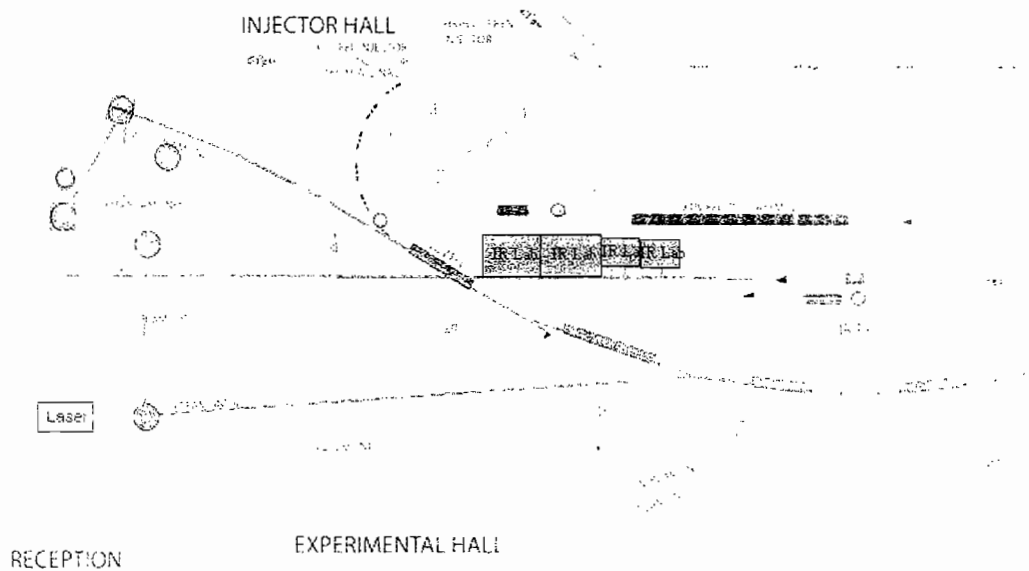
where E is the photon energy in eV

(Exact values depend on pulse and beam profiles)

Combining Sources



Illustrative combinations: IR FEL and THz distribution added



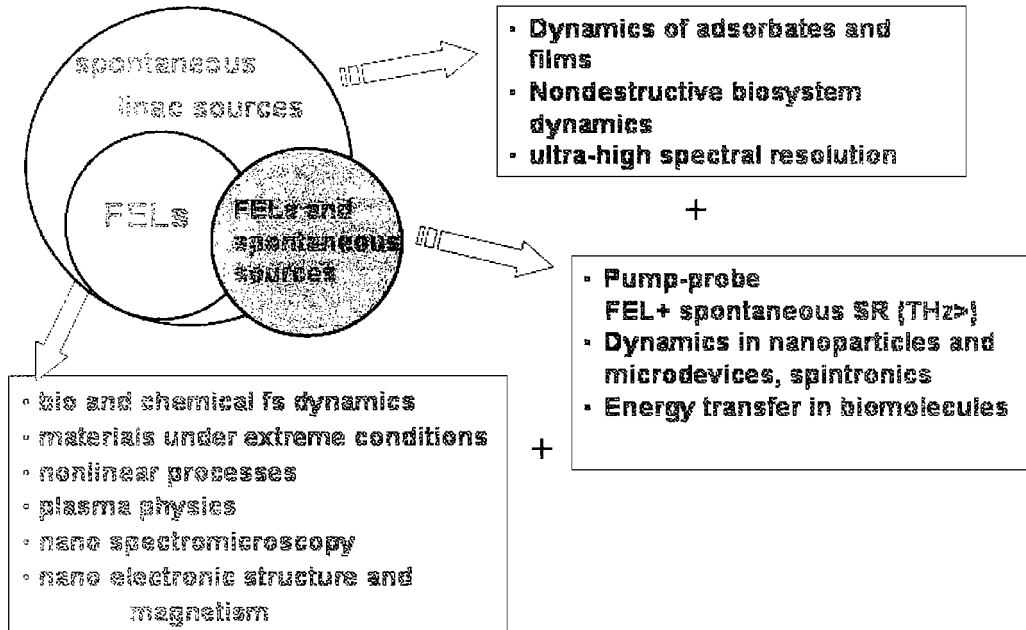
**A suite of light sources optimised for
THz to soft X-ray wavelengths...**



- **free electron lasers**
- **undulators and bending magnets**
THz to soft X-ray
- **combinations of sources**
internal and/or with conventional lasers

**World leading combination -
unique experimental
flexibility and cost effective
delivery**

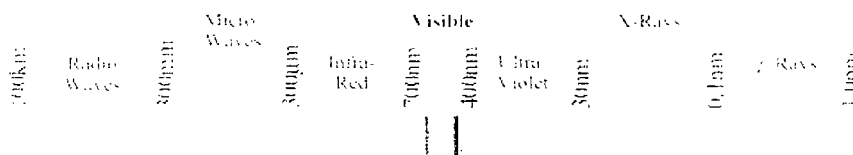
4GLS. Greater than the sum of the parts



4GLS Update



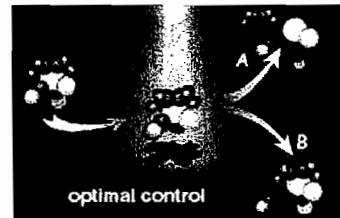
- ➔ Milestones and hurdles
- ➔ 4GLS machine update (focus on longer wavelength systems)
- ➔ Flavour of some of the science potential of 4GLS





Overview

- Unprecedented probe of electron motion in atoms and molecules
- Capability to pioneer a new generation of ultra-fast time resolved experiments revealing short lived intermediates in catalytic reaction pathways



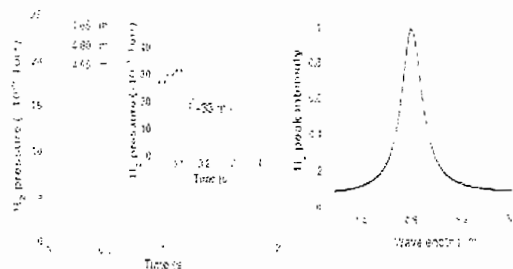
- The technology to underpin the development of the next generation of electronic devices charge and spin dynamics



- Development of innovative dynamic imaging techniques
 - on large scale for disease recognition
 - on nanoscale for biomolecular function in live cells

FEL ALONE: Mode-selective control of chemical reactions, Vanderbilt IR FEL, Liu et al.

Desorption of hydrogen by resonant excitation of the Si-H vibrational stretch



Liu, Feldman, Tolk, Zhang and Cohen, Science **312** 1024 May 2006

Irradiation of a mix of 15%H 85%D atoms on Si(111)
 FEL fluence 0.8J/cm² per macropulse (100mJ per macropulse), 50-90cm⁻¹ bandwidth
 Tuned from 4.2-5.6μm, quadratic laser intensity dependence
 No evidence of bulk heating

Desorption non-statistical 95 % is H₂ <5% HD or D₂
 Peak in H₂ desorption at 4.8 μm (0.26 eV) ν(Si-H) terrace sites

FEL ALONE cont.: Mode-selective control of chemical reactions
Vanderbilt IR FEL, Liu et al.



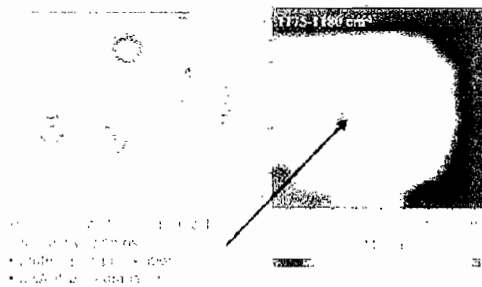
Conventional wisdom large molecules and molecules on surfaces expect many well coupled low frequency modes giving rapid energy randomisation (~ psec). Leads to thermal rather than selective results.

Power and tuneability of IR FEL enabled excitation of a particular vibrational mode and diverted reaction from thermal pathway

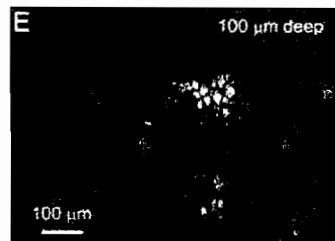
Potential impact on:

- 1 the storage, transport and delivery of hydrogen for the hydrogen economy
- 2 reactive chemistry on surfaces leading to room temperature refining

FEL ALONE cont.: Near-field imaging:
Sub-cellular IR Spectromicroscopy



Cell changes during apoptosis
(P Dumas, SR IR, SOLEIL)

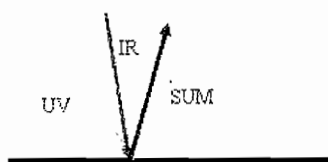


CARS image, mouse ear
(lipid CH₂ symmetric stretch)
Xie et al., PNAS, 102, 16807
(2005)

- Overcome diffraction limit using near-field imaging/IR FEL:
 - ⇒ 30-50 nm resolution cf. current best (microns)

Combined sources

Double resonance Sum Frequency Spectroscopy and imaging: New Horizons

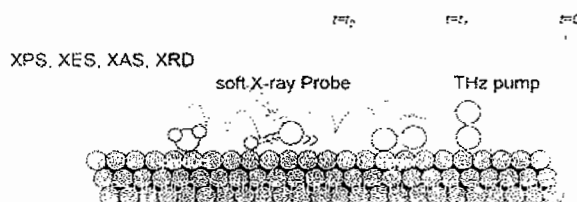


IR $\lambda > 10 \mu\text{m}$
 UV, tune to optimise non-resonant interaction

- Exploits tuneability of both IR FEL and VUV FEL
 - Conformation of large admolecules
 - Adsorbate dynamics
 - Membrane rafts & proteins, lipid bilayers, oxide catalysts...
 - Enormously widens range of surfaces and vibrations
- Imaging applications using near-field SFG signal (SNOM probe): below diffraction limit

Combined sources

Probing elementary surface reactions, Anders Nilsson group and collaborators



4GLS

Pump: THz,

Probe: XPS, XES, XAS, IR

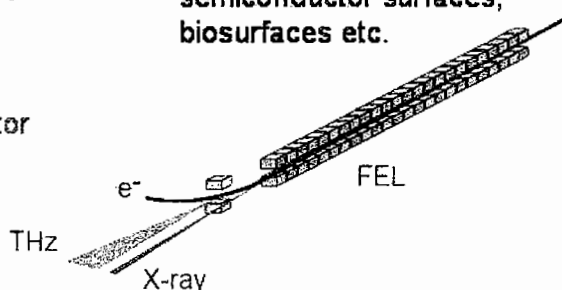
BM & XUV FEL

or far-IR FEL & undulator

Probe of reaction coordinate

Selective detection of surface species


Relevance to catalysis, fuel cells, environmental science, semiconductor surfaces, biosurfaces etc.





- multiuser facility
- state-of-the-art sources by themselves (THz to soft X-ray)
- undulators and FELs
- source combinations including table-top laser
- Bringing together laser and SR expertise and skills

- fully optimised detectors and on line diagnostics crucial for full exploitation






4GLS – the UK's 4th Generation Light Source

4GLS: the next steps

An information and interaction meeting for potential users following publication of the Conceptual Design Report

Daresbury Laboratory

Friday 8th September 2006

Invited speakers:

Markus Drescher (Universität Hamburg & DESY, Germany)

Gwyn P Williams (Jefferson Laboratory, USA)

John Sutherland (East Carolina University, USA)

Norman H Tom (Vanderbilt University, USA)

Antonio Criozetti (ISM-CNR Roma, Italy)

Cheuk-Yu Ng (University of California, Davis, USA)

- The purpose of the meeting is to inform, and consult with, potential users on the design of 4GLS following the recent publication of the Conceptual Design Report.
- A number of international experts will give presentations describing the key science that will be achieved
- Discussion sessions will ensure that the evolving aspirations of the user community continue to be met as the detailed design parameters are confirmed.





International Collaborations

International development programmes

- JLab
- Cornell
- Stanford
- Rossendorf
- DESY
- FERMI@Elettra
- EUROFEL collaboration



4GLS funding

NWDA



northwest
development agency

- Contribution to capital (ca. £4.5 M)
- Provision of 4GLS building thro' leaseback (ca. £24 M + vat)

- ca. £ 80-200 M to build and commission (not including VAT)



Linac-based light sources

